

NEDO特別講座

先進複合材料の製造における高度デジタル人材育成に関する特別講座　第5回：11月26日

複合材航空機の空力構造設計：空力弾性解析から多目的最適化・データ駆動型連成解析まで

阿部 圭晃（東北大学）



Greener Aviation

Sustainable Aviation Fuel (SAF)



Electric / Hybrid aircraft



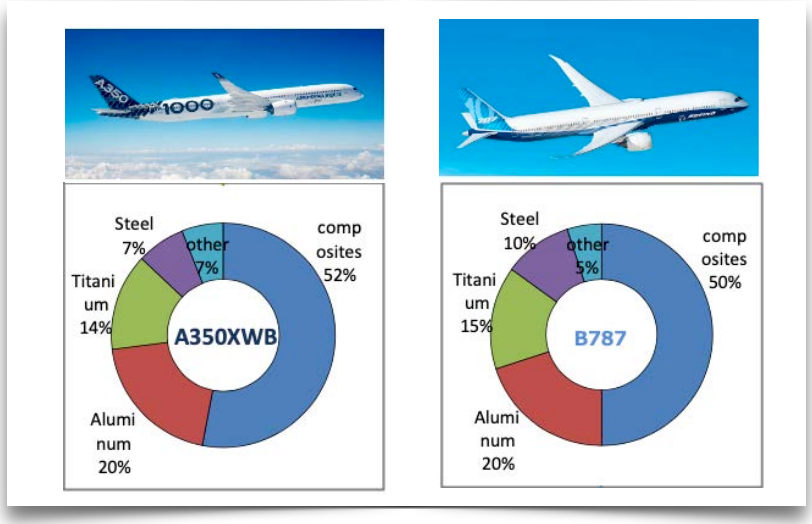
STARC-ABL(NASA)

Hydrogen / Ammonia combustion



ZEROe (Airbus)

Carbon Fiber Reinforced Plastic

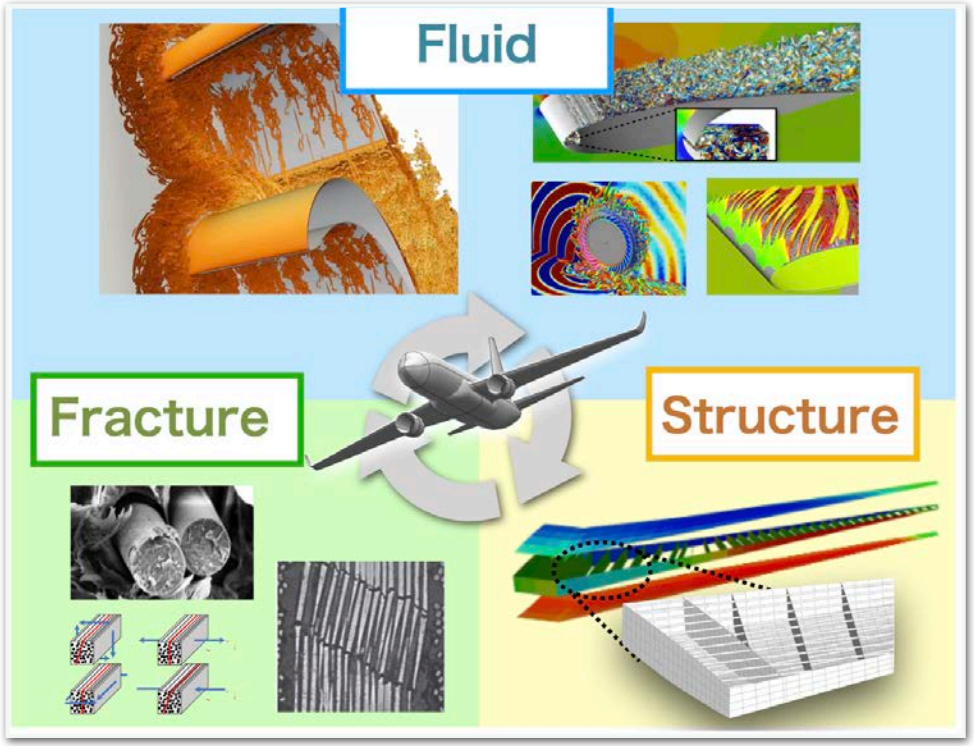


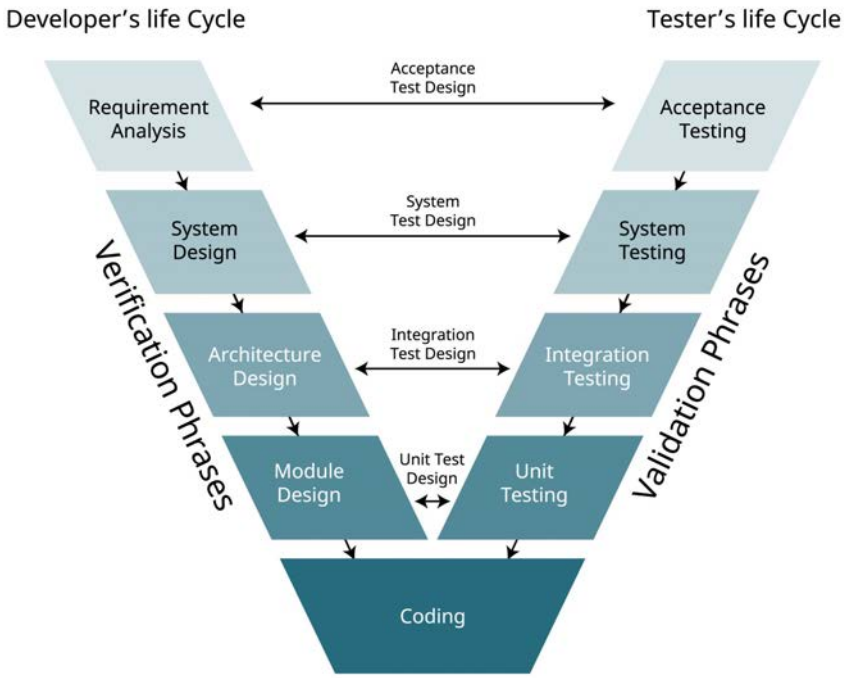
Digital aircraft design for mitigating a development cost / time

Digital aircraft design

Challenges in simulation technologies for digital twin/MBSE:

- **Multidisciplinary Design Optimization (MDO)**
- **Multi-scale / high-fidelity simulation**
- **Highly-parallel / modern hardwares**





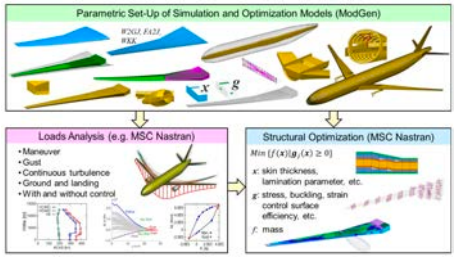
Digital aircraft design

Challenges in simulation technologies for digital twin/MBSE:

- **Multidisciplinary Design Optimization (MDO)**
- **Multi-scale / high-fidelity simulation**
- **Highly-parallel / modern hardwares**

(2022-) **DLR VicToria / VPH / VPH-2.0**

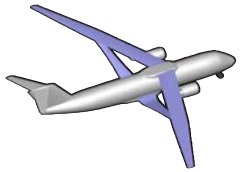
(Virtual Aircraft Technology Integration Platform)



cpacs-MONA: highly parameterized aeroelastic structural design tool

(2024-) **NASA Aviary** openMDAO

AVIARY



- Design aircraft and optimize trajectories simultaneously
- Use gradient-based optimization effectively

FENIAX Imperial College London

- Nonlinear aeroelastic toolbox (geom. nonl. ROM)
- Fully differentiable via AD
- Run on GPU via JAX library



Cea & Palacious, CPC 311 (2025) 109547

Tohoku Uni. TiAD

(Toward Ideal Aircraft Design)

- CFRTP aircraft design
- Virtual Testing

DASH

Digital Aircraft Design tool of Tohoku University

JAXA CHAIN-X

(*2022-*, with MHI/KHI/SUBARU)

- Design DX
- Certification DX (CbA)
- Production DX

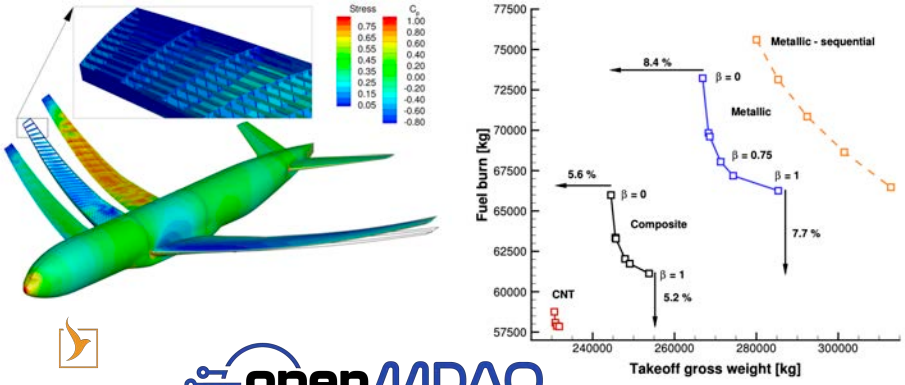
Studies on digital aircraft design

Aerodynamic/structural-coupled-adjoint method

Kennedy et al., AIAA2014-0596, Kenway *et al.*, *AIAA J.*, Vol. 52, No. 5, (2014)
Gray *et al.*, *Struct Multidisc Optim 59, 1075–1104 (2019)*

$$\text{minimize} \quad \beta\text{FB} + (1-\beta)\text{TOGW}$$

$$\text{w.r.t.} \quad \mathbf{x}$$

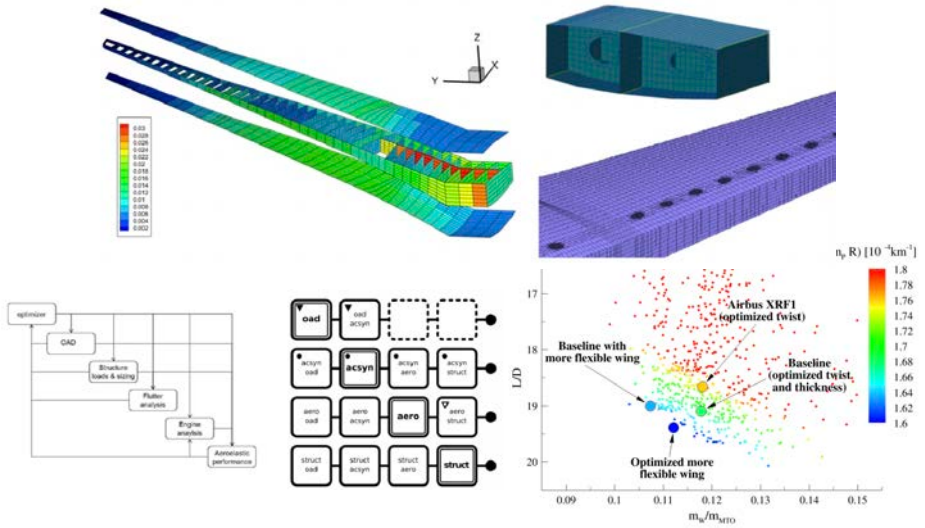


AVIARY openMDAO

- Wing shape optimization by coupled adjoint
- CFD (RANS) and CSD (Linear FEM)
- Less adaptive for new CFRP materials
- Multiple objective function with weight func.

cpacs-MONA: DLR VicToria project for MDO

S. Görtz et al., AIAA 2020-3167
Klimmek et al., IFASD, 2019



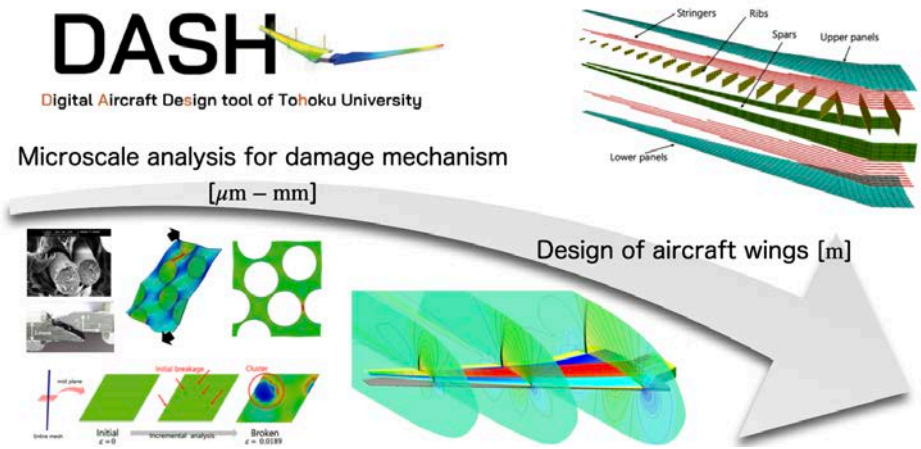
- Integrated high-fidelity aero-structural optimization
- Demonstration of flexible wing potential
- Many-discipline highly-parallel approach
- Gradient-based optimization

- Multiscale framework for estimating CFRP properties
- Global optimization and multiple objective functions (drag and weight reduction)
- Coupling methodologies for integrating high-fidelity / parallel simulations

Contents of my talk

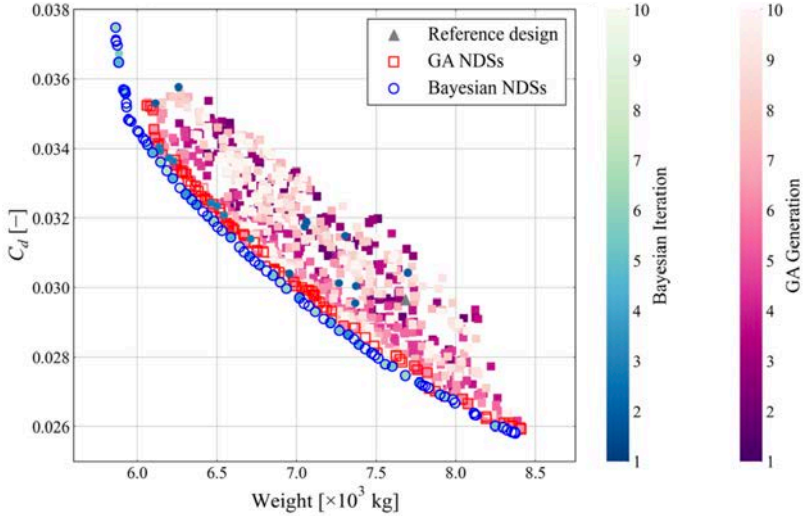
Composite aircraft design tool

Date *et al., AEST 2022, Rashmikant and Abe, AEST 2026*



Design optimization of CFRP wings

Liu *et al., AEST 2025, Comp. Struct. 2026,* Kano *et al., AEST 2025*

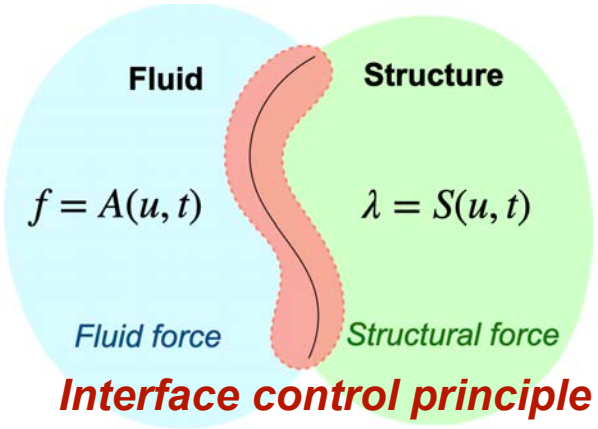


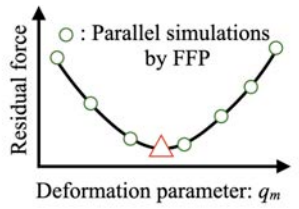
Data-driven/assisted FSI

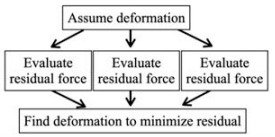
Abe *et al., JSCM, 48, 6 (2022)*

Lee, Abe, et al., J. Fluids and Structures 2026

Yatsu *et al., CM3 Transport 2025*







Composite aircraft design tool

DASH

Digital Aircraft Design tool of Tohoku University

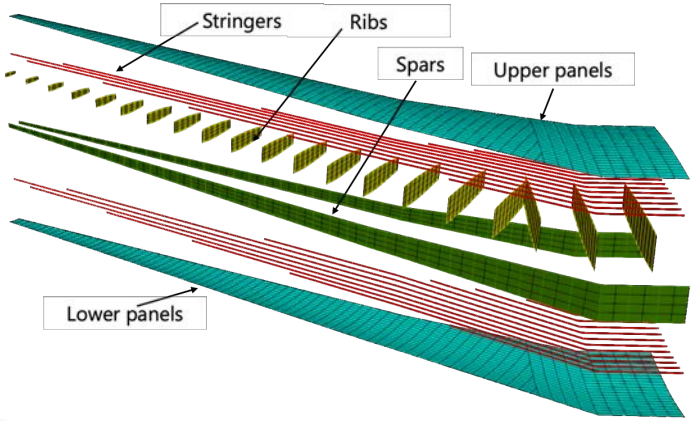
Date, Abe, *et al., J. Aero. Sci. Tech.* 2022

Liu, Abe, *et al., J. Aero. Sci. Tech.* 2025

Kano, *et al., J. Aero. Sci. Tech.* 2025

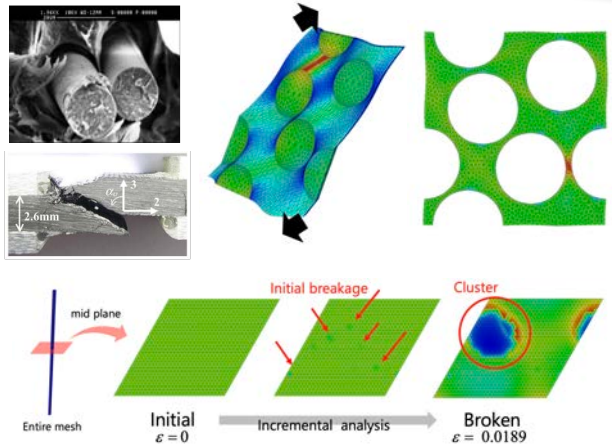
Liu, Abe, *et al., Comp. Struct.* 2026



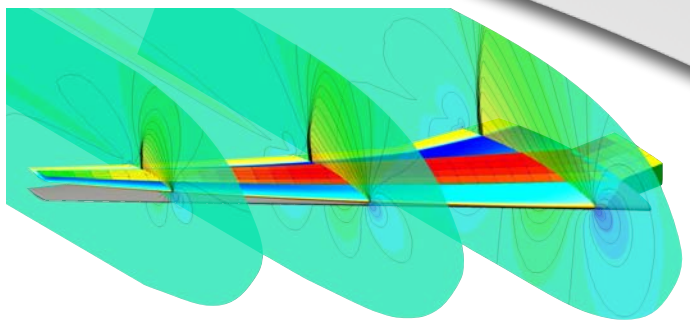


Microscale analysis for damage mechanics

$[\mu\mathrm{m} - \mathrm{mm}]$



Design of aircraft wings [m]



Multiscale Analysis for Aircraft Design

Microscale

Fibers

Stiffness parameters

$E_{ij}^{\mathrm{f}},\ \nu_{ij}^{\mathrm{f}}$

Strength parameters

$\sigma_{01},\ \sigma_{02},\ m_1,\ m_2$

Matrix

Stiffness parameters

$E^{\mathrm{m}},\ \nu^{\mathrm{m}},\ H_{\mathrm{p}}$

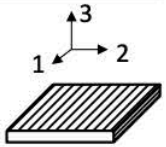
Strength parameters

σ_{Y}

Composites

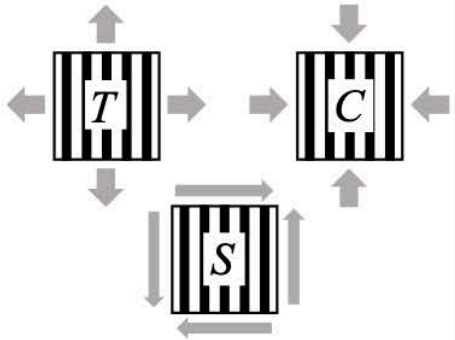
Stiffness parameters

$E_{ij}^{\mathrm{c}},\ \nu_{ij}^{\mathrm{c}}$



Strength parameters

$T_{ii},\ C_{ii},\ S_{ij}$

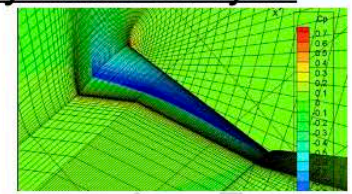


$E_{ij}^{\mathrm{c}},\ \nu_{ij}^{\mathrm{c}}$
$T_{ii},\ C_{ii},\ S_{ij}$

Macroscale

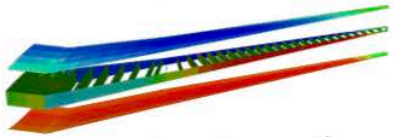
Wings

Aerodynamic analysis



Coupled

Structural analysis



Failure criteria

$$\left(\frac{1}{T_{11}}-\frac{1}{C_{11}}\right)\sigma_{11}+\frac{\sigma_{11}^2}{T_{11}C_{11}}-\frac{1}{4}\left(\frac{1}{T_{11}}+\frac{1}{C_{11}}\right)^2\sigma_{11}\sigma_{22}\le 1$$

$$\left(\frac{1}{T_{22}}-\frac{1}{C_{22}}\right)\sigma_{22}+\frac{{\sigma_{22}}^2}{T_{22}C_{22}}+\frac{\sigma_{12}^2}{S_{12}^2}\le 1$$

Microscale analysis

- Estimation of stiffness parameters
- Estimation of strength parameters

Macroscale analysis

- Fluid-structural coupling
- Failure analysis & sizing process

Shugo Date, Ph.D Thesis (Tohoku University), 2021

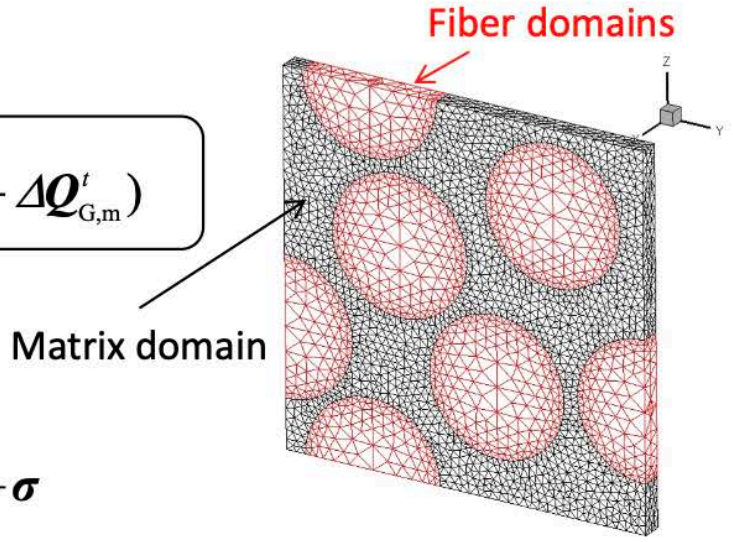
Microscale Analysis for Aircraft Design

Prediction of transverse and shear strength (T_{22}, C_{22}, S_{12})

- Periodic unit cell (PUC) analysis *

Stiffness equation

$$(\boldsymbol{K}_{\mathrm{f}}^{t}+\boldsymbol{K}_{\mathrm{m}}^{t})\Delta\boldsymbol{U}_{\mathrm{L}}=-(\boldsymbol{Q}_{\mathrm{f}}^{t}+\boldsymbol{Q}_{\mathrm{m}}^{t})+\boldsymbol{Q}_{\mathrm{V}}^{t}+\boldsymbol{Q}_{\mathrm{Dam}}^{t}-(\Delta\boldsymbol{Q}_{\mathrm{G,f}}^{t}+\Delta\boldsymbol{Q}_{\mathrm{G,m}}^{t})$$



Unit cell model

- Constitutive laws

Fibers $\quad \dot{\boldsymbol{\sigma}}=\boldsymbol{C}_{\mathrm{f}}:\dot{\boldsymbol{\varepsilon}}$

Matrix $\quad \dot{\boldsymbol{\sigma}}=\left(1-D^{*}\right)\boldsymbol{C}_{\mathrm{m}}:\dot{\boldsymbol{\varepsilon}}-\left(1-D^{*}\right)\dfrac{3\mu\dot{\bar{\varepsilon}}^{\mathrm{p}}}{\bar{\sigma}}\boldsymbol{\sigma}'-\dfrac{\dot{D}^{*}}{1-D^{*}}\boldsymbol{\sigma}$

$\boldsymbol{K}_{\mathrm{f}}$	: stiffness matrix of fiber
$\boldsymbol{K}_{\mathrm{m}}$	: stiffness matrix of matrix
$\boldsymbol{Q}_{\mathrm{f}}$	: internal force vector of fiber
$\boldsymbol{Q}_{\mathrm{m}}$	: internal force vector of matrix

- Failure criteria

Under elastic deformation (Asp et al. **)

$$U_{V}\geq\frac{3(1-2\nu)}{2E_{\mathrm{m}}}\sigma_{\mathrm{m}}^{2}$$

Under plastic deformation (Nishikawa et al. ***)

$$D\geq D^{\mathrm{crit}}$$

$$\dot{D}=H\left(\bar{\sigma}-\sigma_{\mathrm{Y}}\right)\left(1-D\right)C\left\langle\dot{\varepsilon}_{\mathrm{m}}^{\mathrm{p}}\right\rangle+\left(B_{0}+B_{1}D\right)\dot{\bar{\varepsilon}}^{\mathrm{p}}$$

Shugo Date, Ph.D Thesis (Tohoku Uni.), 2021

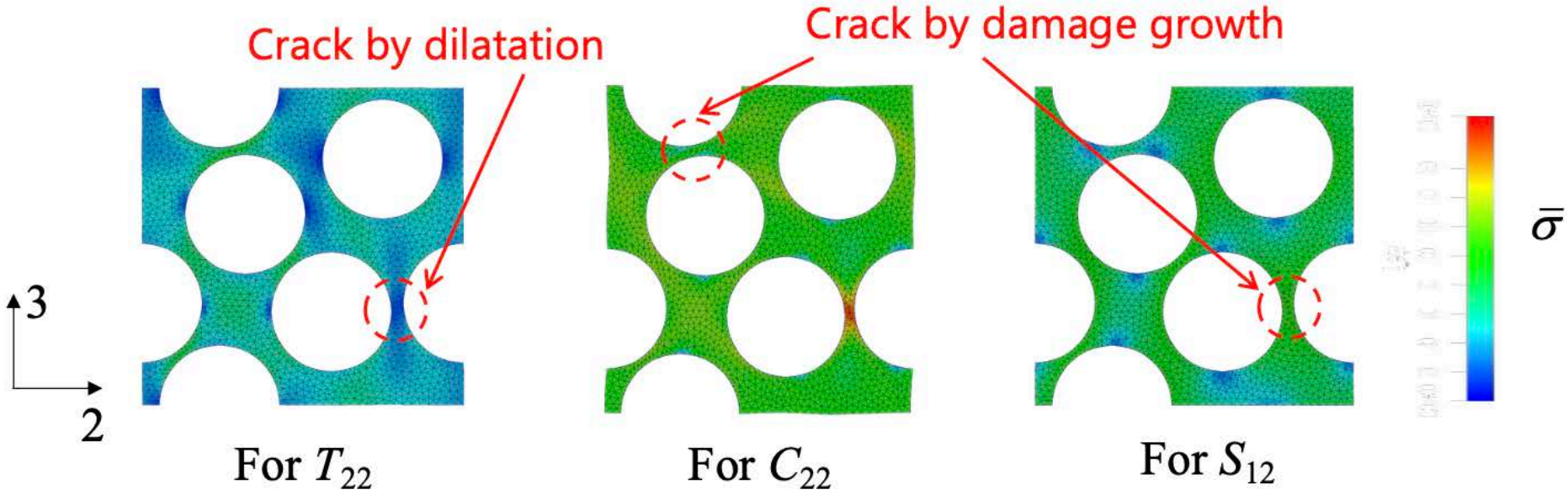
* Okabe, *Creep Damage Mechanics to Homogenization Methods,* 201
** Asp et al., *Composites Science and Technology,* 1996.
*** Nishikawa, *Ph. D thesis,* 2008.

Microscale Analysis for Aircraft Design

Prediction of transverse and shear strength (T_{22}, C_{22}, S_{12})

Example of PUC analysis (case: T800S)

Shugo Date, Ph.D Thesis (Tohoku Uni.), 2021



Almost the same strength for each fiber

	T700S	T800S	T1100G
T_{22} [MPa]	71.78	69.96	69.55
C_{22} [MPa]	161.3	160.6	160.8
S_{12} [MPa]	63.40	63.40	63.40

Microscale Analysis for Aircraft Design

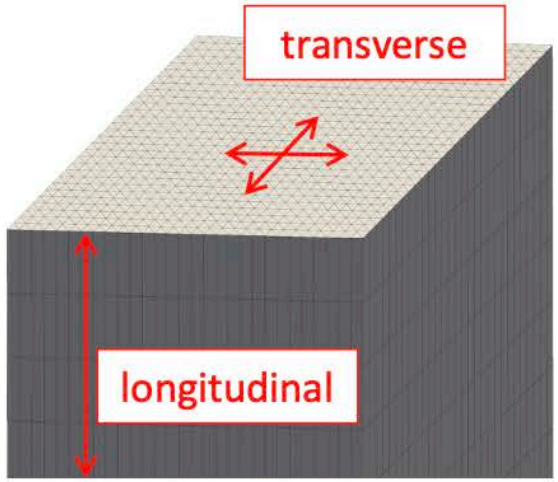
Prediction of longitudinal tensile strength (T_{11})

- Spring element model *

  Fiber : longitudinal spring element
  Matrix : transverse spring element

  Stiffness equation

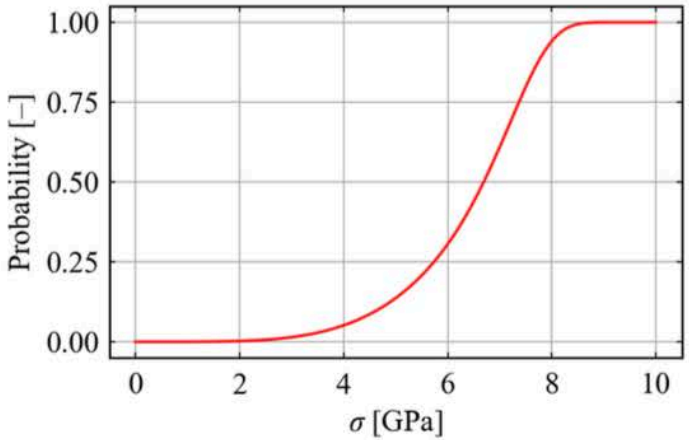
$$\left[\sum_{e=1}^{N_f-N_B-N_S} \boldsymbol{K}_f + \sum_{e=1}^{N_m} \boldsymbol{K}_m\right]\boldsymbol{w} + \sum_{e=1}^{N_{SL}} \pi R^2 \int_0^l \boldsymbol{B}^T \sigma_S dz = 0$$



Mesh of spring element model

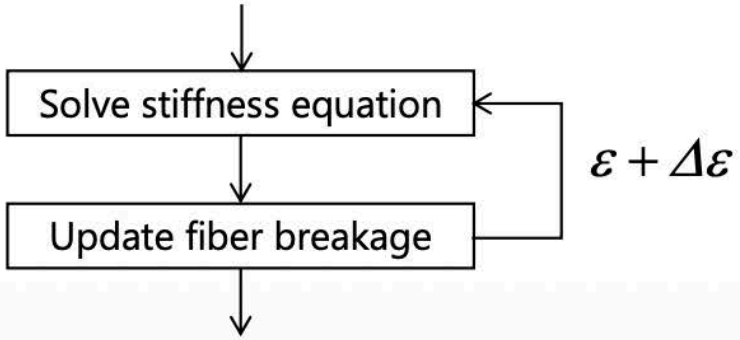
- Bimodal Weibull distribution

$$P(\sigma) = 1 - \exp\left\{-\frac{L}{L_0}\left(\frac{\sigma}{\sigma_{01}}\right)^{m_1} - \frac{L}{L_0}\left(\frac{\sigma}{\sigma_{02}}\right)^{m_2}\right\}$$



Bimodal Weibull distribution

- Incremental calculation



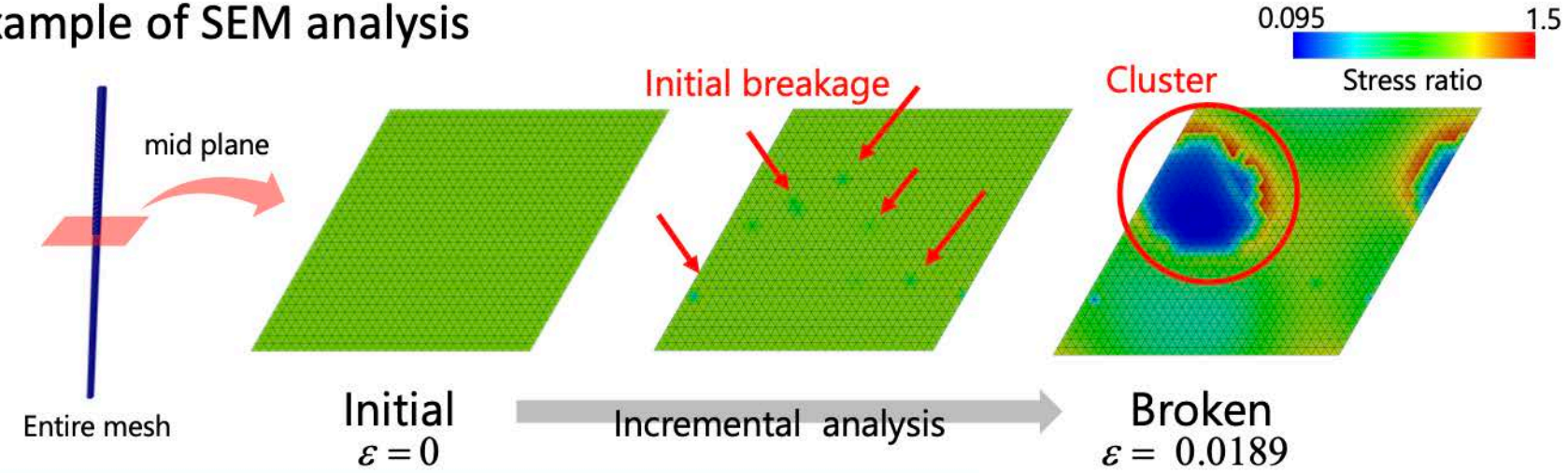
Okabe et al., Comp. Sci. and Tech. 2015
Shugo Date, Ph.D Thesis (Tohoku Uni.), 2021

Microscale Analysis for Aircraft Design

Longitudinal tensile strength (T_{11})

Okabe et al., Comp. Sci. and Tech. 2015
Shugo Date, Ph.D Thesis (Tohoku Uni.), 2021

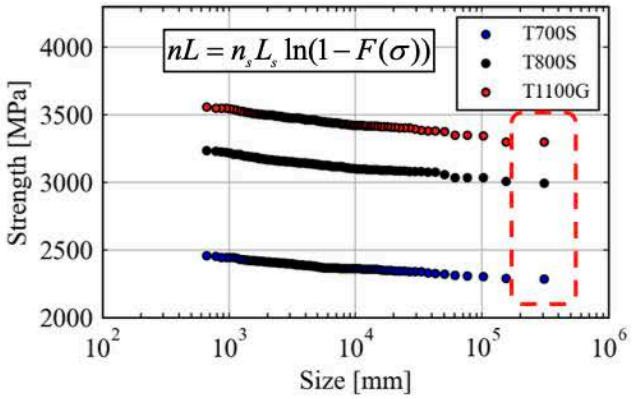
Example of SEM analysis



T1100G fiber exhibits higher strength

	T700S	T800S	T1100G
T_{11} [Mpa]	2290	2997	3301

Fiber strength directly affects the UD laminate strength



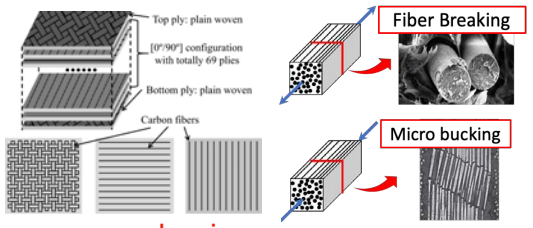
Microscale Analysis for Aircraft Design

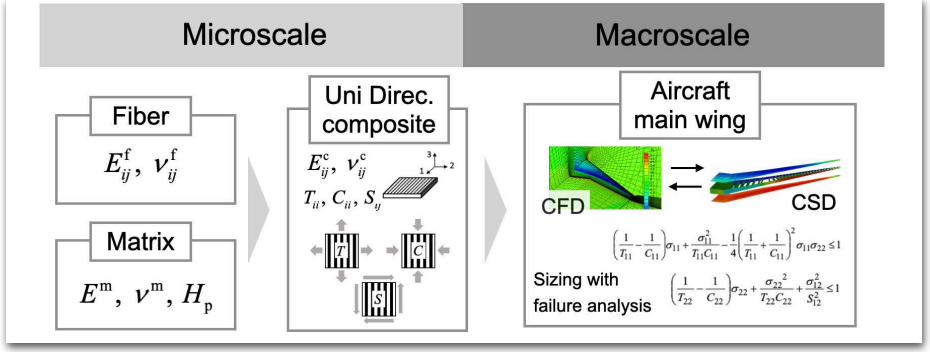
From micro/meso to macroscale (fiber/resin properties => CFRP laminate)

Fiber ⊕ **Matrix resin**

- ✓ High specific strength
- ✓ Anisotropic/complex damage mechanism

Li *et al., Int. J. Adv. Manu. Tech.*, 113 (2021)

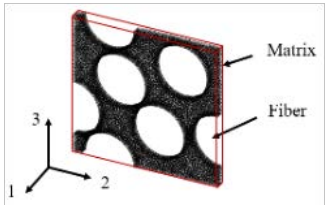




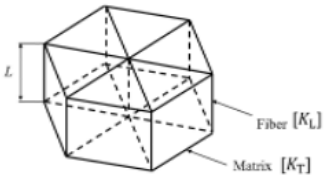
Key technologies for micro/mesoscale analysis

Prediction of UD laminate properties

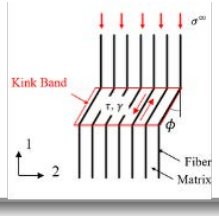
Periodic unit cell (PUC)



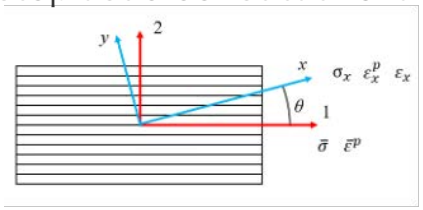
Spring element model



Sun-Jun / Knock-down Budiansky-Fleck model

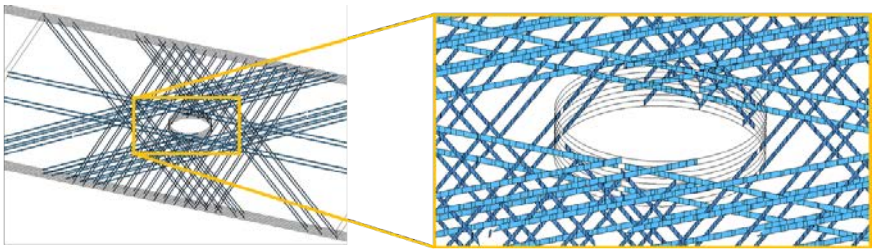


Elastoplastic constitutive law



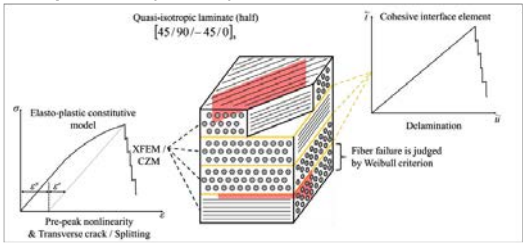
XFEM for OHT/C (open-hole tension/compression)

transverse crack, delamination by CZM



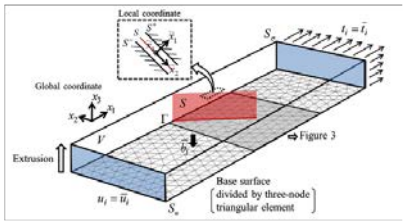
OHC

- Kink band propagation by energy dissipation (SCM)

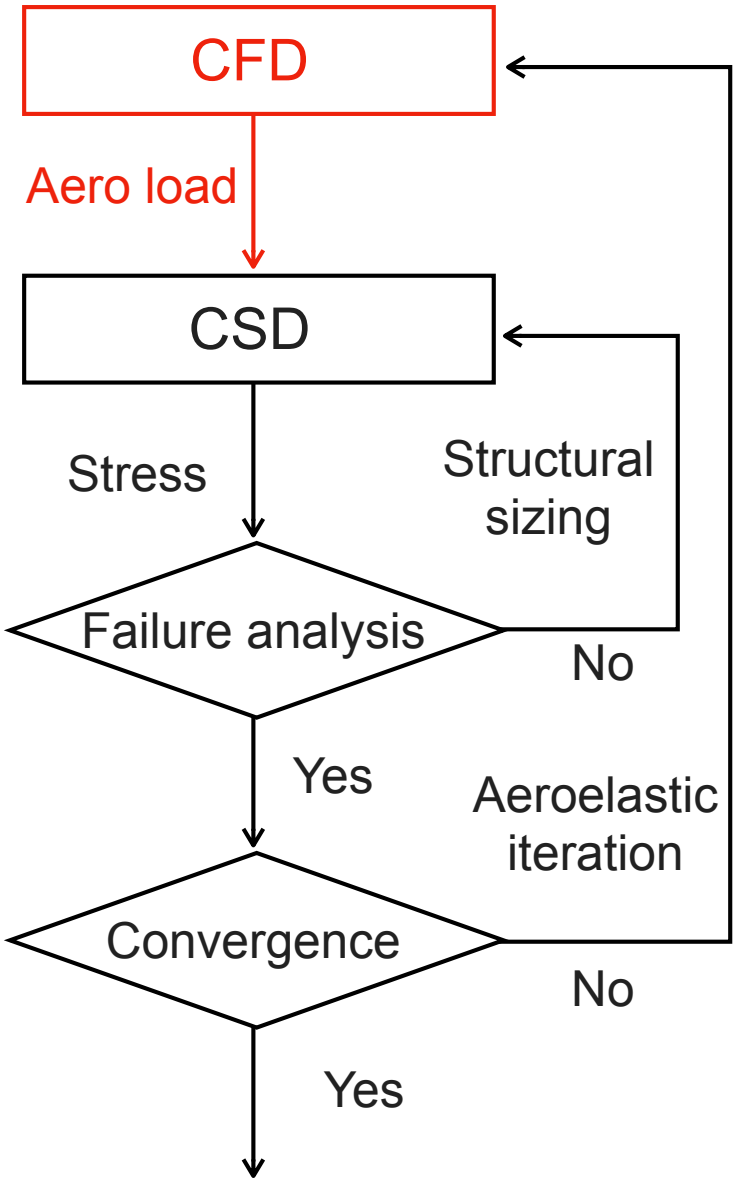


OHT

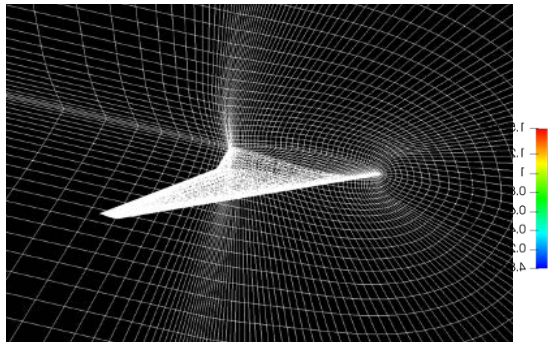
- Failure of 0° plies (Weibull criterion)

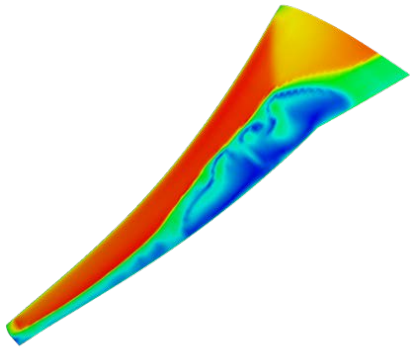


Macroscale Analysis for Aircraft Design



CFD





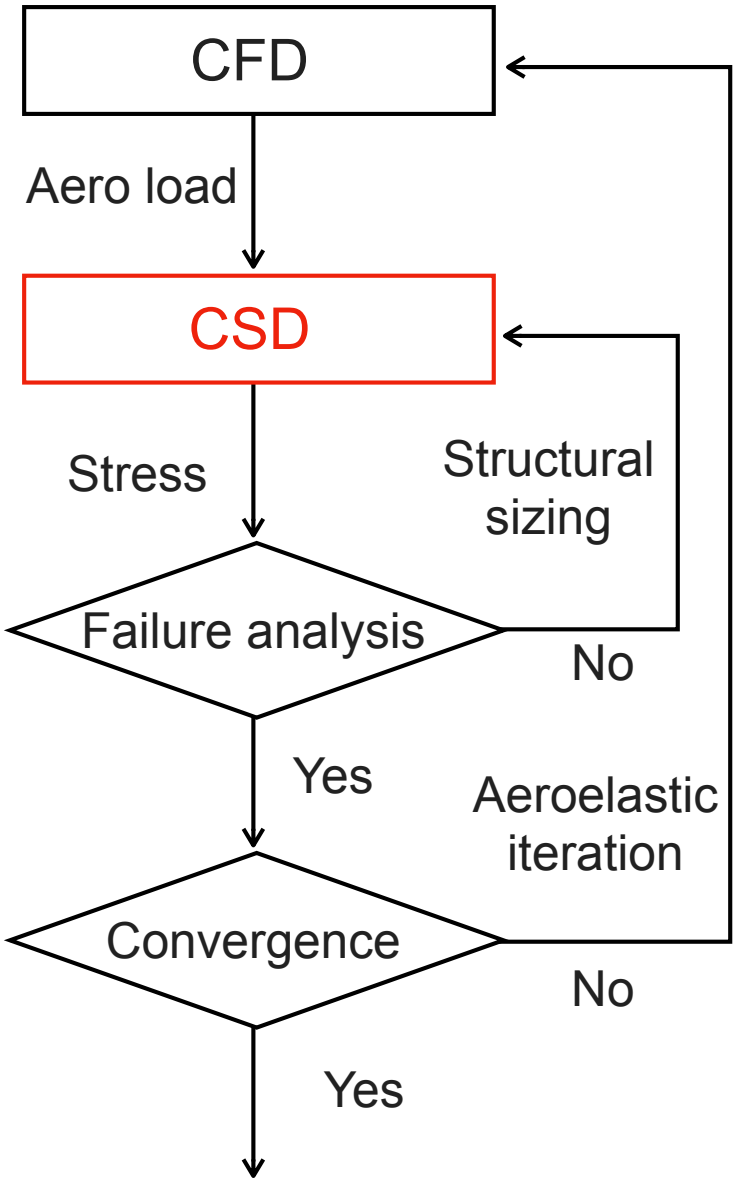
Governing eq.	Compressible Euler
Discretization	2nd-order MUSCL
Inviscid flux	SHUS

Load transfer

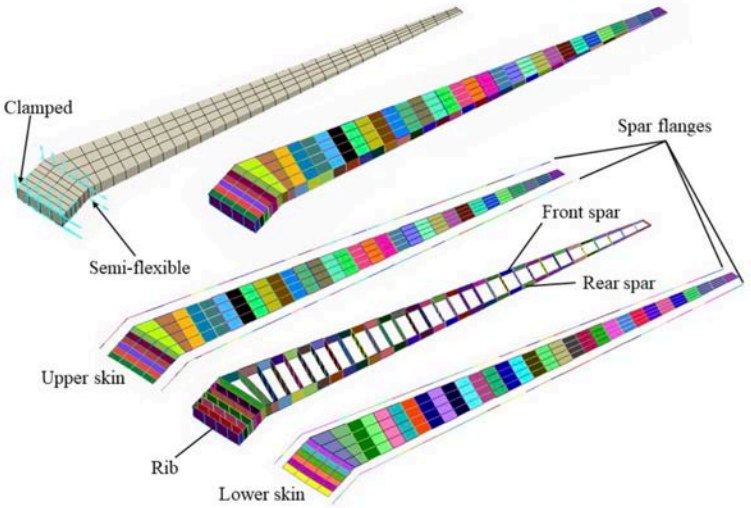
RBF (Radial basis function) based transfer between nonconforming meshes

$$\boldsymbol{f}_{\mathrm{st}}^{(\mathrm{n}+1)} = \mathbf{M}^{T} \boldsymbol{f}_{\mathrm{aero}}^{(\mathrm{n})}$$

Macroscale Analysis for Aircraft Design

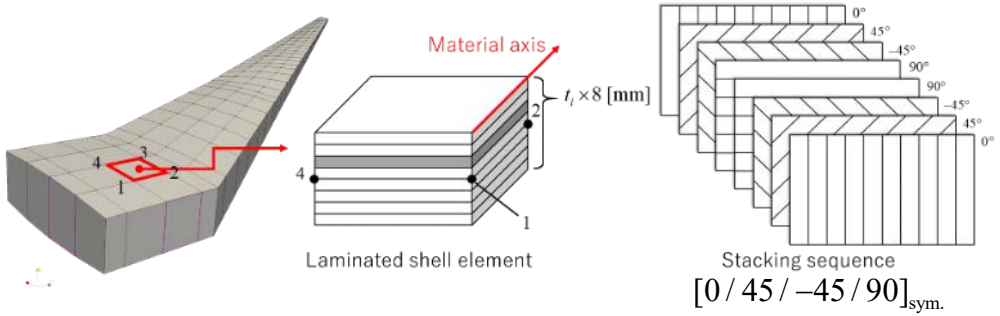


CSD

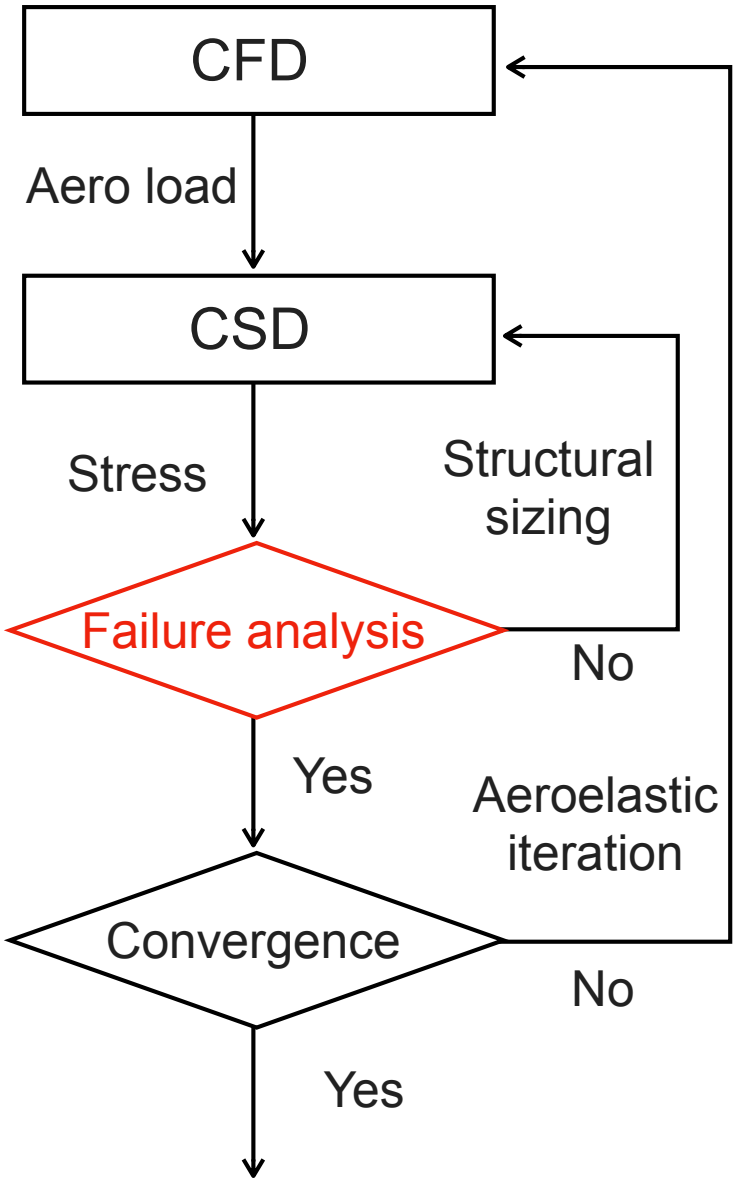


FEM: static analysis (geometrically linear/nonlinear)

Skin, Spar webs, Ribs	MITC4 Shell	Uni-directional lamina
Spar flanges	Rod element	Qusi-iso. lamina



Macroscale Analysis for Aircraft Design



- Failure analysis for shell element

Local Buckling failure criteria

Axial buckling & Shear buckling

$$F_{shell}^{buckling} = \begin{cases} \dfrac{|\sigma_{11}|}{\sigma_{cr}^{axial}} \le 1 & (axial\ bucking) \\ \dfrac{|\sigma_{12}|}{\sigma_{cr}^{shear}} \le 1 & (shear\ buckling) \end{cases}$$

Strength failure criteria (Christensen criteria)

Fiber dominant failure & matrix dominant failure

$$F_{shell}^{strength} = \begin{cases} \left(\dfrac{\sigma_{11}}{T_{11}} - \dfrac{\sigma_{11}}{C_{11}}\right) + \dfrac{\sigma_{11}^2}{T_{11}C_{11}} - \dfrac{1}{4}\left(\dfrac{1}{T_{11}} + \dfrac{1}{C_{11}}\right)^2 \sigma_{11}\sigma_{12} \le 1 & (Fiber\ dominant) \\ \left(\dfrac{1}{T_{22}} - \dfrac{1}{C_{22}}\right)\sigma_{22} + \dfrac{\sigma_{22}^2}{T_{22}C_{22}} + \dfrac{\sigma_{12}^2}{S_{12}^2} \le 1 & (Matrix\ dominant) \end{cases}$$

- Failure analysis for rod element

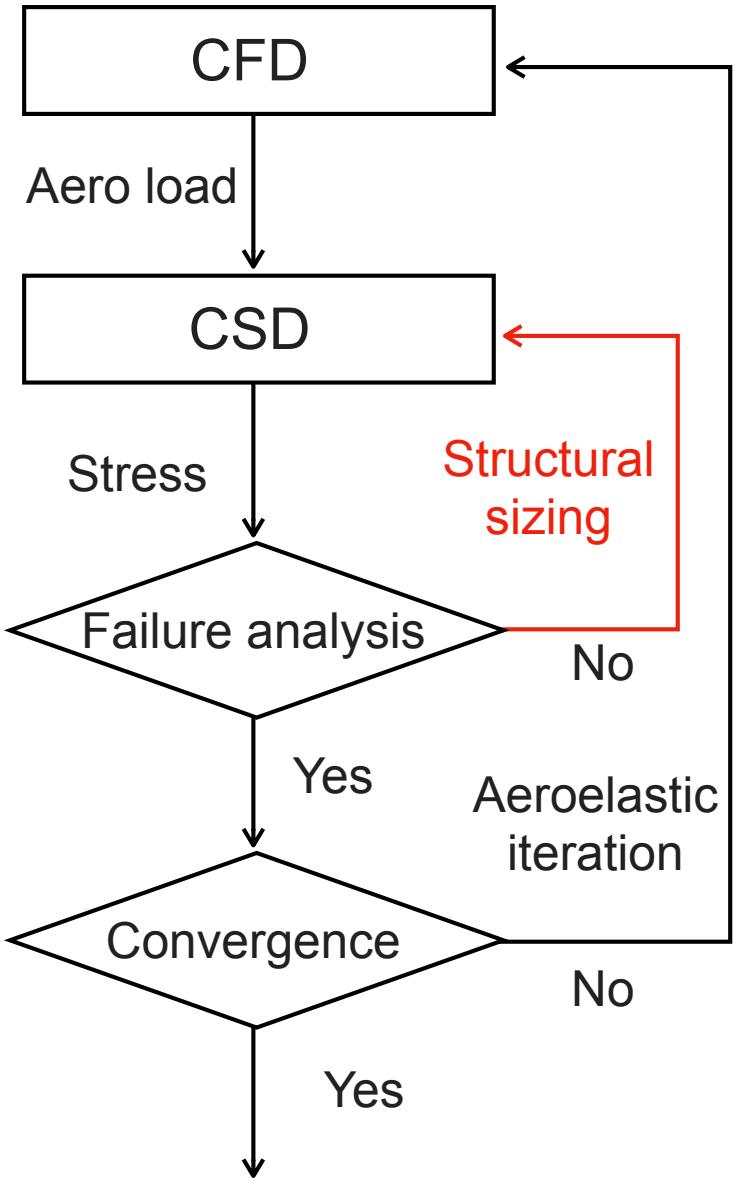
Local Buckling failure criteria (Johnson-Euler buckling criterion)

$$F_{rod}^{buckling} = \frac{|\sigma|}{\sigma_{cr}} \le 1 \qquad \sigma_{cr} = \begin{cases} C\left(1 - \dfrac{C}{4\pi^2 E}\left(\dfrac{l}{r}\right)^2\right), & \left(\dfrac{l}{r}\right) \le \sqrt{\dfrac{2\pi^2 E}{C}} \quad (Johnson\ buckling) \\ \pi^2 E\left(\dfrac{r}{l}\right)^2, & \left(\dfrac{l}{r}\right) > \sqrt{\dfrac{2\pi^2 E}{C}} \quad (Euler\ buckling) \end{cases}$$

Strength failure criteria

$$F_{rod}^{strength} = max\left\{\frac{\sigma}{T}, -\frac{\sigma}{C}\right\} \le 1$$

Macroscale Analysis for Aircraft Design



Structural sizing

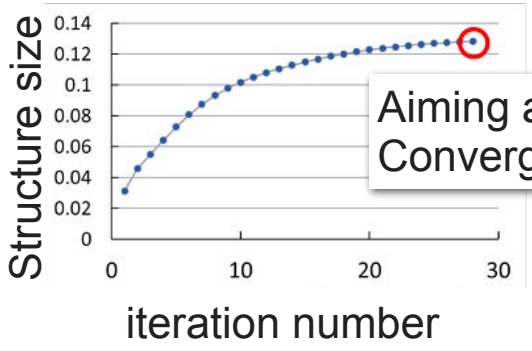
Margin of safety (M.S.)

$$M.S. = \frac{\sigma_{\mathrm{cr}}}{\sigma} - 1 \qquad \sigma_{\mathrm{cr}}: \text{Critical stress (strength)}$$

Fully stressed design (Lansing 1971)

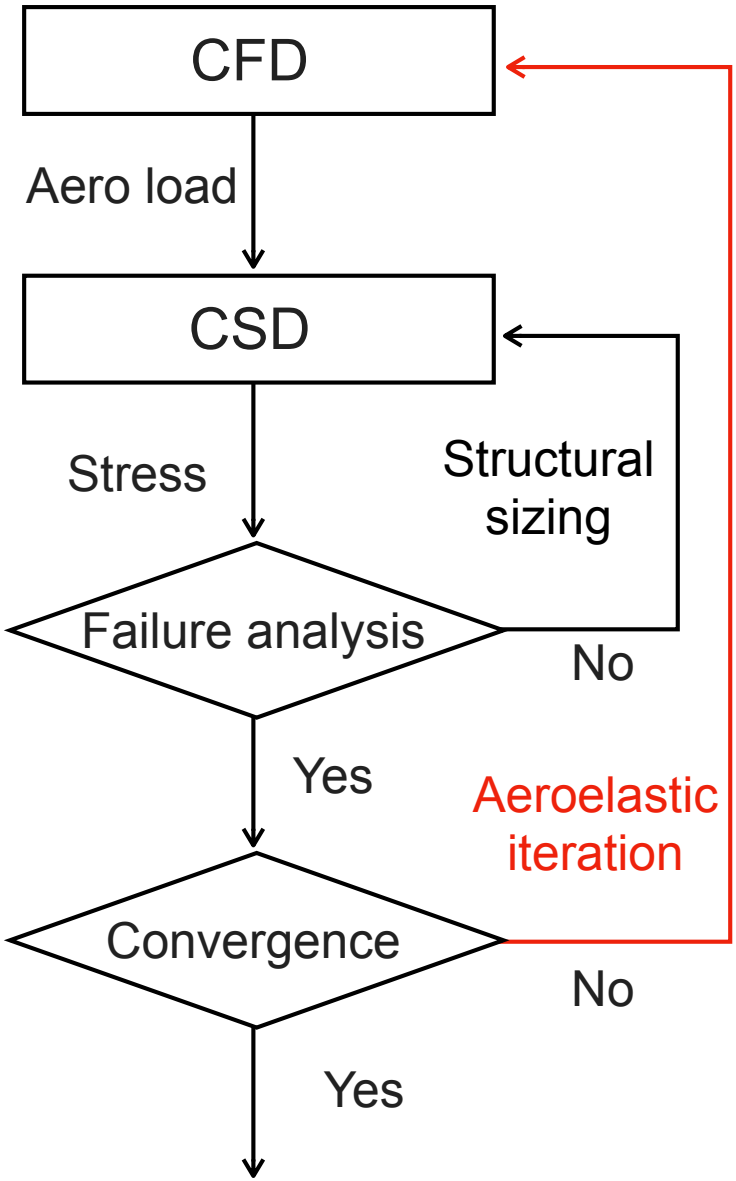
$$g_{i+1}^{k} = g_{i}^{k}\left(\frac{1.05\sigma_{i}^{k}}{\sigma_{\mathrm{cr}}}\right)^{\beta}$$

g : structure size (e.g., thickness)
i : iteration number
β : 0.33 for shell
0.5 for rod



Aiming at M.S. = 0.05,
Convergence if 0 < M.S. < 0.1

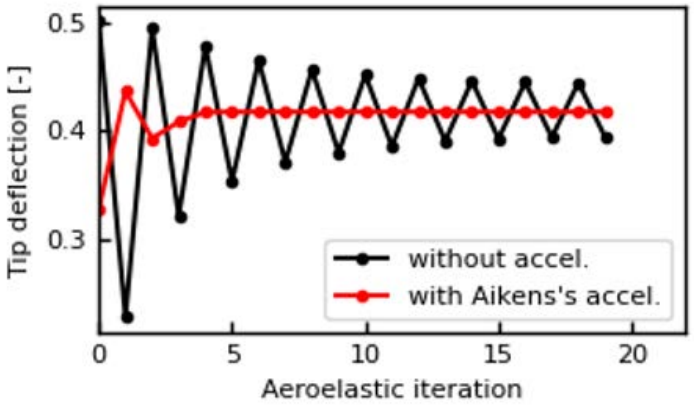
Macroscale Analysis for Aircraft Design



Aeroelastic iteration

Update structural deformation

Aitken's relaxation: $\boldsymbol{u}_{\mathrm{st}}^{(n)} = \theta^{(n)} \tilde{\boldsymbol{u}}_{\mathrm{st}}^{(n)} + (1-\theta^{(n)}) \boldsymbol{u}_{\mathrm{st}}^{(n-1)}$



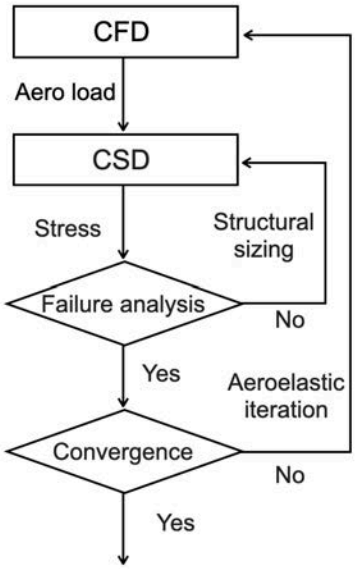
Transfer deformation to aero mesh

RBF (Radial basis function) based transfer between nonconforming meshes

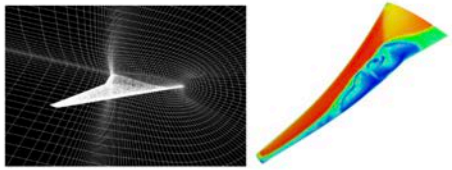
$$\boldsymbol{u}_{\mathrm{aero}}^{(\mathrm{n+1})} = \mathbf{M}\boldsymbol{u}_{\mathrm{st}}^{(\mathrm{n})}$$

Macroscale Analysis for Aircraft Design

Macroscale analysis (structural sizing with static aeroelastic iteration)



CFD



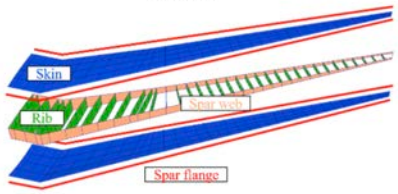
Governing eq.	Euler / RANS
Discretization	2nd-order MUSCL
Inviscid flux	SHUS

Load transfer

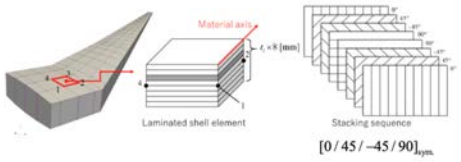
RBF (Radial basis function) based transfer between nonconforming meshes

$$\boldsymbol{f}_{\mathrm{st}}^{(\mathrm{n+1})} = \mathbf{M}^{T} \boldsymbol{f}_{\mathrm{aero}}^{(\mathrm{n})}$$

CSD



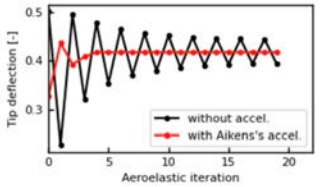
FEM: linear static analysis	
Skin, Spar webs, Ribs	Shell element
Spar flanges	Rod element



Aeroelastic iteration

Update structural deformation

Aitken's relaxation: $\boldsymbol{u}_{\mathrm{st}}^{(n)} = \theta^{(n)} \tilde{\boldsymbol{u}}_{\mathrm{st}}^{(n)} + (1-\theta^{(n)}) \boldsymbol{u}_{\mathrm{st}}^{(n-1)}$



Transfer deformation to aero mesh

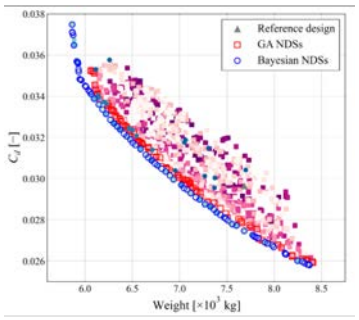
RBF (Radial basis function) based transfer between nonconforming meshes

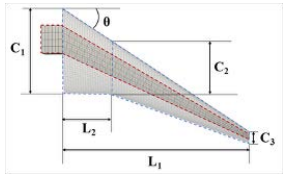
$$\boldsymbol{u}_{\mathrm{aero}}^{(\mathrm{n+1})} = \mathbf{M} \boldsymbol{u}_{\mathrm{st}}^{(\mathrm{n})}$$

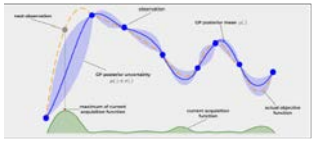
Key technologies for macroscale analysis

Multi-objective optimization

Bayesian optimization / Genetic algorithm







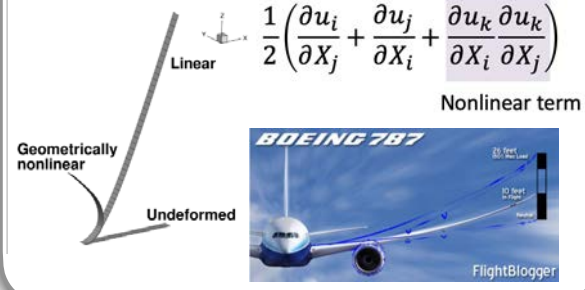
Geometrical nonlinear FEM

Large deformation for CFRP

Green-Lagrange strain tensor

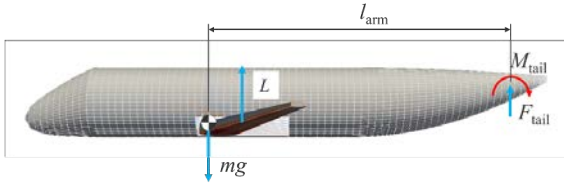
$$\frac{1}{2}\left(\frac{\partial u_i}{\partial X_j} + \frac{\partial u_j}{\partial X_i} + \frac{\partial u_k}{\partial X_i}\frac{\partial u_k}{\partial X_j}\right)$$

Nonlinear term



Inertia relief analysis

Equilibrium for lift/drag/inertia force

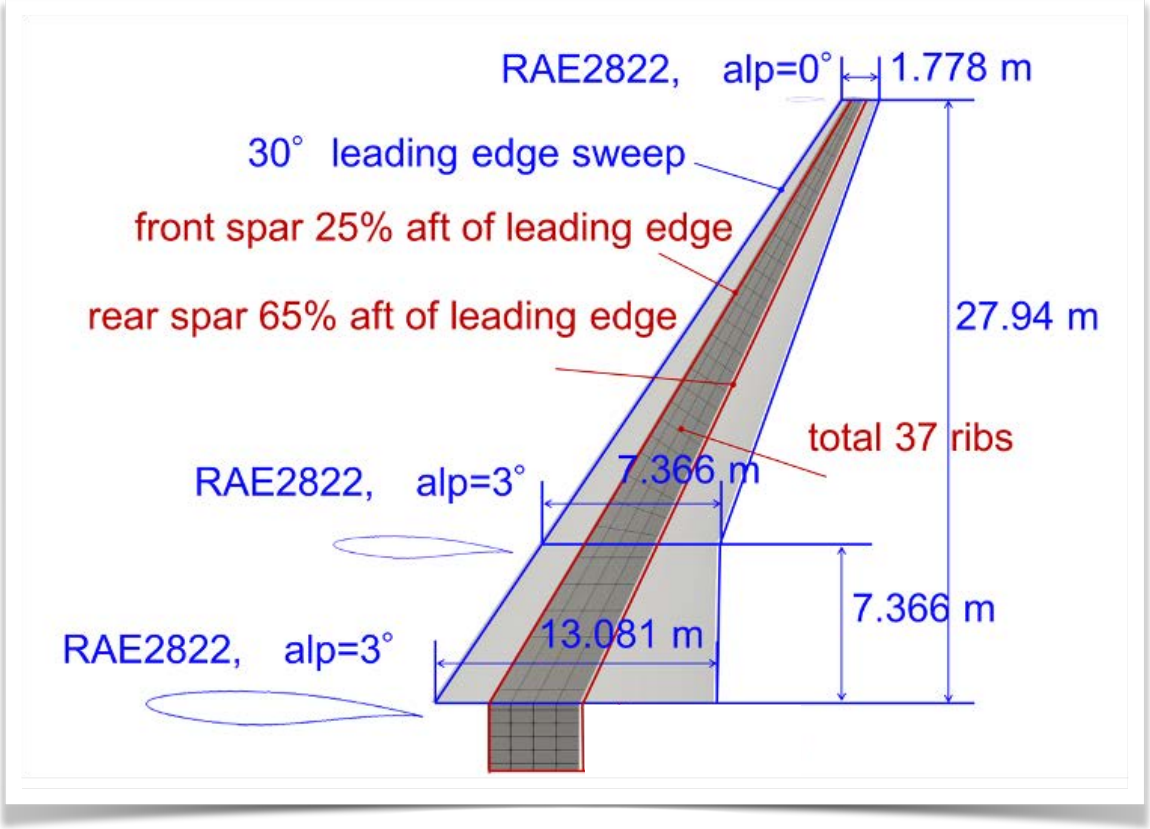


$$\boldsymbol{KU} = \boldsymbol{F} - \boldsymbol{MT}\left(\boldsymbol{T}^{\mathrm{T}}\boldsymbol{MT}\right)^{-1}\boldsymbol{T}^{\mathrm{T}}\boldsymbol{F}$$

Inertia force

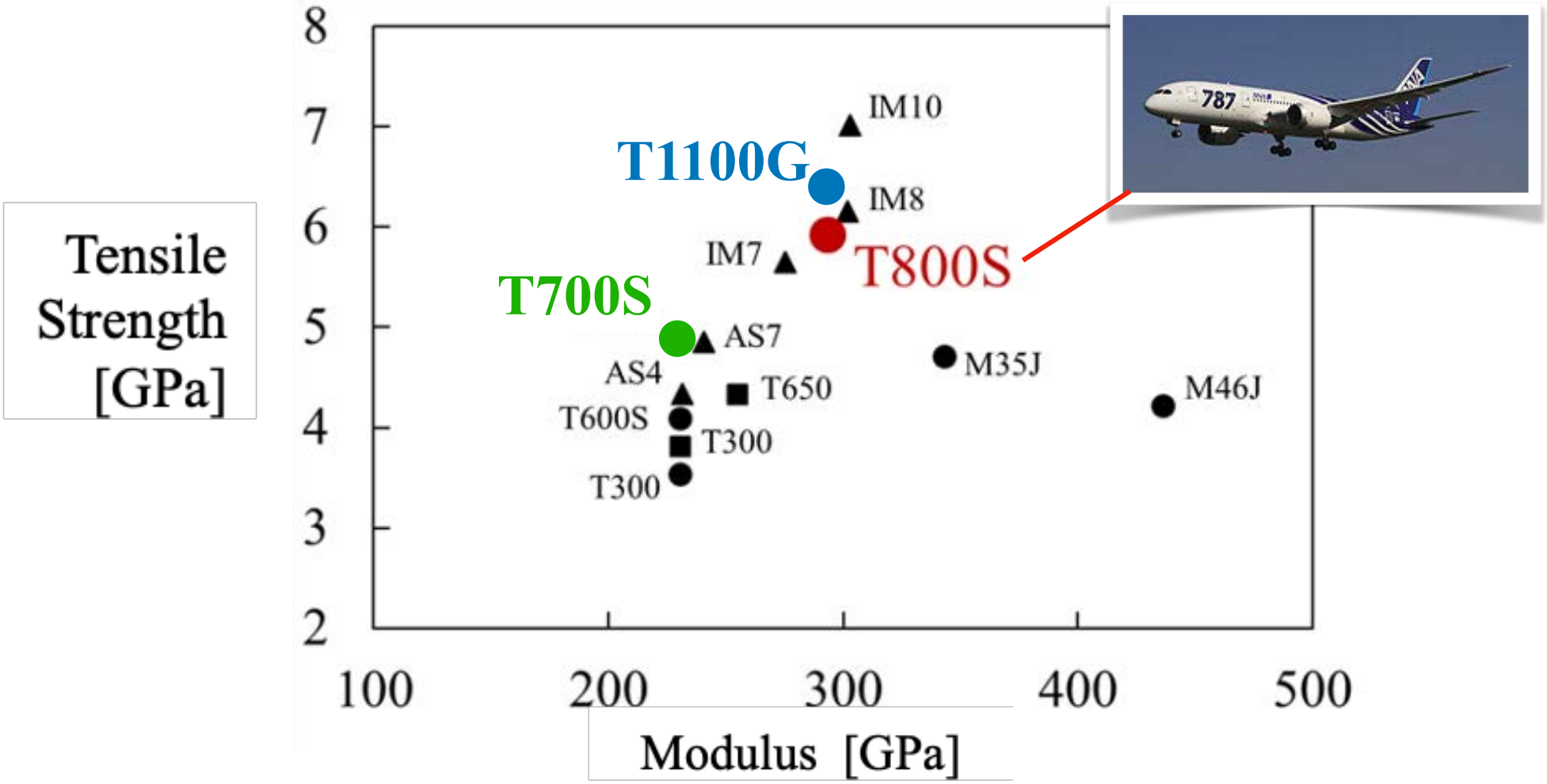
Problem Settings

- Wing geometry and cruise conditions
  - B777-like geometry / RAE2822 airfoil
  - Mach 0.84, Alt. 10,000m
  - 2.5G and -1G condition for structural sizing
  - C_L=0.5 by adjusting the AoA



Problem Settings

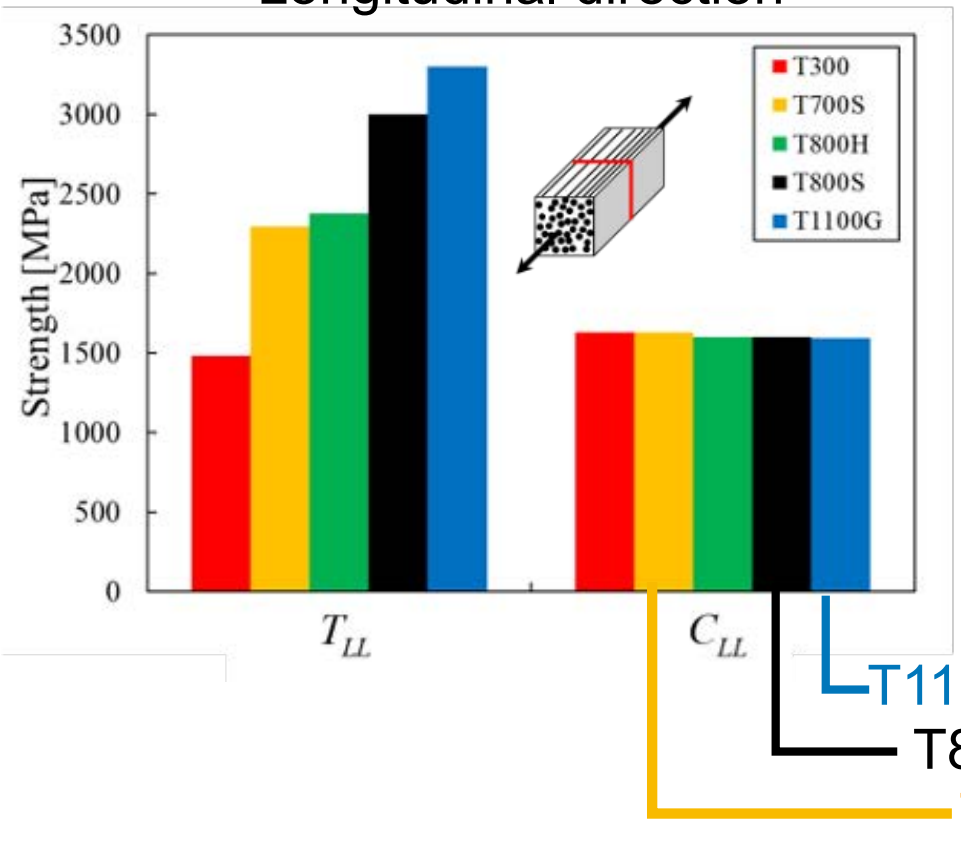
- Fiber and matrix for CFRP
  - Fibers: T700S, T800S, T1100G
  - Matrix: #3900-2B



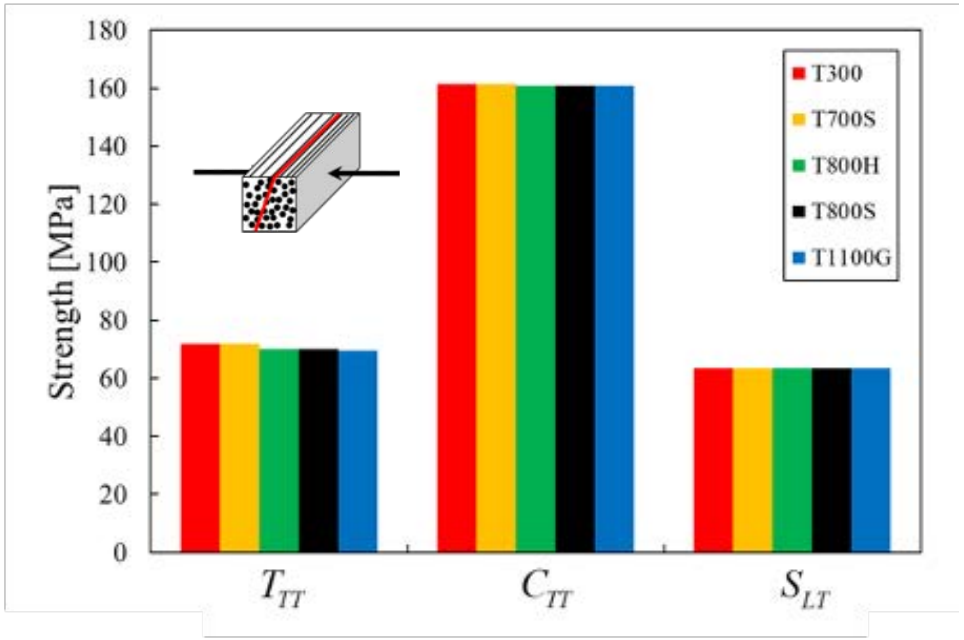
Results of microscale analysis

- Summary of strength for different fibers

Longitudinal direction



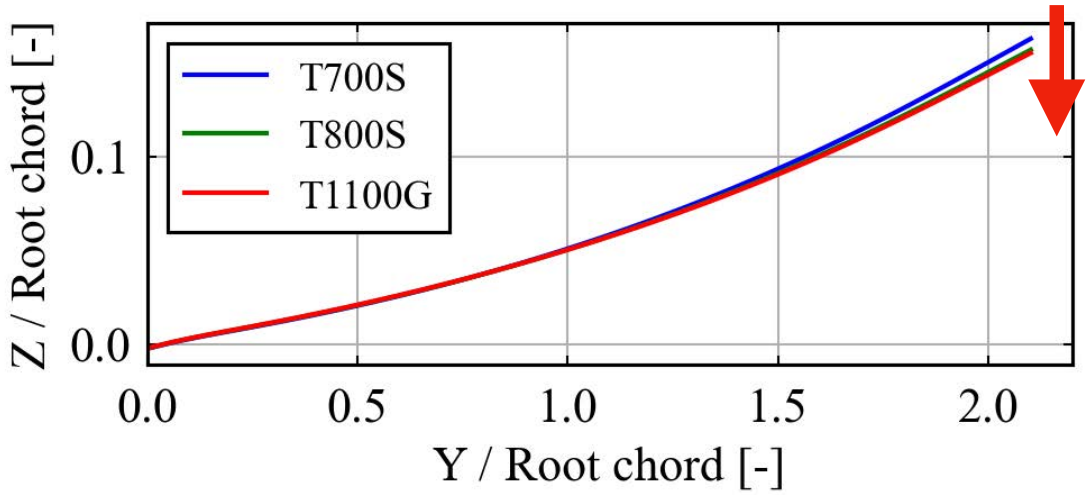
Transverse direction



- Tensile strength in longitudinal direction is different while others not.

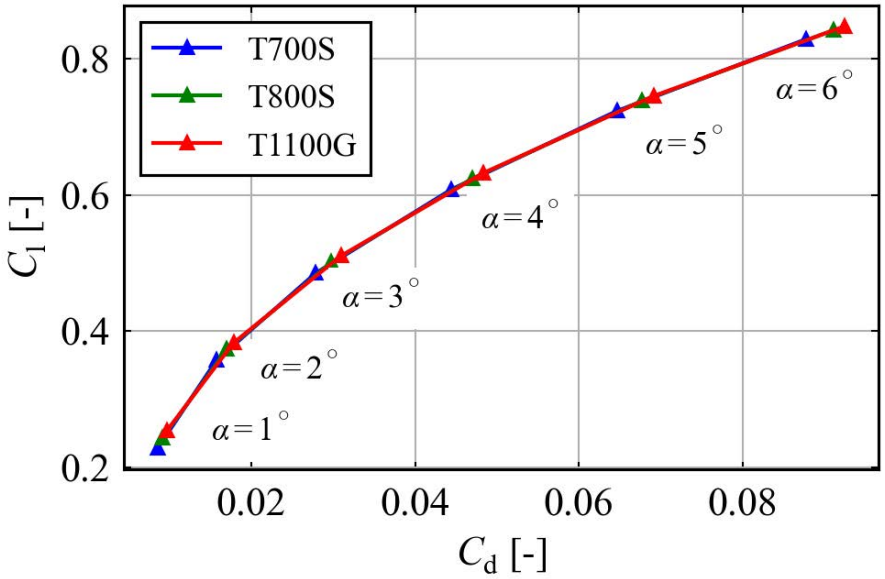
Deformation and aerodynamic performance

- Leading-edge deformation under C_L=0.5 constraint



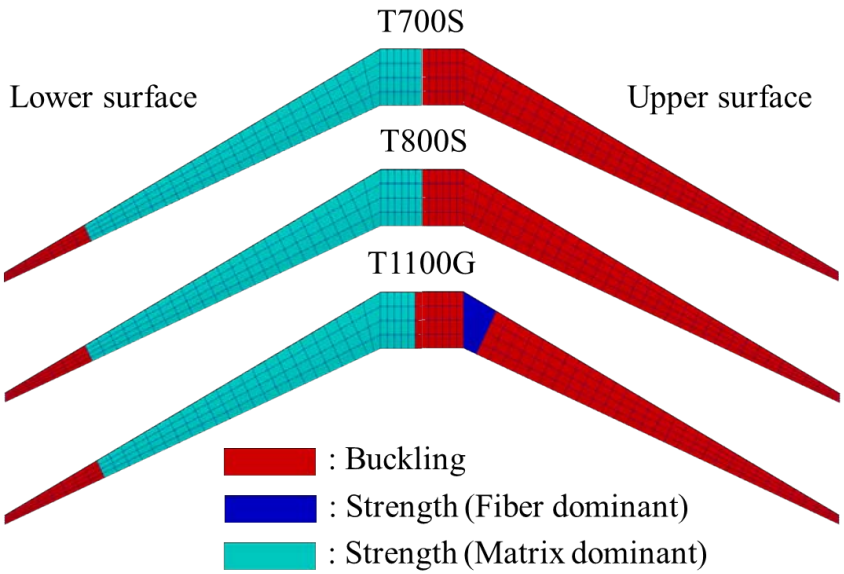
- Stiffer fiber achieves smaller deformation

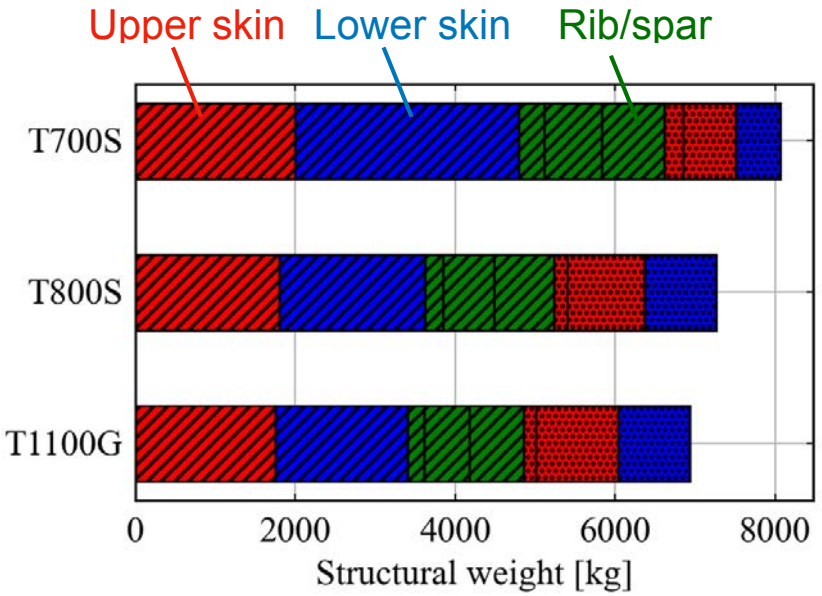
- C_L-C_D curve with various angle of attacks



- Collapsed to the C_L-C_D single curve
- Stiffer fiber achieves lower AoA under the same C_L

Failure modes and structural weight

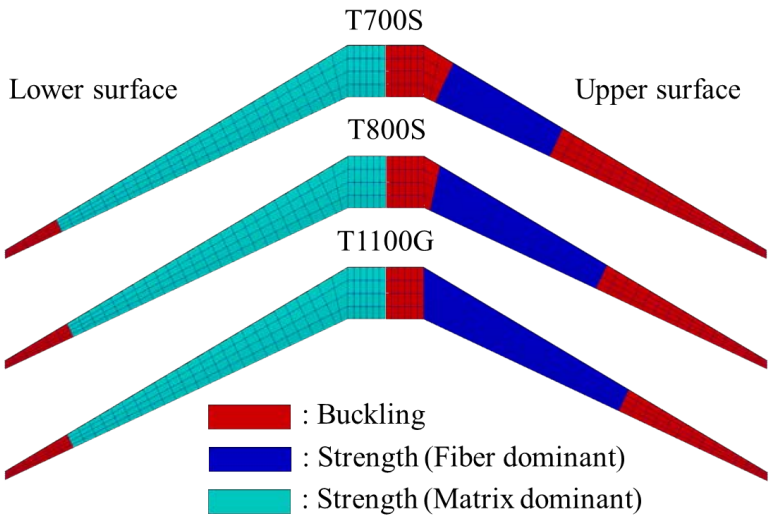


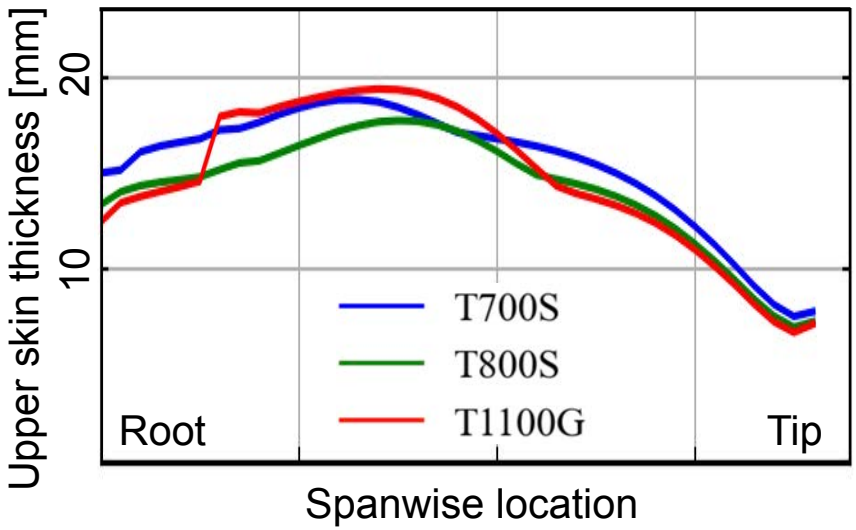


- The upper skin (shell element) is dominated by a buckling failure
- The lower skin is dominated by a matrix failure
- T1100G structure leads to the lightest wingbox structure

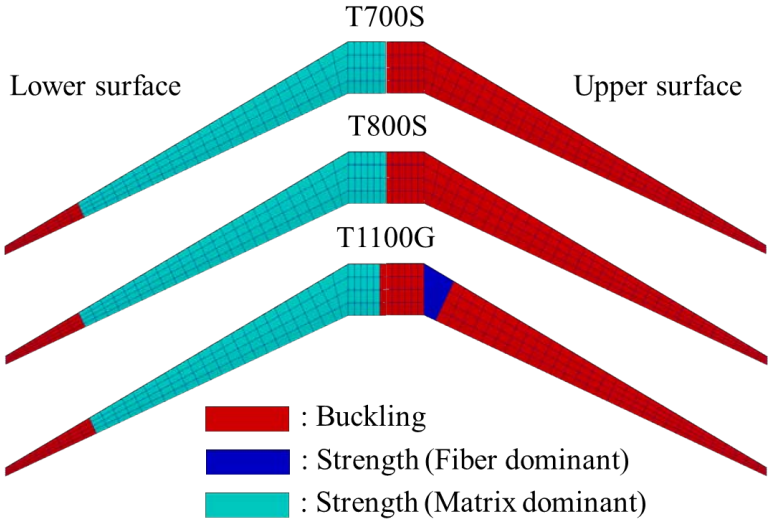
Failure modes and structural weight

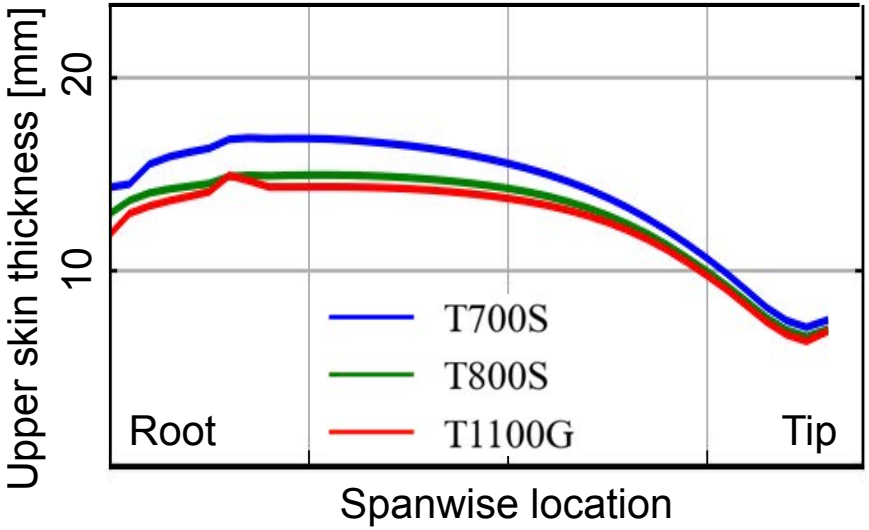
One-way (CFD → CSD)





Two-way (CFD ⇄ CSD)

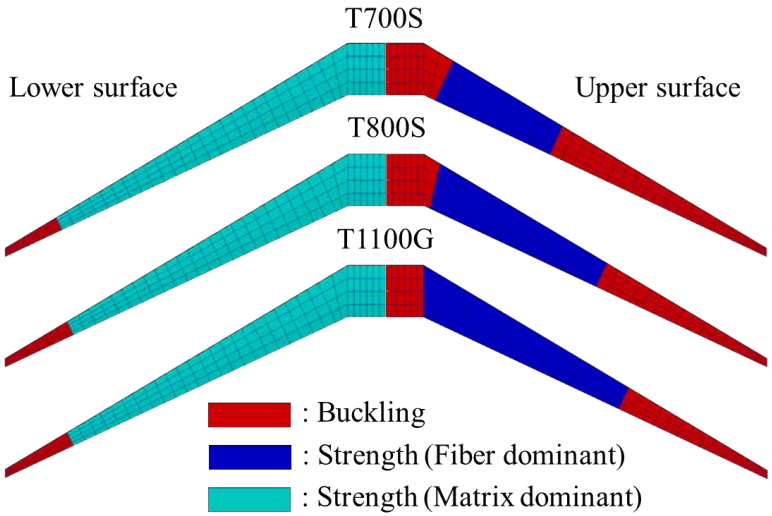


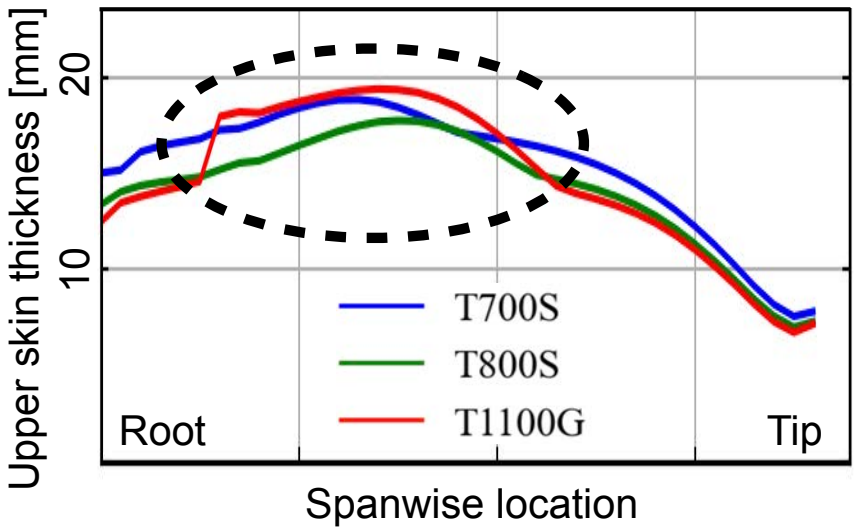


- Failure mode cannot be accurately captured by one-way coupled analysis

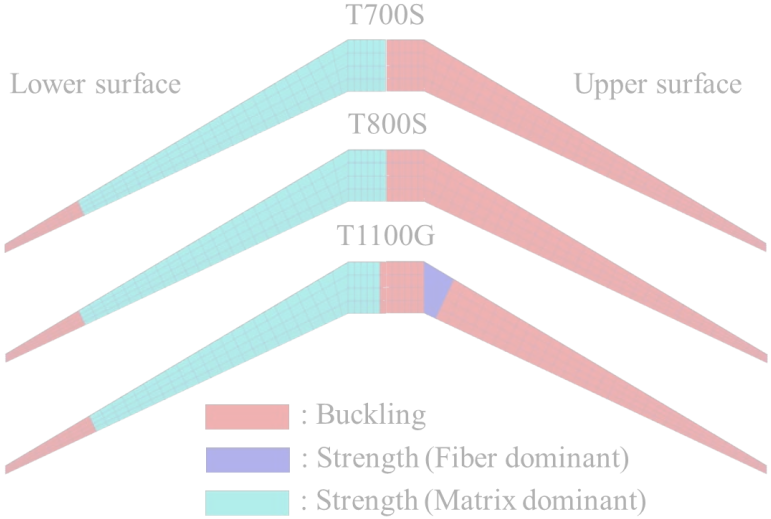
Failure modes and structural weight

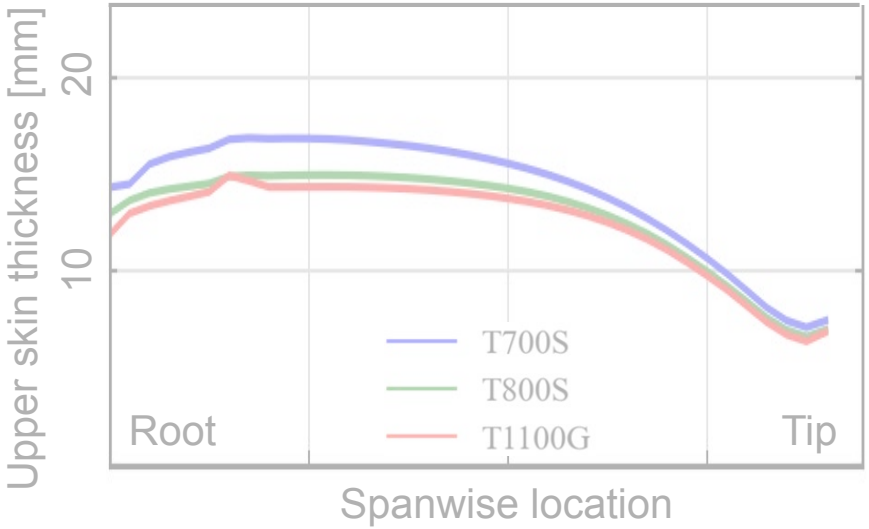
One-way (CFD → CSD)





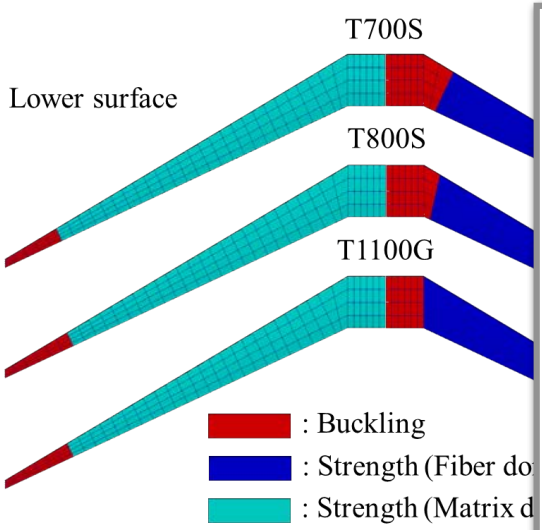
Two-way (CFD ⇄ CSD)





Failure modes and structural weight

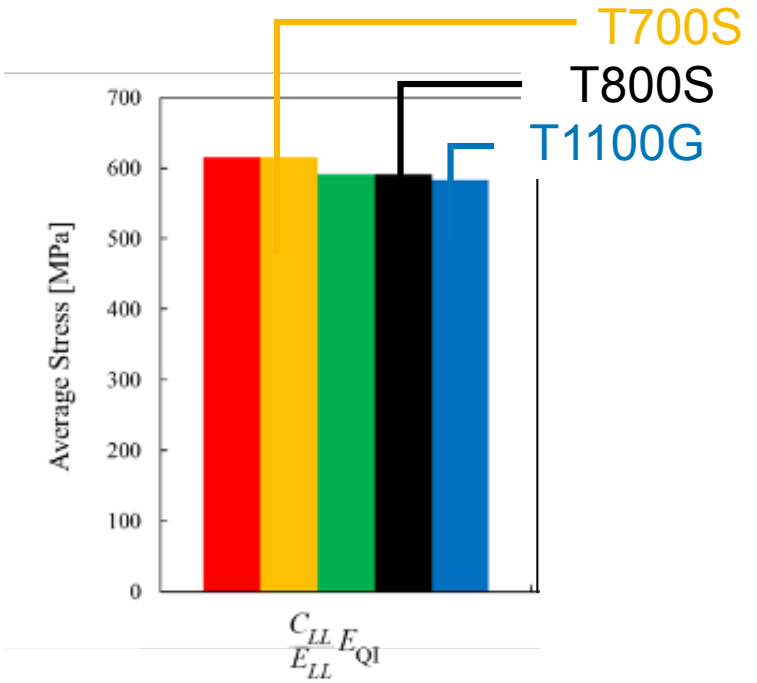
One-way (CFD → CSD)

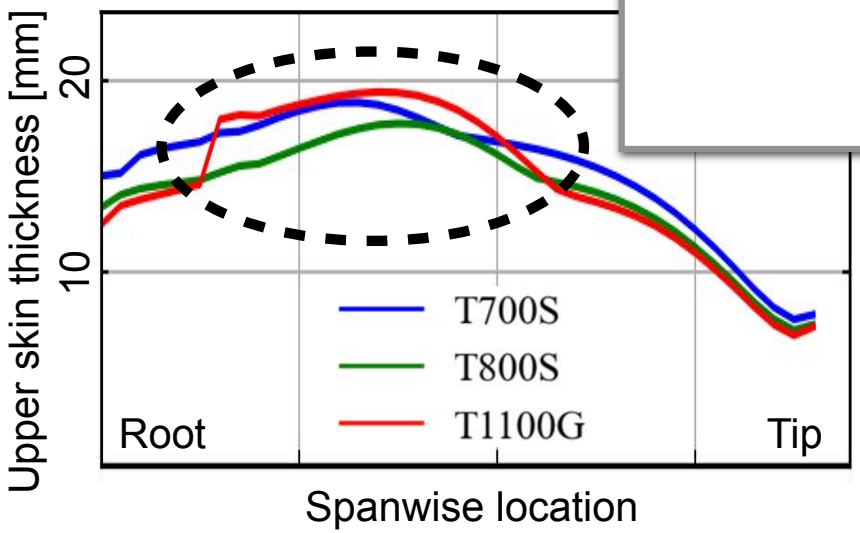


T1100G ≒ T800S ≒ T700S

$$C_{\mathrm{QI}} = \overbrace{C_{LL}}\,\underbrace{\frac{E_{\mathrm{QI}}}{E^{c}_{LL}}}$$

T1100G < T800S < T700S

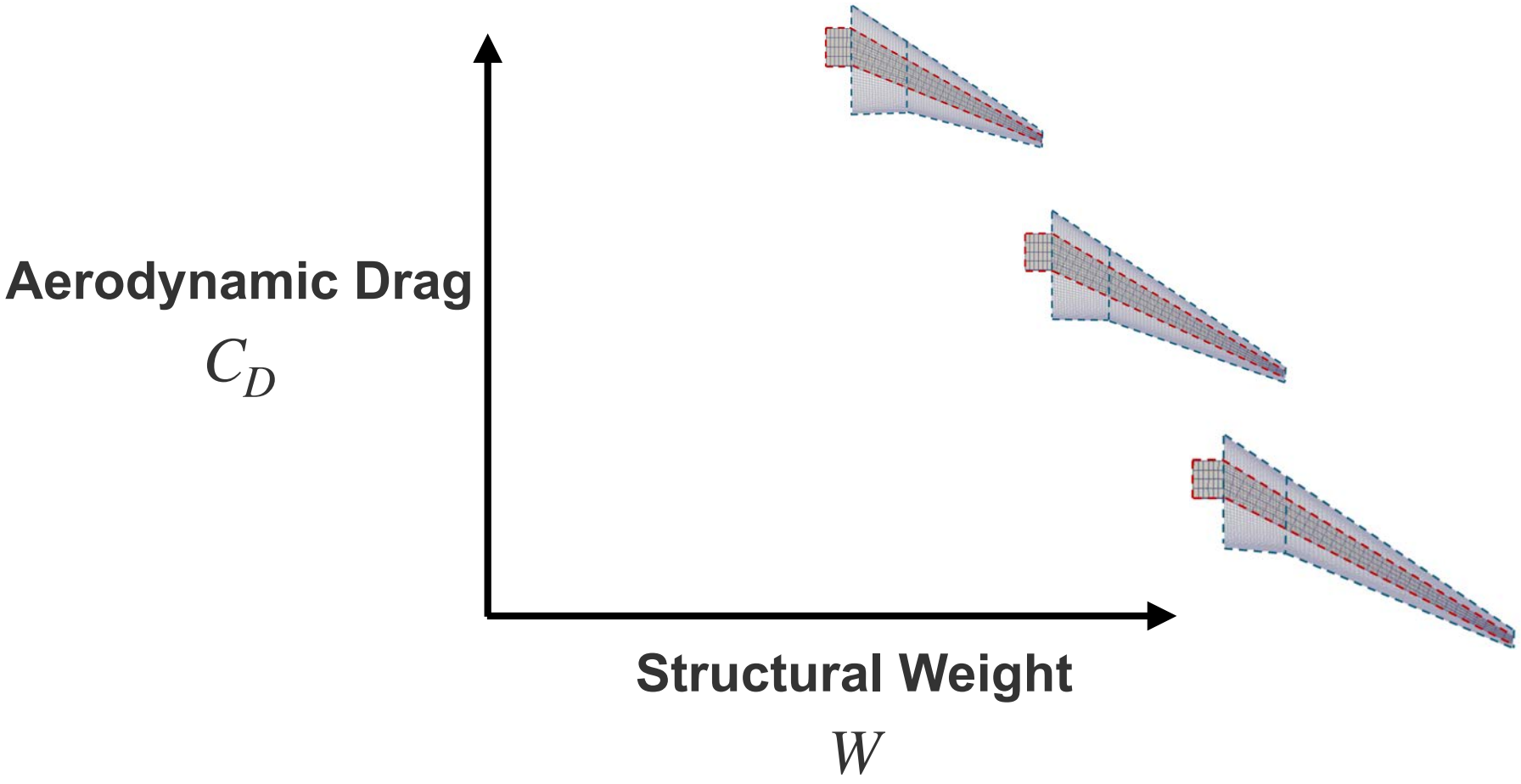




- Although the stiffness of the fibers is T1100G > T800S > T700S, the thickness of the upper skin is T700S < T800S < T1100G
- This is because the compressive strength of the quasi-isotropic laminates decreases as the stiffness of the fiber increases

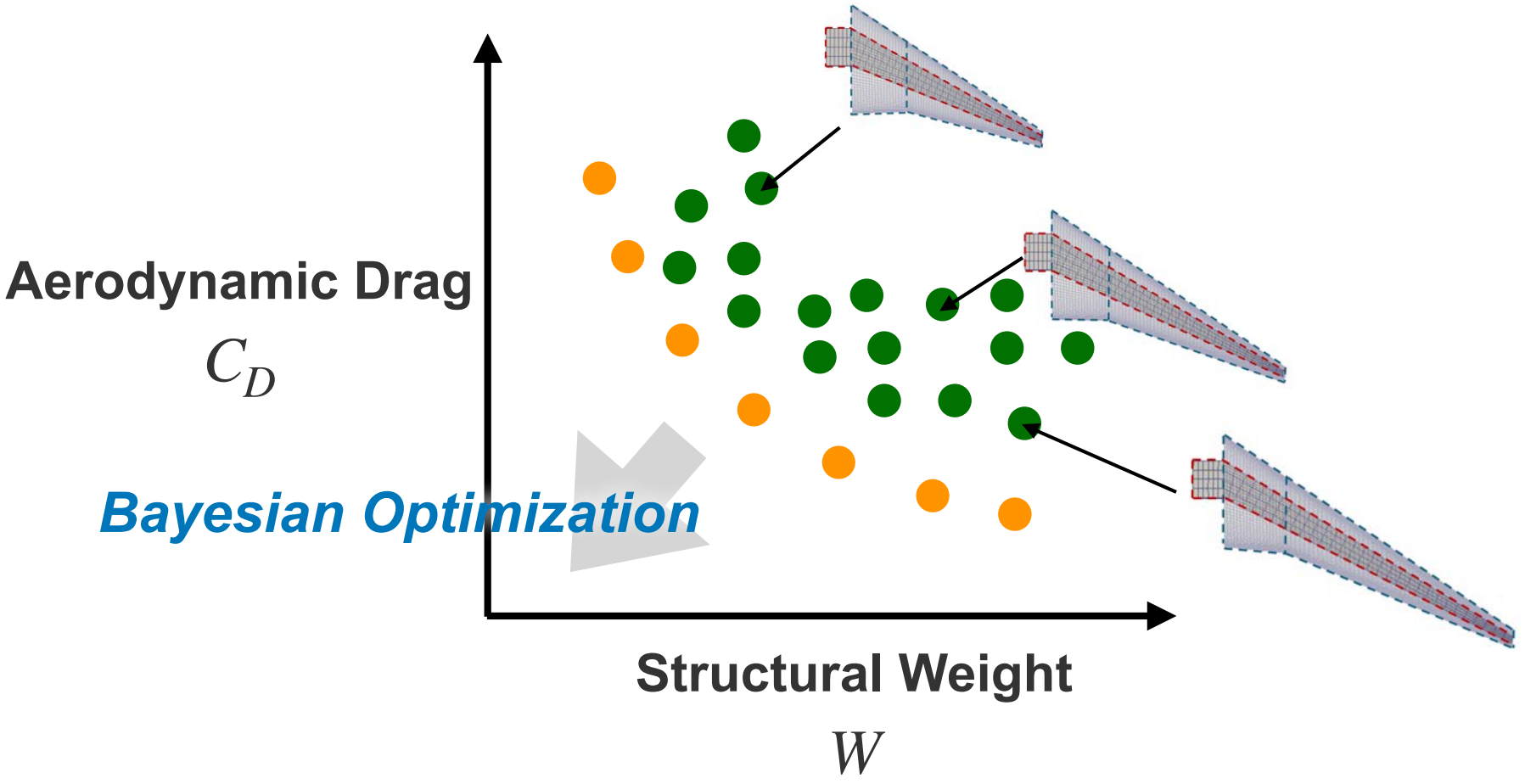
Difficulty in Aircraft Wing Design

Objectives: Decrease structural weight / Decrease aerodynamic drag — **Trade-off**

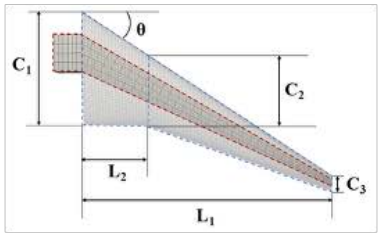


Difficulty in Aircraft Wing Design

Objectives: Decrease structural weight / Decrease aerodynamic drag — **Trade-off**



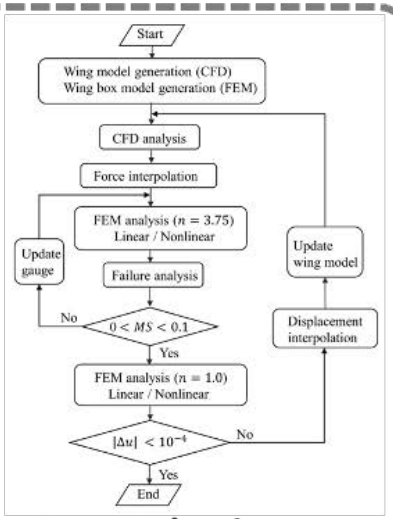
Multi-objective Optimization



$$\boldsymbol{x} = \begin{Bmatrix} \theta \\ C_1 \\ C_2 \\ C_3 \\ L_2 \end{Bmatrix}$$

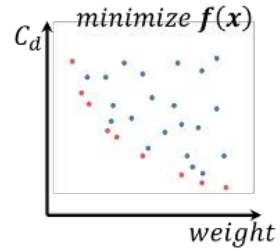
Design Variables

Input



True Evaluation

Output

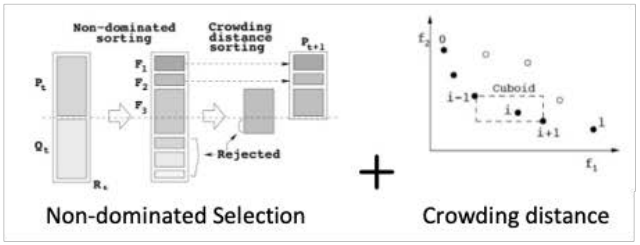


$$\boldsymbol{f}(\boldsymbol{x}) = \begin{Bmatrix} f_1(\boldsymbol{x}) \\ f_2(\boldsymbol{x}) \end{Bmatrix} = \begin{Bmatrix} weight(\boldsymbol{x}) \\ C_d(\boldsymbol{x}) \end{Bmatrix}$$

Objective Functions

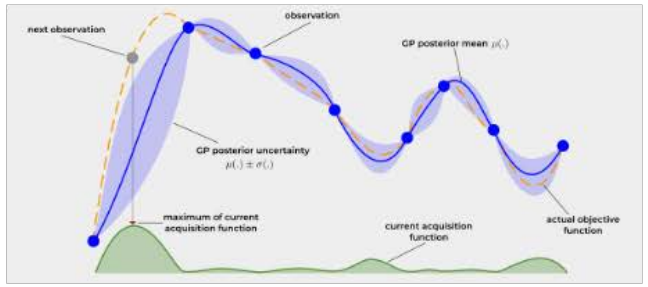
Genetic Algorithm (NSGA-II) [1]

Selection Crossover Mutation



Bayesian Optimization [2]

Surrogate model (Kriging)



/https://firasalhafez.com/2021/05/12/finding-the-optimal-learning-rate-using-bayesian-optimization

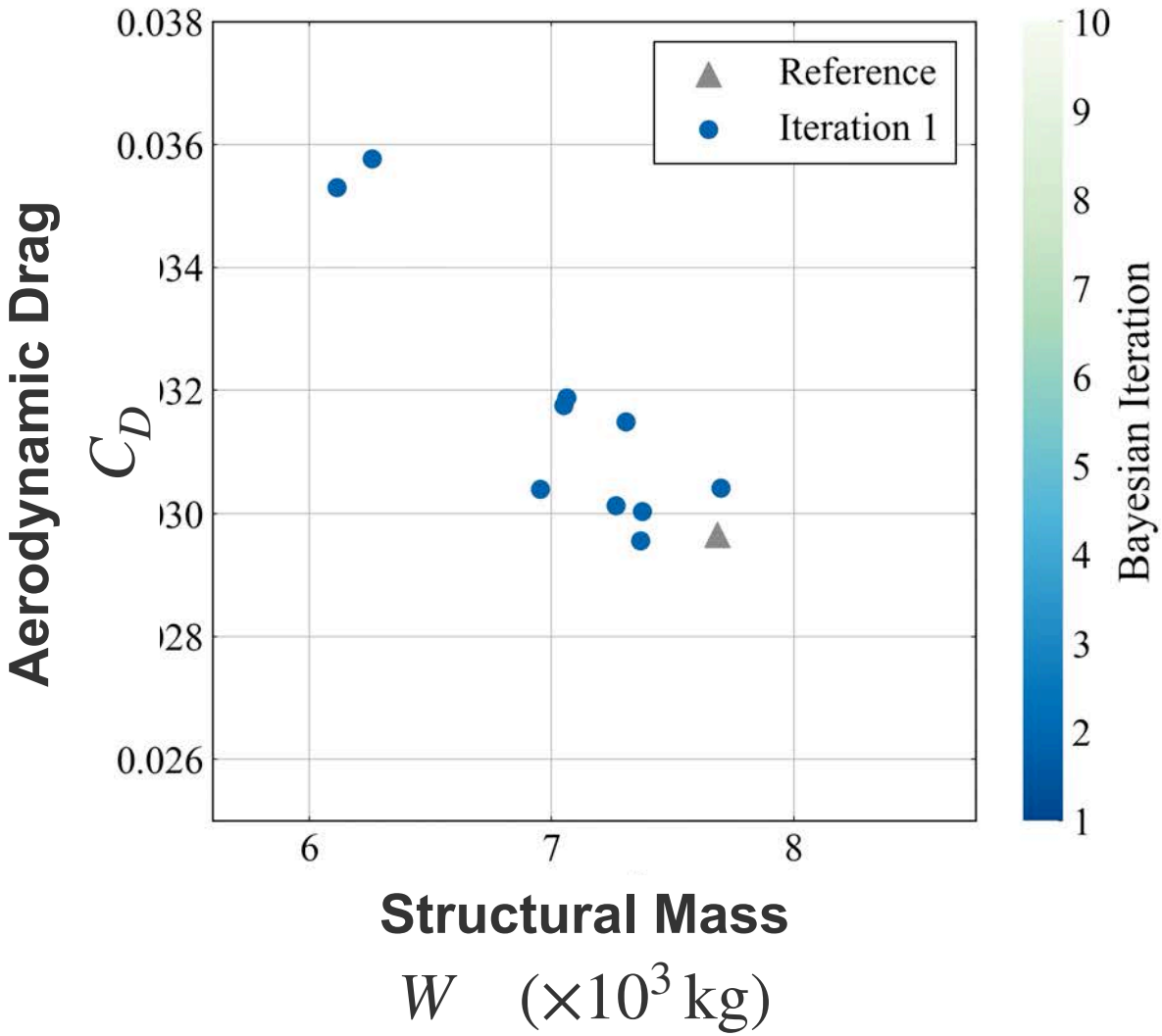
Multi-objective optimization strategies

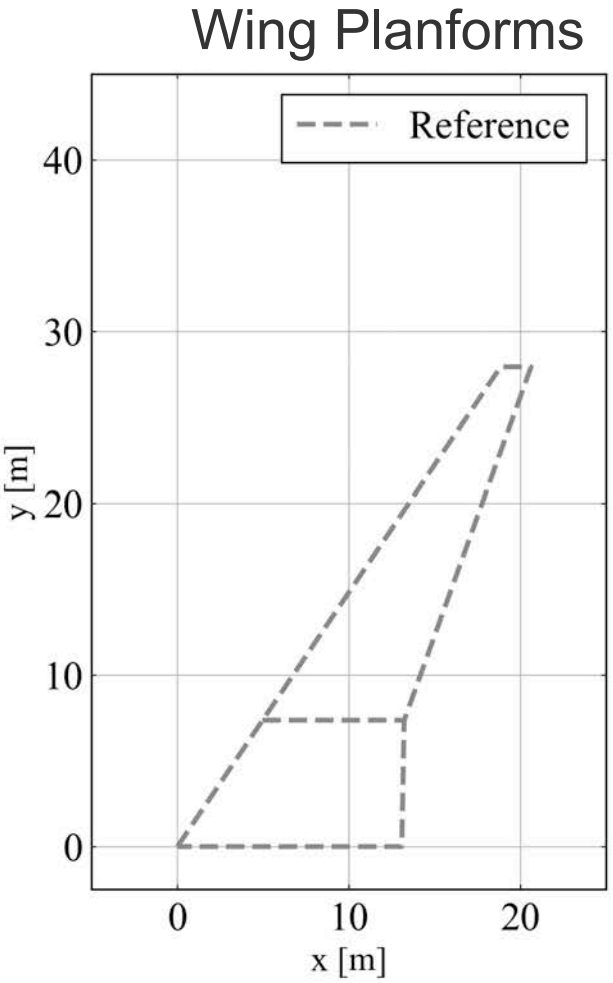
- quantify the trade-off between different objectives
- provides a set of designs (**Pareto set**) rather than a single design

[1] Kalyanmoy Deb, et al. IEEE-TEC. 2002
[2] N. Namura, et al. IEEE-TEC. 2017

Multi-objective Optimization

Bayesian Optimization





Multi-objective Optimization

Genetic Algorithm (GA) Optimization

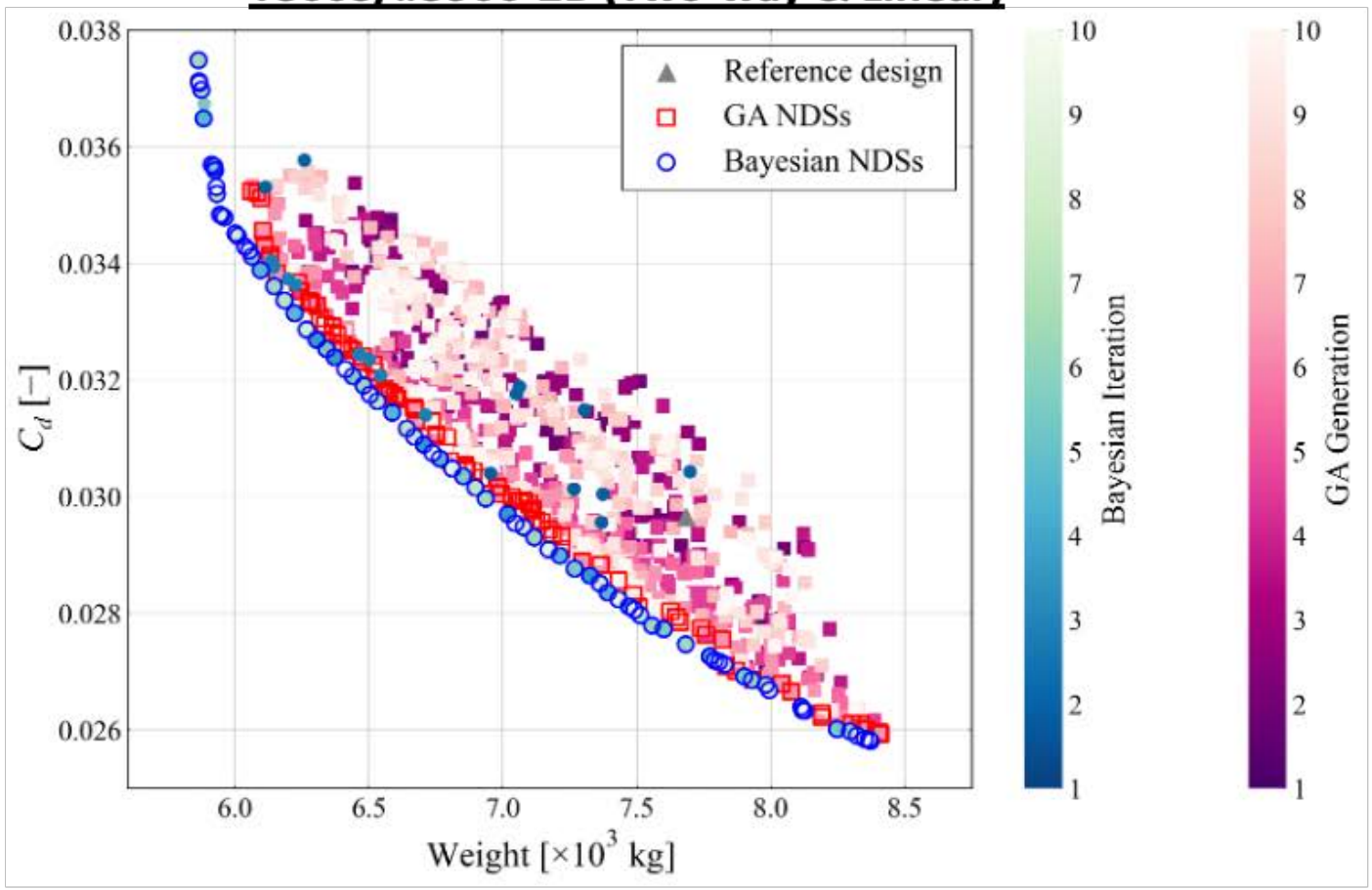
Optimizer : **NSGA-II** [1]
Material : **T800S/#3900-2B**
Population size : **100**
No. of Generation: **10**
No. of total evaluation: **1000**
Probability of crossover : 0.8
Probability of mutation : 0.17

Multi-objective Bayesian Optimization (MBO)

Optimizer : **Bayesian** [2]
Material : **T800S/#3900-2B**
Population size : **10**
No. of Iteration: **10**
No. of total evaluation: **100**
Criteria: EPBII+SRVA
Kernal: Gaussian

Optimization Results

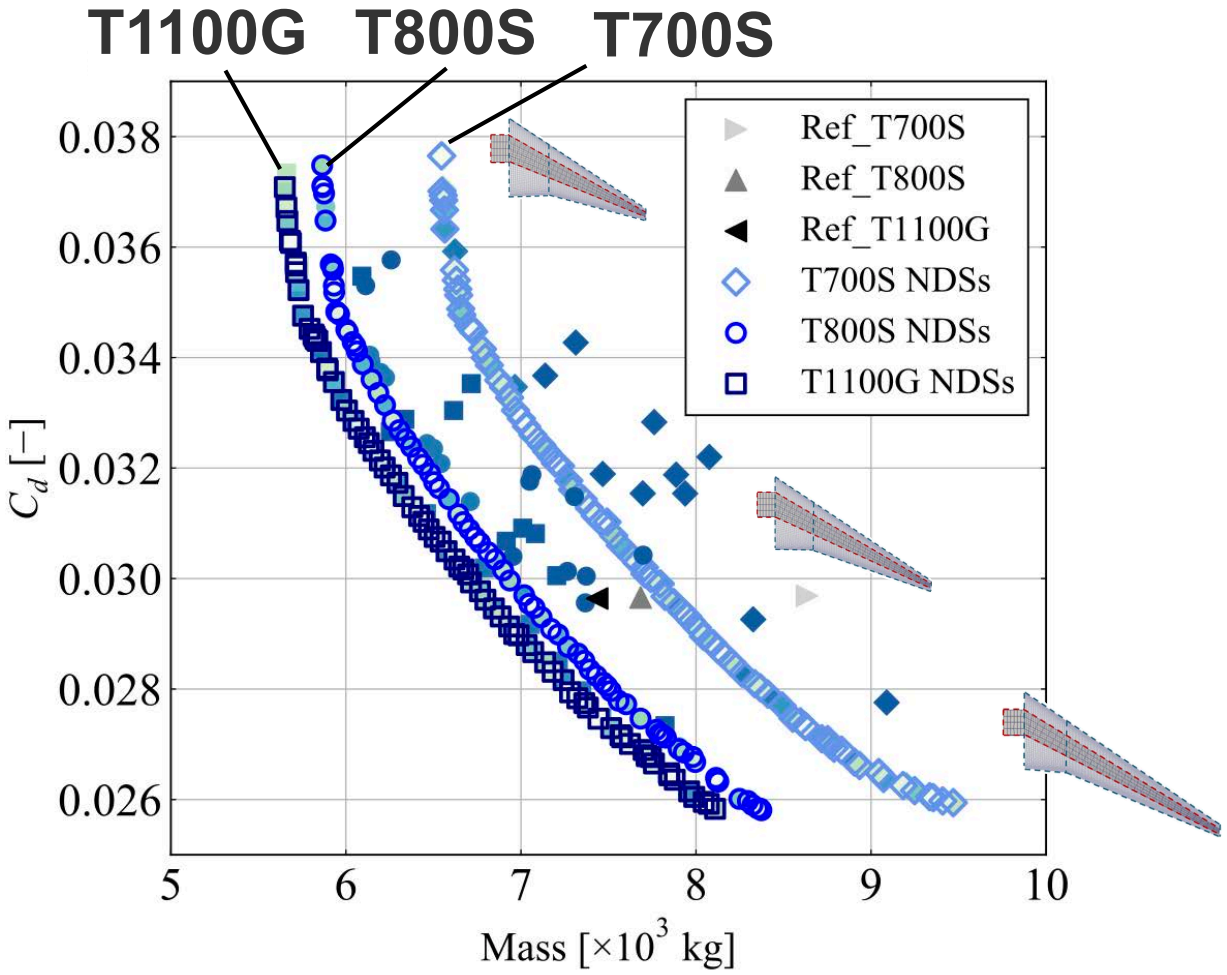
T800S/#3900-2B (Two-way & Linear)



- Bayesian optimization Pareto front is more advanced than that of GA optimization

[1] Kalyanmoy Deb, et al. IEEE-TEC. 2002
[2] N. Namura, et al. IEEE-TEC. 2017

Comparison of fiber properties on design



The Pareto fronts with T700S / T800S / T1100G were compared

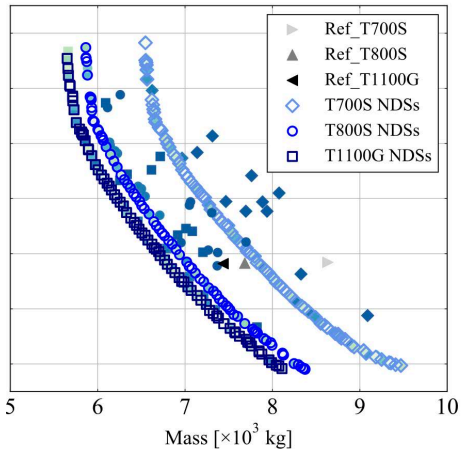
The weights are uniformly shifted over the Pareto front

Comparison of fiber properties on design

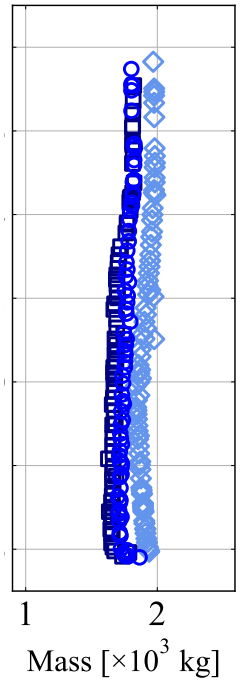


Upper panel　　Lower panel　　Rear spar

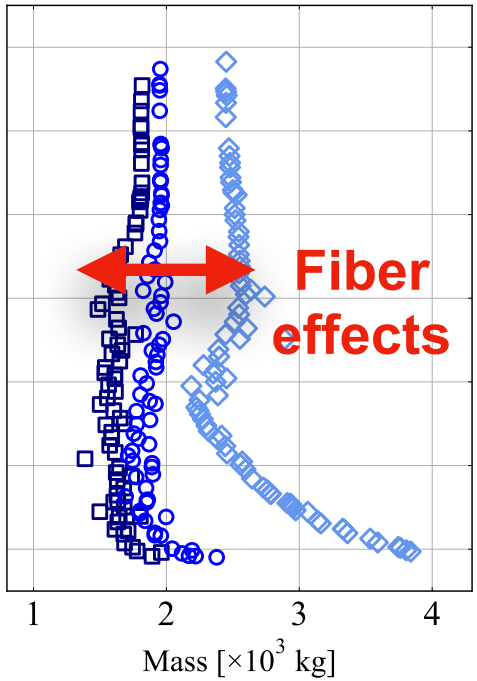
Total weights



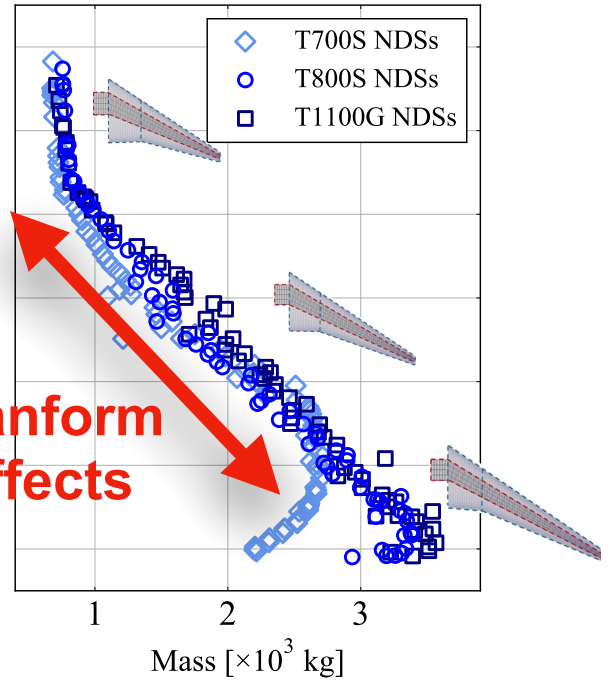
≃



+



+



Component-wise weights are not uniformly in the order of fiber stiffness

Lower panel = fiber effects, but rear spar = planform effects

Geometrical Nonlinearity

Linear solver

- Infinitesimal (Engineering) strain tensor:

$$\varepsilon_{ij} = \frac{1}{2}\left(\frac{\partial u_i}{\partial x_j} + \frac{\partial u_j}{\partial x_i}\right)$$

- Cauchy stress tensor (σ_{ij}):

  True stress relative to the deformed configuration

Geometrical nonlinear solver

(Total Lagrangian formulation)

- Green-Lagrange strain tensor:

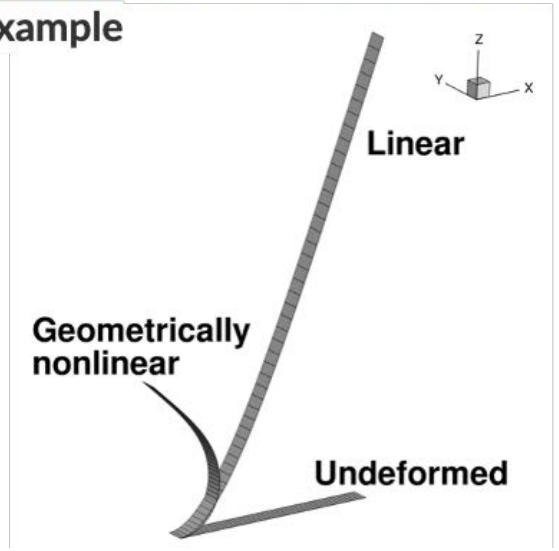
$$E_{ij} = \frac{1}{2}\left(\frac{\partial u_i}{\partial X_j} + \frac{\partial u_j}{\partial X_i} + \frac{\partial u_k}{\partial X_i}\frac{\partial u_k}{\partial X_j}\right)$$

Nonlinear term

- Second Piola-Kirchhoff stress tensor (S_{ij}):

  Stress relative to the reference (initial) configuration (work-conjugate to E_{ij})

Example



A cantilever beam under a uniformly distributed follower pressure load.

Linear:

- Transverse deflection only (no rotational effect)
- Unphysical stretching of the beam

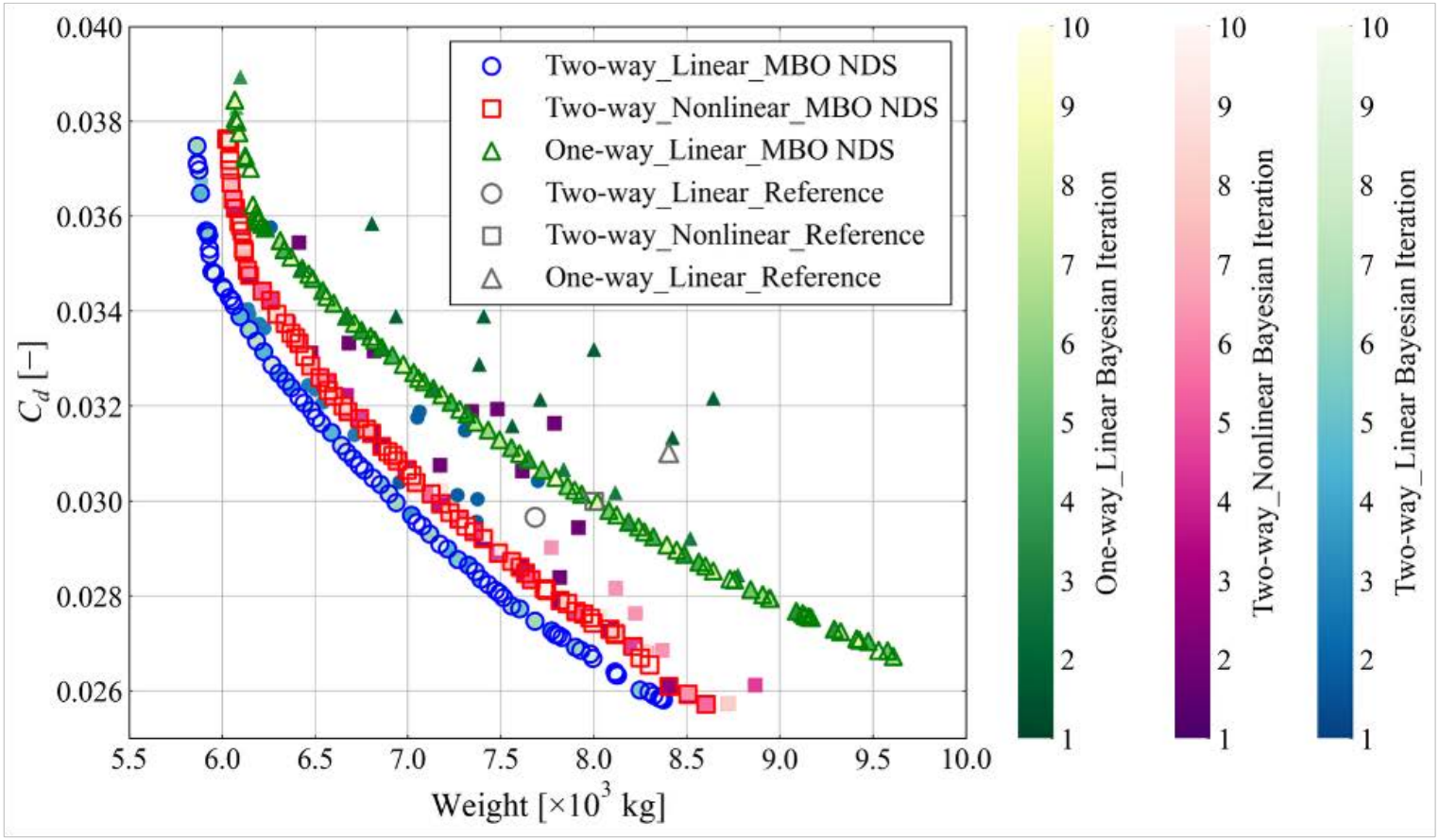
Geometrical nonlinear:

- Bends back on itself as load direction updates
- Correctly retains original length

Source: A. Gray, MSc thesis, University of Michigan, 2020

Aeroelasticity and Geometrical Nonlinearity

Two-way/One-way/Nonlinear/Linear (T800S/#3900-2B)

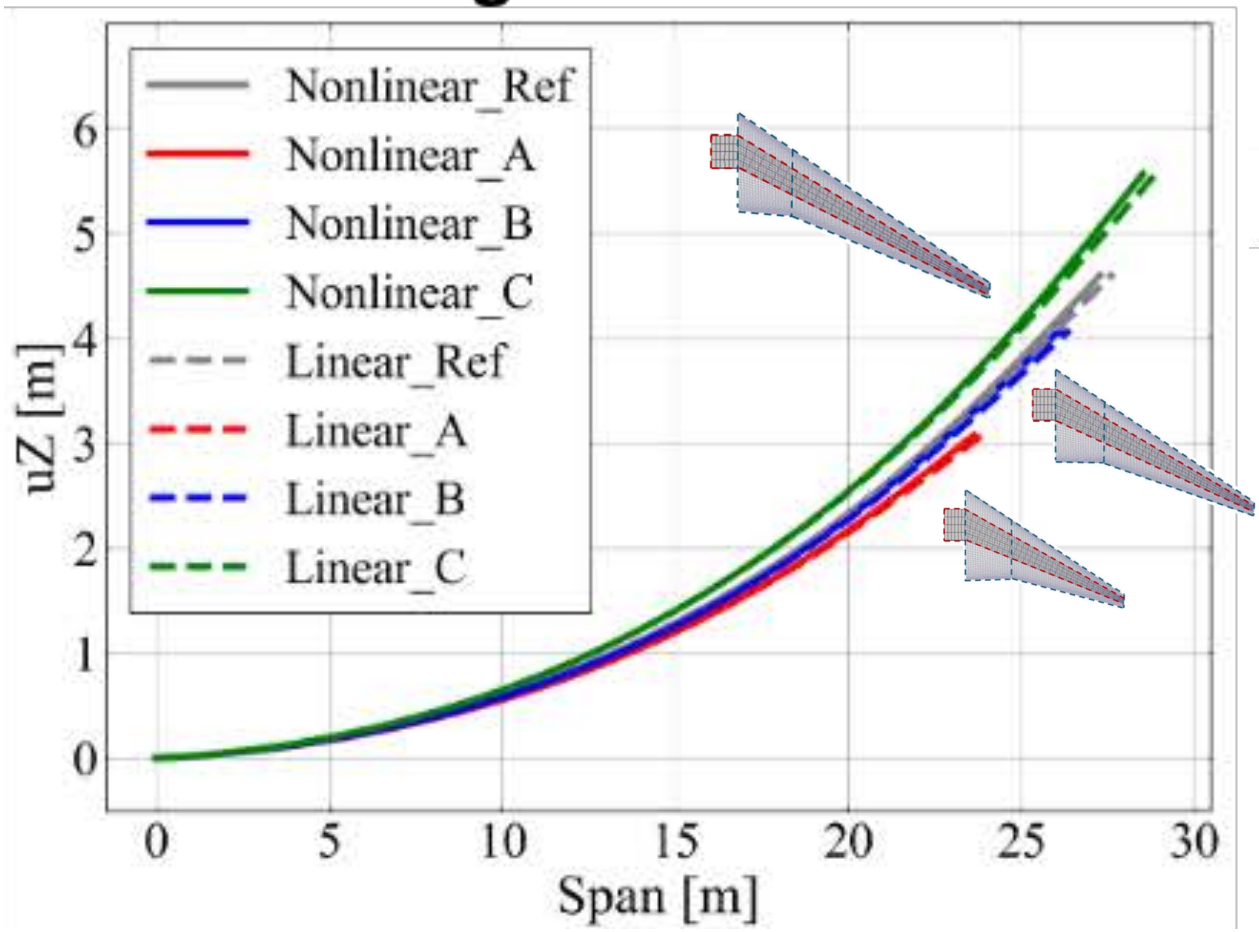


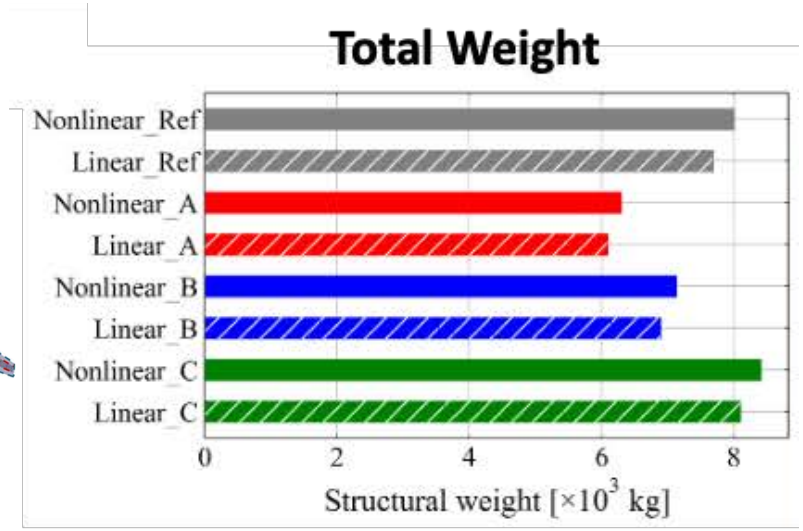
Baseline: *Two-way Nonlinear* strategy (higher physical fidelity)
combines two-way aeroelastic coupling with a geometrically nonlinear FEM solver.

Linear FEM analysis (*Two-way Linear*) tends to underestimate structural weight.
One-way coupling method (*One-way Linear*) tends to overestimate both structural weight and drag.

Geometrical Nonlinearity

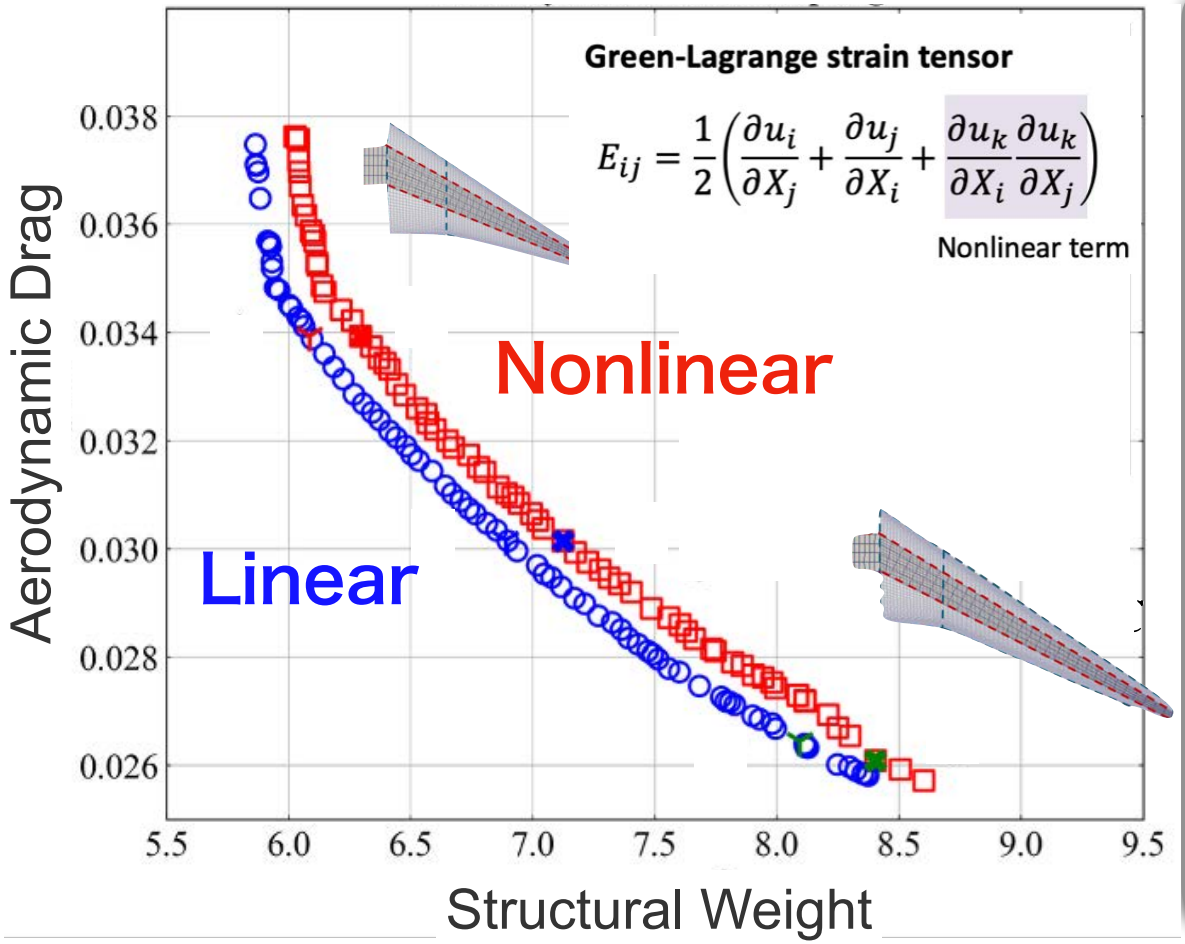
Wing Deflection



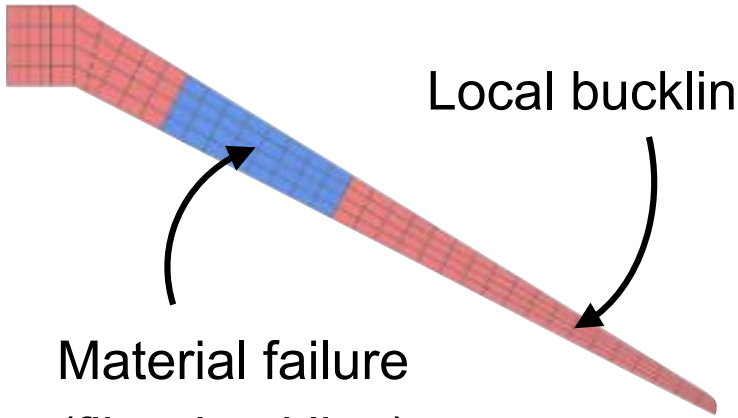


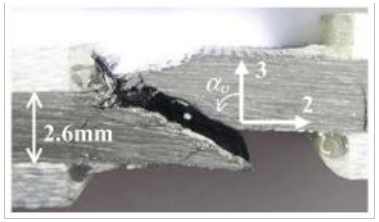
- Nonlinear analyses exhibit slightly more pronounced wing bending effects (greater wingtip shortening), especially for longer-wingspan designs.

Geometrical Nonlinearity



Failure modes on upper surface



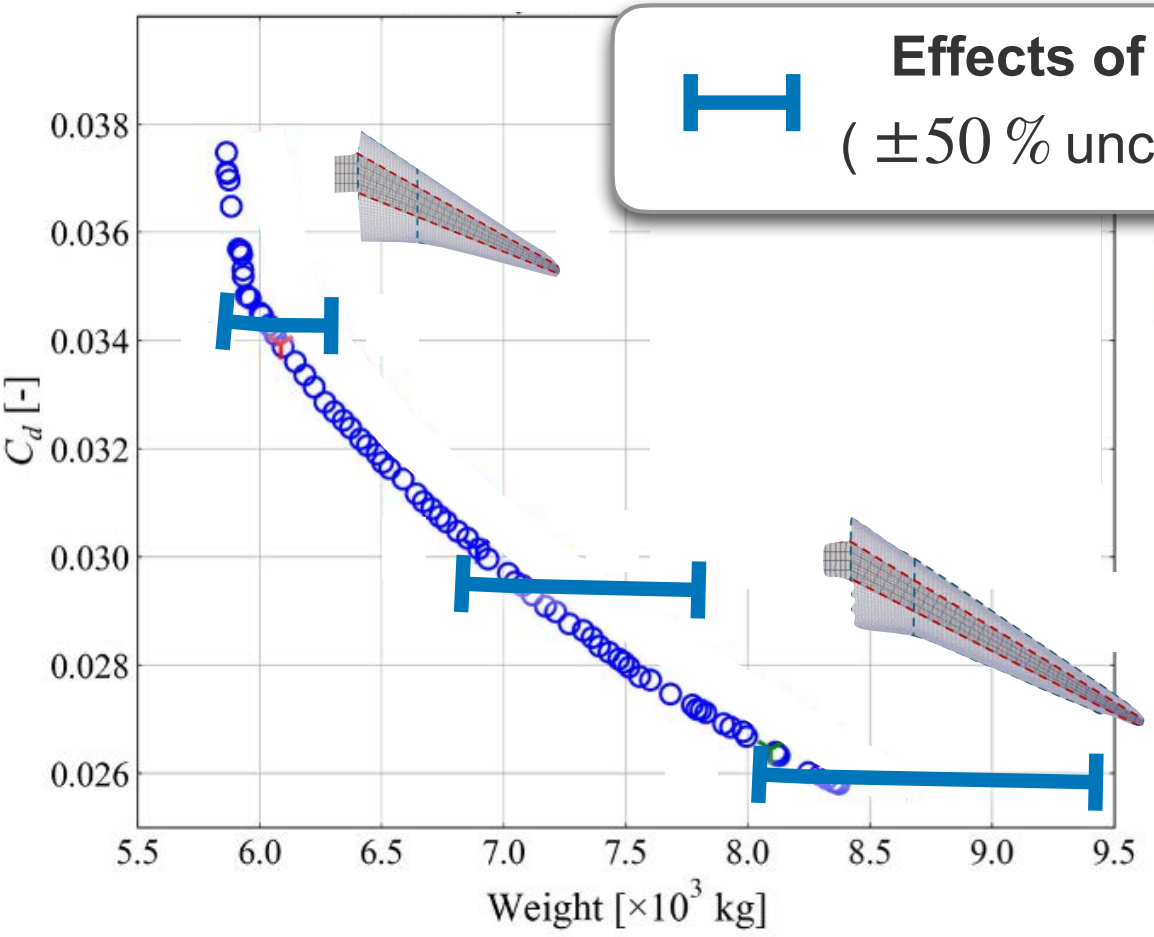




- First fully global multi-objective optimization with GN analysis

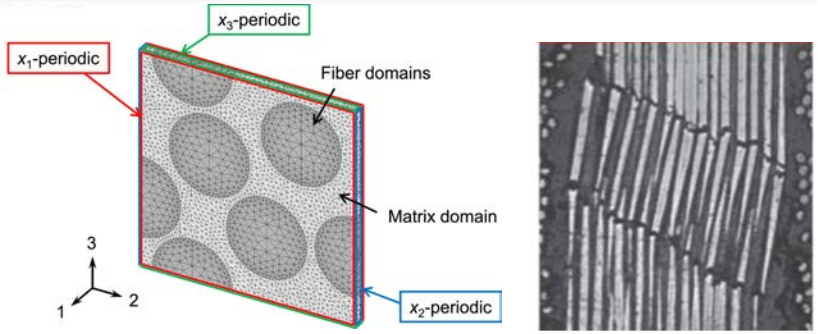
Liu et al., AEST (2025) , Liu, Abe et al., (under review)

Effects of fiber misalignment on design



Effects of Initial Fiber Misalignment

(±50 % uncertainty in carbon-fiber angle)



$$C11 = \frac{G}{1 + n\left(\frac{3}{7}\right)^{\frac{1}{n}}\left(\frac{\phi_0 \frac{G}{\tau_y}}{n-1}\right)^{\frac{n-1}{n}}}$$

Budiansky & Fleck (1933)

- First fully global multi-objective optimization with GN analysis

Liu et al., AEST (2025) , Liu, Abe et al., (under review)

- **Initial fiber misalignment in manufacturing can be assessed**

Liu & Abe et al., (Composite & Structures 2026)

Contents lists available at ScienceDirect

Composite Structures

journal homepage: www.elsevier.com/locate/compstruct

Multi-objective Bayesian optimization of composite aircraft wings using various carbon fibers

Yajun Liu [a,1], Yoshiaki Abe [a,*,1], Ryosuke Kano [b,a], Yuki Yatsu [b,a], Katsumi Nakamura [b,a], Koji Shimoyama [d], Tomonaga Okabe [b,c], Shigeru Obayashi [a]

[a] Institute of Fluid Science, Tohoku University, 2-1-1, Katahira, Aobaku, Sendai, 980-8577, Japan
[b] Department of Aerospace Engineering, Tohoku University, 6-6-01, Aramaki-Aza-Aoba, Aobaku, Sendai, 980-8579, Japan
[c] Department of Materials Science and Engineering, University of Washington, BOX 352120, Seattle, WA 98195, USA
[d] Department of Mechanical Engineering, Kyushu University, Fukuoka, 819-0395, Japan

Read the full paper

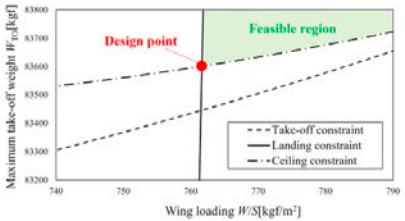
Composite Structures 383 (2026) 120105 · Open Access

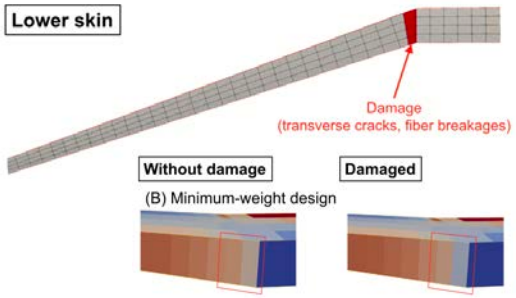
Ongoing works on our aircraft design tool

Integration with conceptual design and damage mechanics

DASH
Digital Aircraft Design tool of Tohoku University

Kano *et al., AEST (2025)*





Integration with high-fidelity CFDs

First wall-modeled LES for ETW aeroelastic experiment

DASH
Digital Aircraft Design tool of Tohoku University

Full-configuration model with CFRP/CFRTP

DASH

Next-gen B737 aircraft is proposed to OEM via Tier 1 industry using DASH tool (Jan. 2025 -)

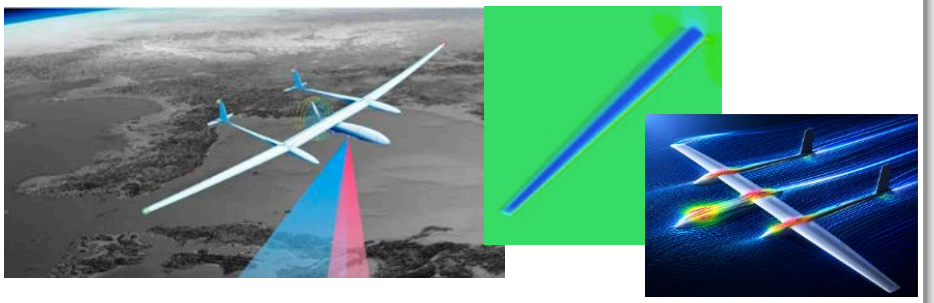
$$T^T F = (T^T M T)\ddot{u}_{ref}$$

$$\ddot{u}_{ref} = (T^T M T)^{-1} T^T F$$

Rashmikant et al., AEST (2026)

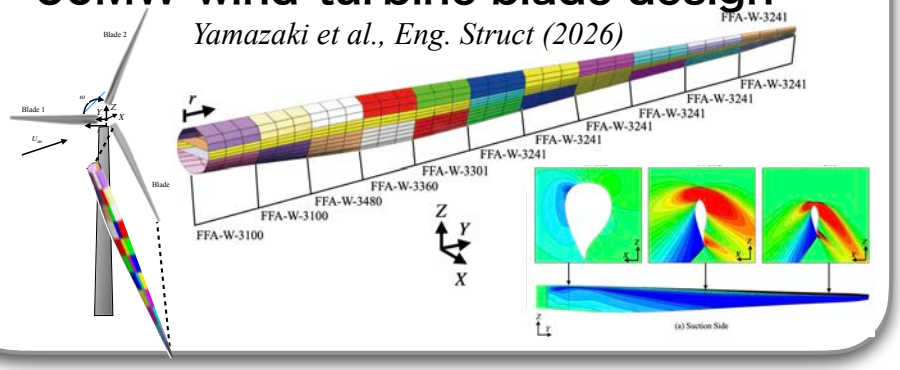
SUBARU Kawasaki

High Altitude Pseudo Satellite (HAPS)



50MW-wind-turbine blade design

Yamazaki et al., Eng. Struct (2026)



Ongoing works on our aircraft design tool

Integration with conceptual design and damage mechanics

DASH
Digital Aircraft Design tool of Tohoku University

Kano *et al., AEST (2025)*

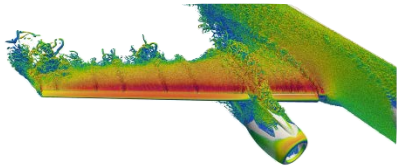
Integration with high-fidelity CFDs

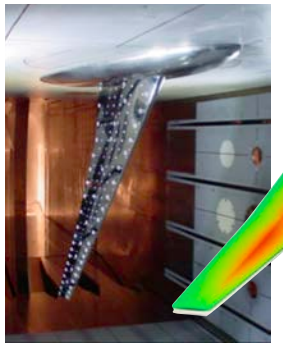
First wall-modeled LES for ETW aeroelastic experiment

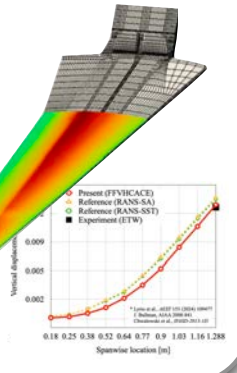
DASH
Digital Aircraft Design tool of Tohoku University

Fugaku

JAXA



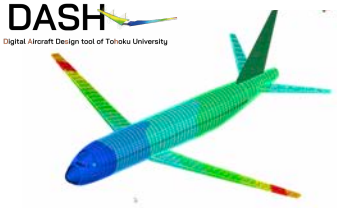


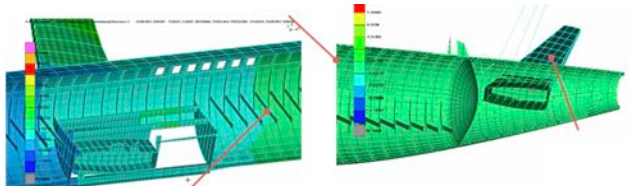


Full-configuration model with CFRP/CFRTP

DASH
Digital Aircraft Design tool of Tohoku University

Rashmikant et al., AEST (2026)

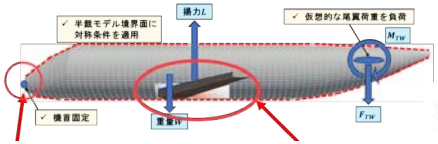


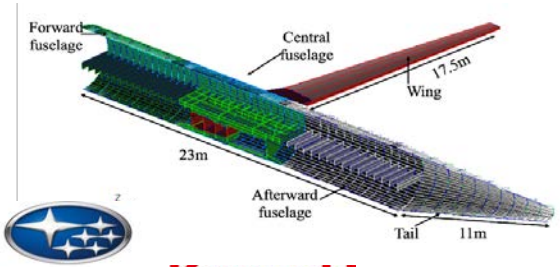


Next-gen B737 aircraft is proposed to OEM via Tier 1 industry using DASH tool (Jan. 2025 -)

$$T^T F = (T^T M T)\ddot{u}_{ref}$$

$$\ddot{u}_{ref} = (T^T M T)^{-1} T^T F$$





SUBARU Kawasaki

High Altitude Pseudo Satellite (HAPS)

50MW-wind-turbine blade design

Yamazaki et al., Eng. Struct (2026)

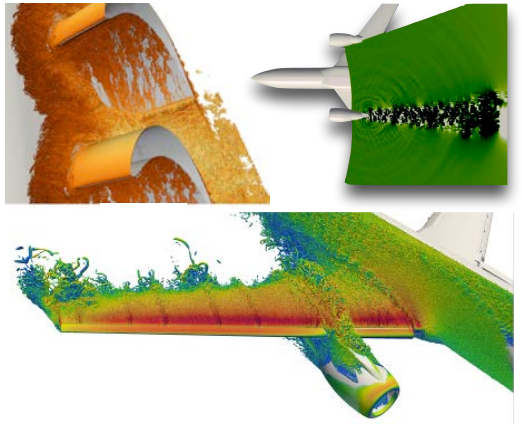
Ongoing works on our aircraft design tool

Integration with conceptual design and damage mechanics

DASH
Digital Aircraft Design tool of Tohoku University

Kano *et al., AEST (2025)*

Integration with high-fidelity CFDs





Modern hardwares

Full-configuration model with CFRP/CFRTP

DASH
Digital Aircraft Design tool of Tohoku University

Next-gen B737 aircraft is proposed to OEM via Tier 1 industry using DASH tool (Jan. 2025 -)

$$T^T F = (T^T M T)\ddot{u}_{ref}$$

$$\ddot{u}_{ref} = (T^T M T)^{-1} T^T F$$

Rashmikant *et al., AEST (2026)*

SUBARU Kawasaki

High Altitude Platform Station (HAPS)

50MW-wind-turbine blade design

Yamazaki *et al., Eng. Struct (2026)*

high-fidelity CFD with modern hardwares

PyFR

- *Open source* platform (FR/DG scheme)
- International collaborative project

IMPERIAL

Université Concordia University

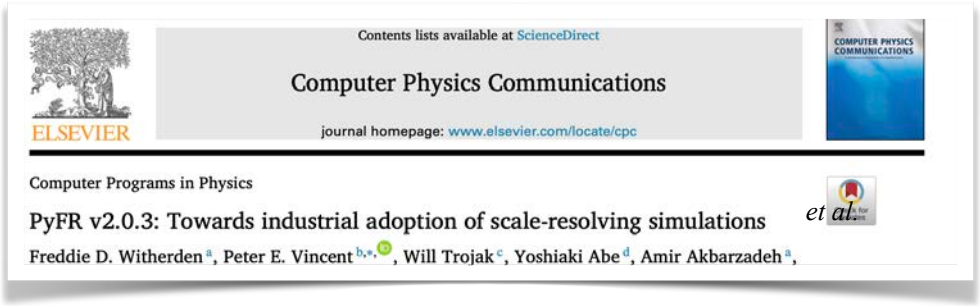
TEXAS A&M UNIVERSITY

TOHOKU UNIVERSITY

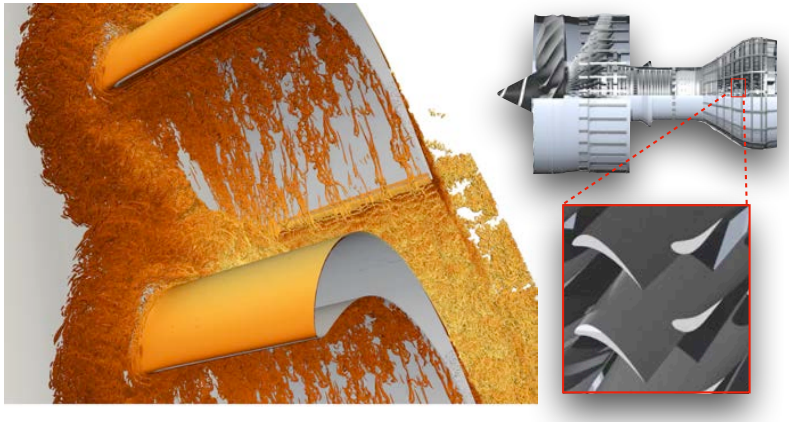
INHA UNIVERSITY 1954

Led by

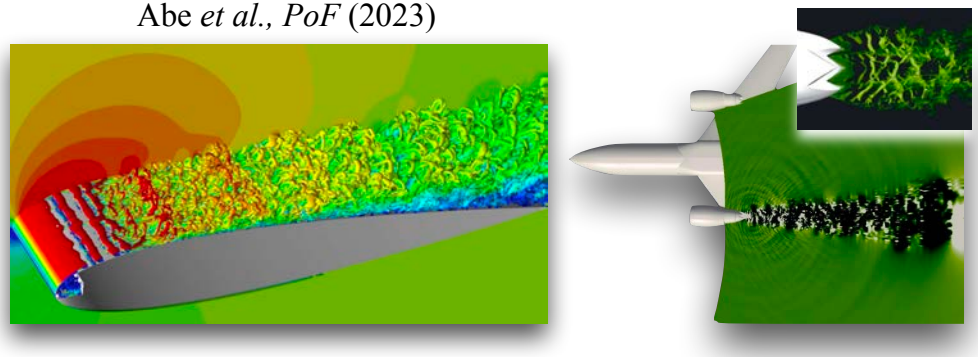
Dr./Prof. Peter Vincent & Freddie Witherden



Iyer, Abe, *et al.*, *Computers & Fluids* (2021)



Abe *et al.*, *PoF* (2023)



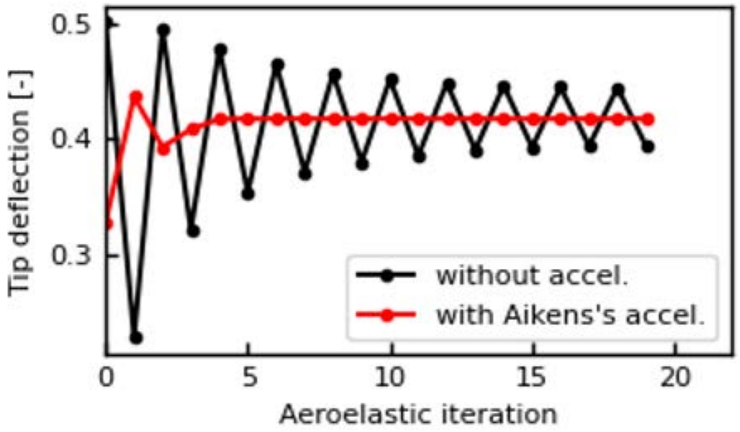
So, how can we integrate high-fidelity simulations to FSI / Aircraft Design?

Structural design at equilibrium condition

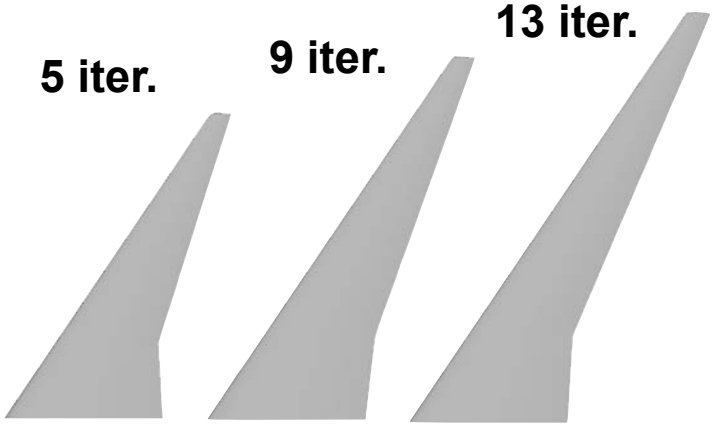
Sequential iteration

✓ 5 - 20 times aeroelastic iteration

✓ 50 - 200 times structural-sizing iter.

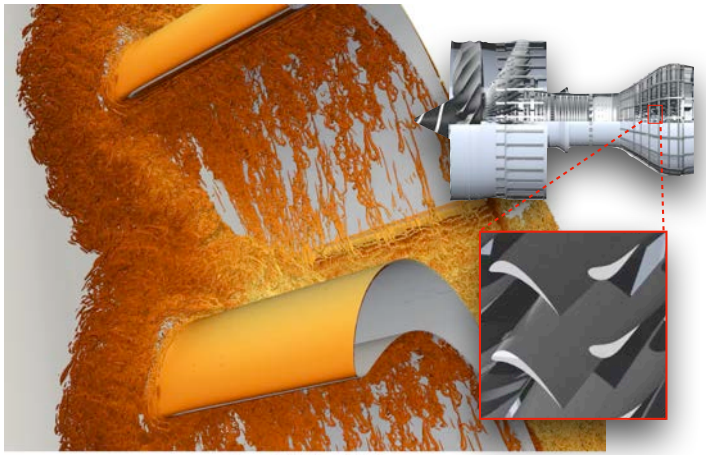


✓ High-aspect-ratio wing requires larger iter.

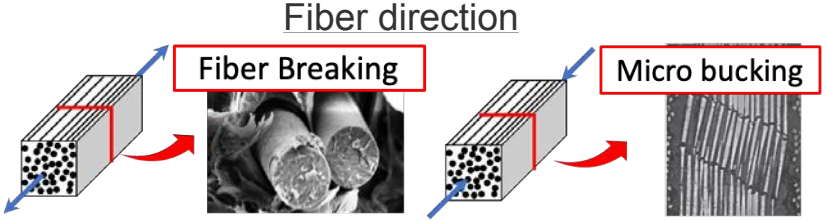


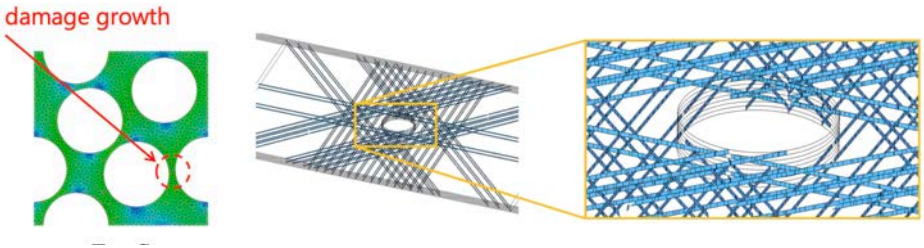
High-fidelity models

✓ CFD at real high-load conditions



✓ CSD with damage propagation





Contents of my talk

Composite aircraft design tool

Date *et al., AEST 2022, Rashmikant and Abe, AEST 2026*

Design optimization of CFRP wings

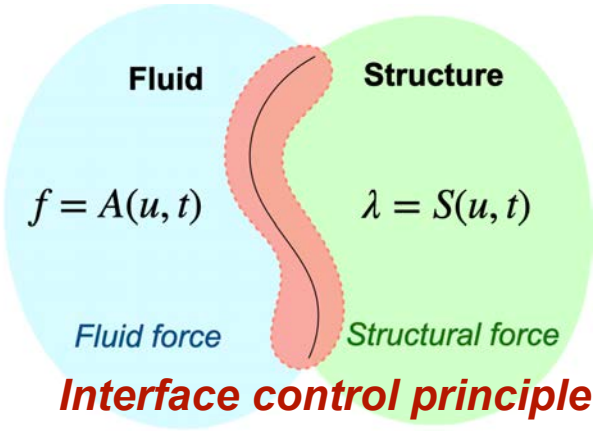
Liu *et al., AEST 2025, Comp. Struct. 2026,* Kano *et al., AEST 2025*

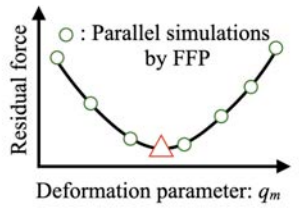
Data-driven/assisted FSI

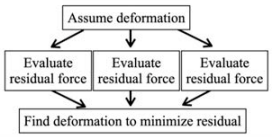
Abe *et al., JSCM, 48, 6 2022*

Lee, Abe, et al., J. Fluids and Structures 2026

Yatsu *et al., CM3 Transport 2025*







Conventional iterative method for static FSI

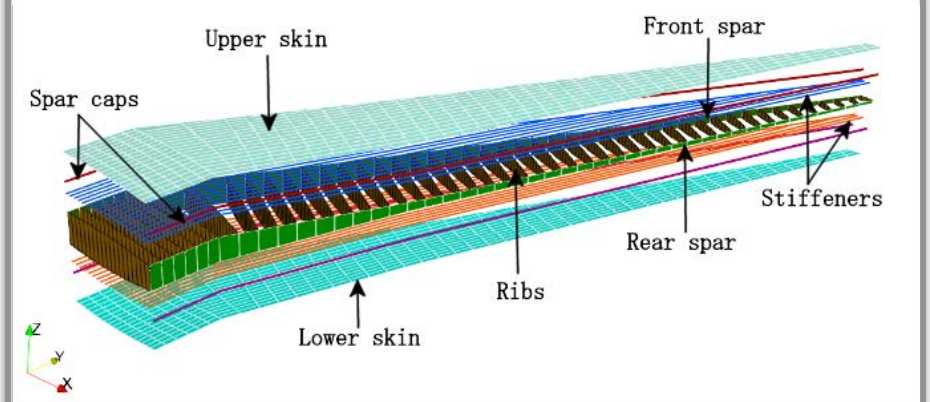
- Structural deformation in equilibrium condition

$$\boldsymbol{\lambda}_{\mathrm{S}}(\boldsymbol{u}_{\mathrm{S}}) - \boldsymbol{f}_{\mathrm{S}}(\boldsymbol{u}_{\mathrm{S}}) = 0 \qquad (\boldsymbol{u}_{\mathrm{S}} : \text{displacement})$$

Internal force

$$\boldsymbol{\lambda}_{\mathrm{S}} = \mathcal{S}^{*}(\boldsymbol{u}_{\mathrm{S}})$$

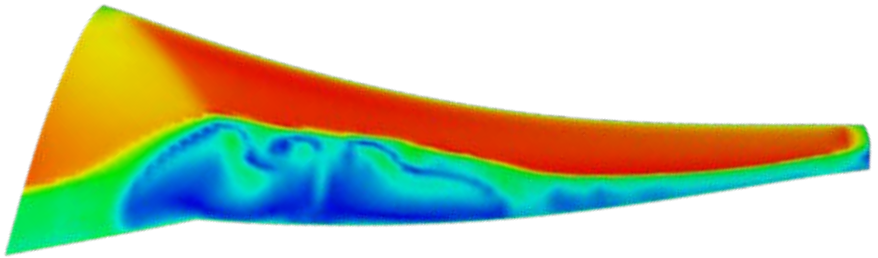
Structural solver



External force

$$\boldsymbol{f}_{\mathrm{S}} = \boldsymbol{T}^{T}\mathcal{A}(\boldsymbol{x}_{\mathrm{Av}}^{(0)}, \boldsymbol{T}\boldsymbol{u}_{\mathrm{S}})$$

Flow solver



Conventional iterative method for static FSI

- Nonlinear Block Gauss-Seidel (**BGS**)

Iteration

Flow solver

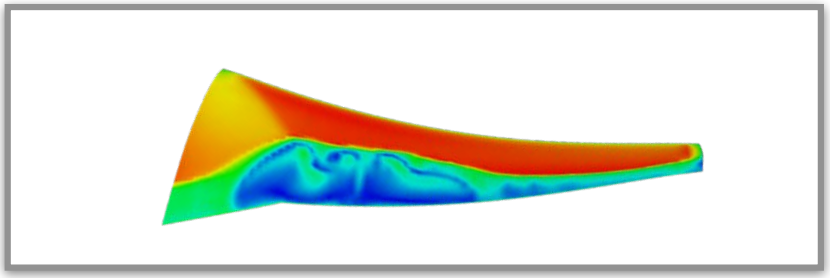
$$\boldsymbol{f}_{\mathrm{S}} = \boldsymbol{T}^{T}\mathcal{A}(\boldsymbol{x}_{\mathrm{Av}}^{(0)}, \boldsymbol{T}\boldsymbol{u}_{\mathrm{S}})$$

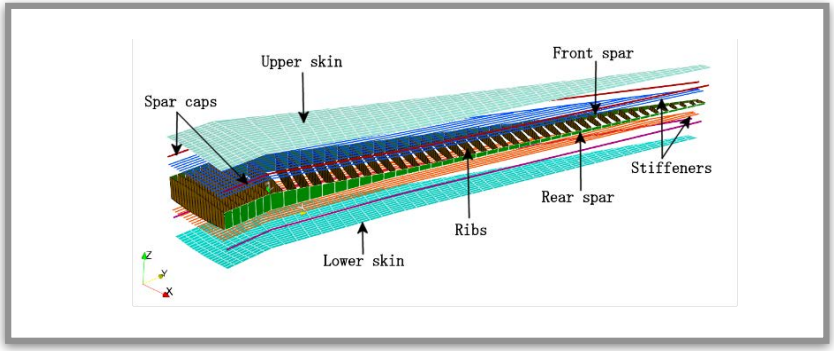
Structural solver

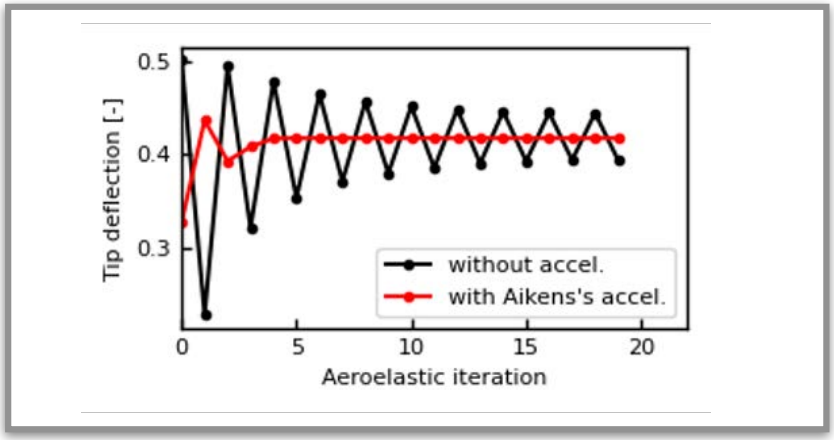
$$\boldsymbol{u}_{\mathrm{S}}^{*(i)} = \mathcal{S}(\boldsymbol{f}_{\mathrm{S}}^{(i)})$$

Relaxation

$$\boldsymbol{u}_{\mathrm{S}}^{(i)} = \boldsymbol{u}_{\mathrm{S}}^{(i-1)} + \theta^{(i)}\Delta\boldsymbol{u}_{\mathrm{S}}^{*(i)}$$







Fully-partitioned method for static FSI

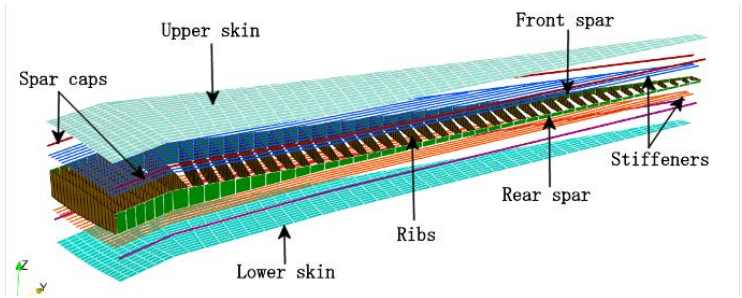
- Force-based fully partitioned (**FFP**)

$$\boldsymbol{\lambda}_{\mathrm{S}}(\boldsymbol{u}'_{\mathrm{S}}) - \boldsymbol{f}_{\mathrm{S}}(\boldsymbol{u}'_{\mathrm{S}}) = R(\boldsymbol{u}'_{\mathrm{S}}) \to 0 \quad (\boldsymbol{u}'_{\mathrm{S}}\text{: non-equilibrium disp.})$$

Internal force

$$\boldsymbol{\lambda}_{\mathrm{S}} = \mathcal{S}^*(\boldsymbol{u}'_{\mathrm{S}})$$

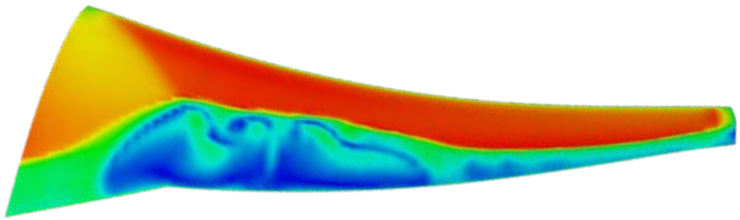
Structural solver



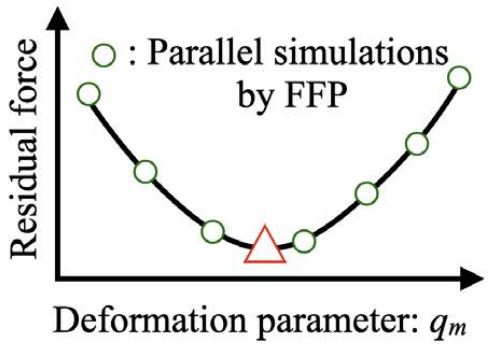
External force

$$\boldsymbol{f}_{\mathrm{S}} = \boldsymbol{T}^T \mathcal{A}(\boldsymbol{x}^{(0)}_{\mathrm{Av}}, \boldsymbol{T}\boldsymbol{u}'_{\mathrm{S}})$$

Flow solver



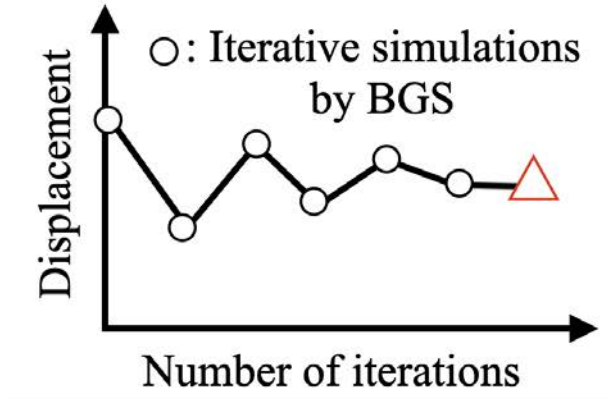
- ✓ Response surface of the residual force: $R(\boldsymbol{u}_{\mathrm{S}})$
- ✓ Find the deformation minimizing $R(\boldsymbol{u}_{\mathrm{S}})$

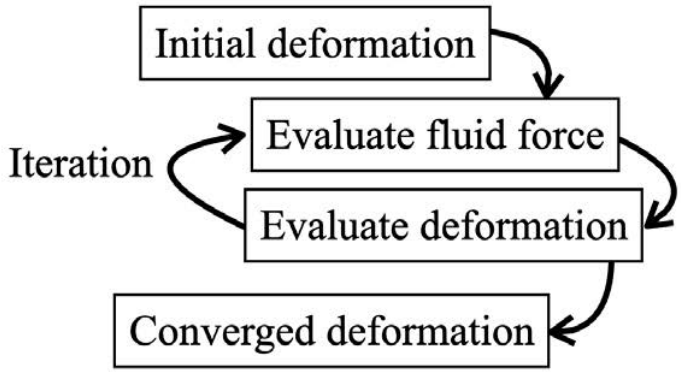


Fully-partitioned method for static FSI

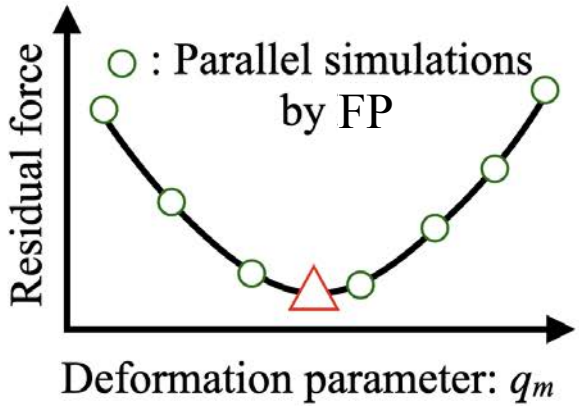
- **Sequential / iterative simulation is required in the conventional BGS.**
  - ✓ Infeasible cost with a large number of iterations, *e.g.,* WMLES for high-AR wing
  - ✓ Sequential process is *not* parallelizable → fully-partitioned method (FP)

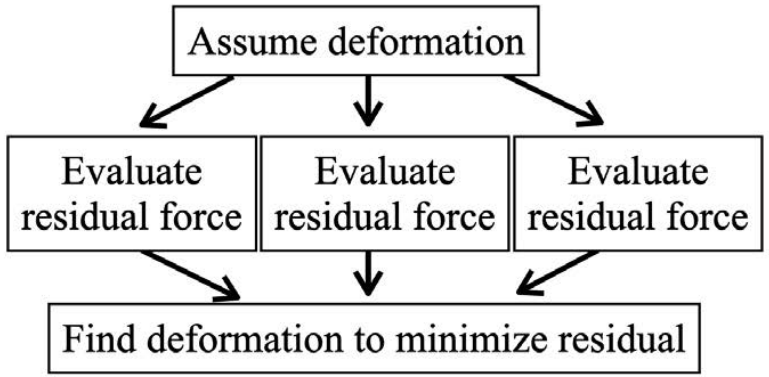
- Nonlinear Block Gauss-Seidel (**BGS**)





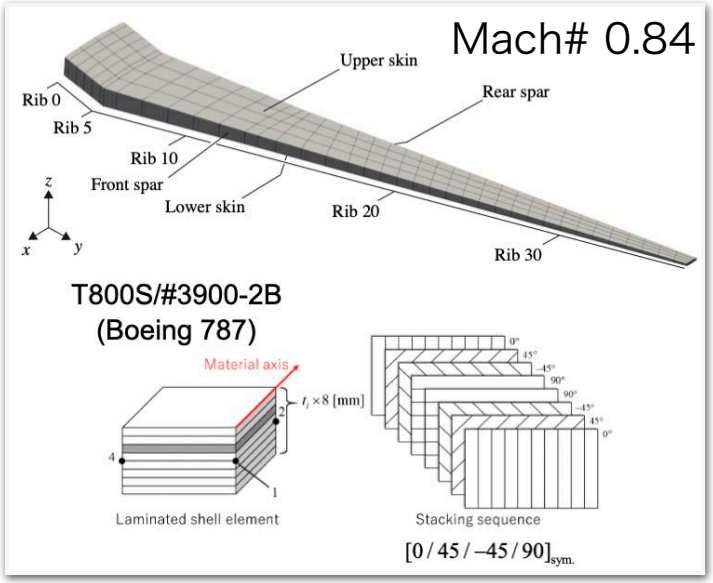
- Fully partitioned (**FP**)





Fully-partitioned method for static FSI

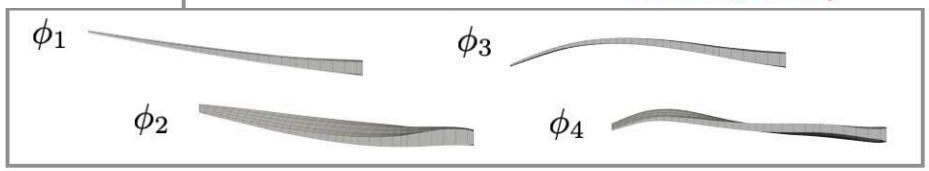
Assume deformation by modal analysis



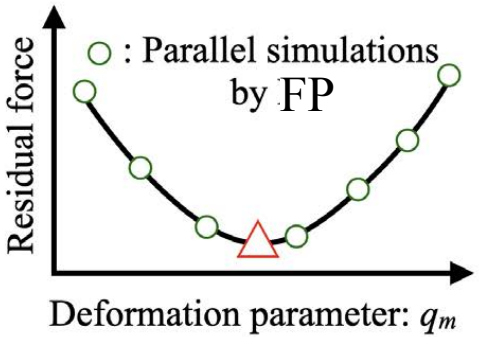
$$\boldsymbol{u}_S = \boldsymbol{\Phi q} = [\phi_1 \quad \phi_2 \ldots \phi_N][q_1 \quad q_2 \ldots q_N]^T$$

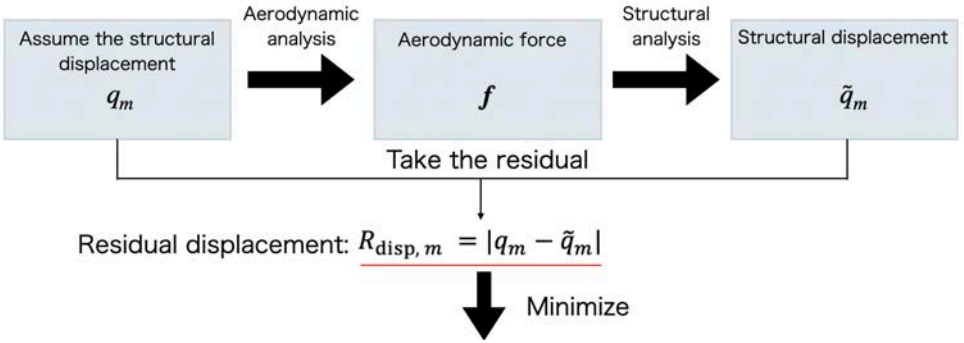
mode shapes (precomputed)

modal coordinates (parameter of deformation to be solved)



Fully partitioned (FP)



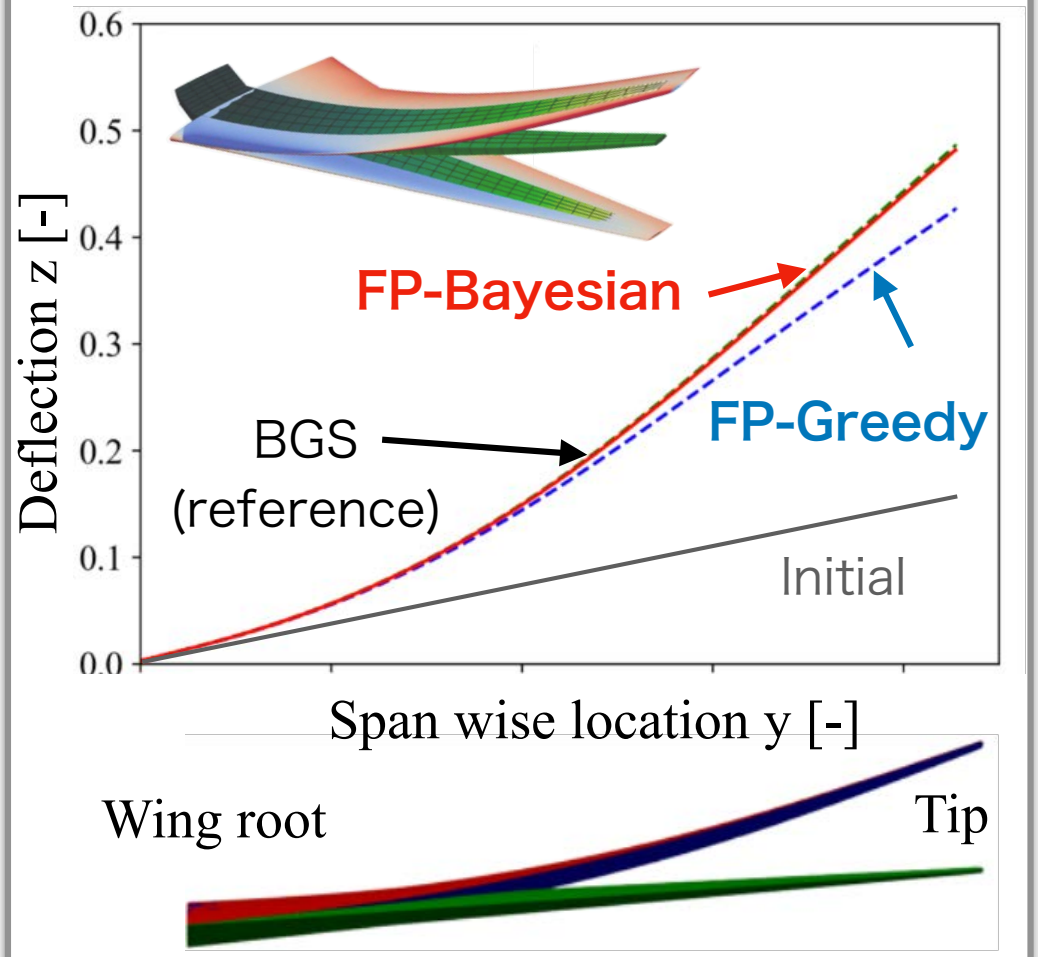


Optimization problem to solve mutiphysics problem

- ✓ **Greedy method**
- ✓ **Bayesian optimization**

Fully-partitioned method for static FSI

Results of leading-edge deformation



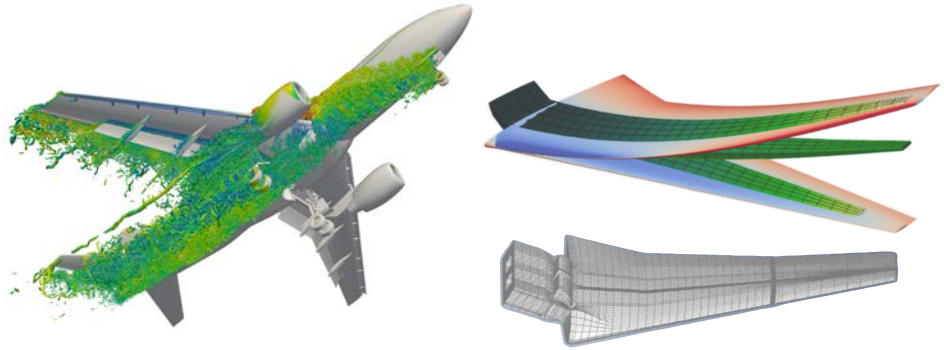
Comparison of simulation cost

Effective number of iterations

AoA	BGS	FP-Greedy	FP-Bayesian
0 deg	11	5	3
3 deg	13	5	3

Approx. 4 times speed-up

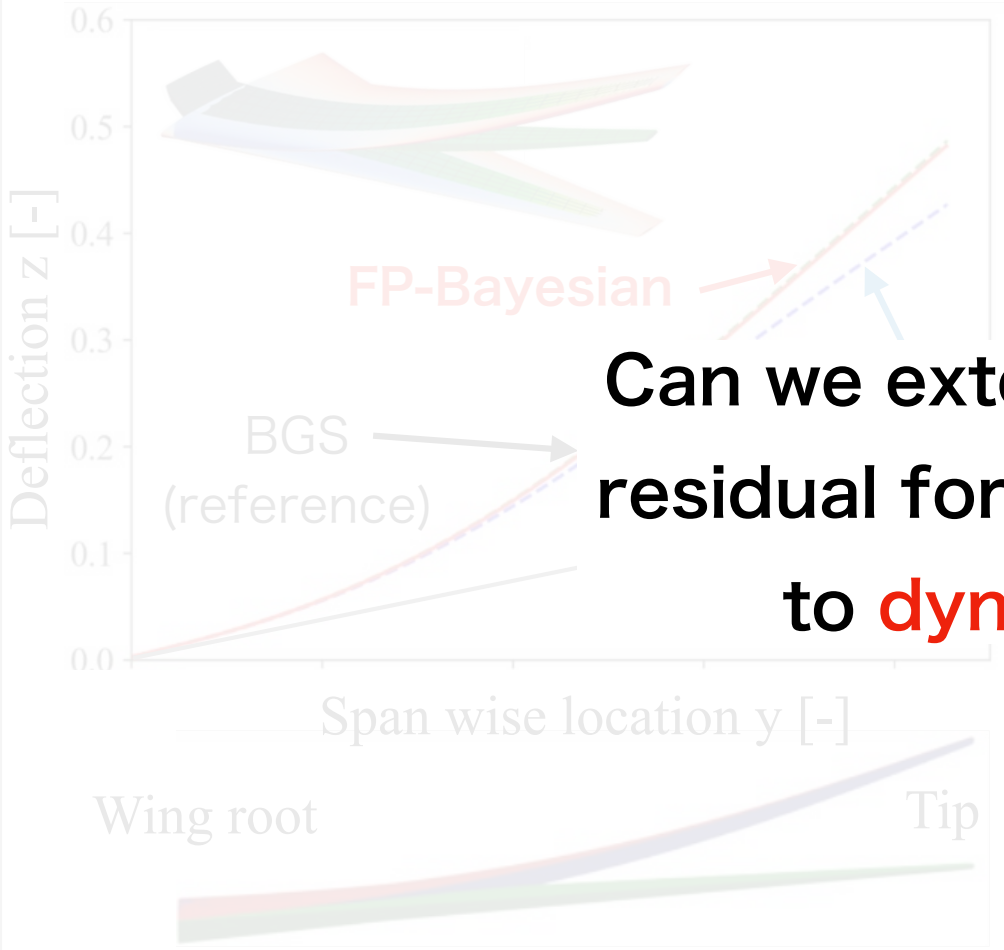
Potential for highly parallel hardwares



- Full-scale wall-modeled LES (WMLES)

Fully-partitioned method for static FSI

Results of leading-edge deformation



Comparison of simulation cost

Effective number of iterations

AoA	BGS	FP-Greedy	FP-Bayesian
0 deg	11	5	3
3 deg	13	5	3

times speed-up

parallel hardwares

Full-scale wall-modeled LES (WMLES)

Can we extend this idea of residual force minimization to dynamic FSI ?

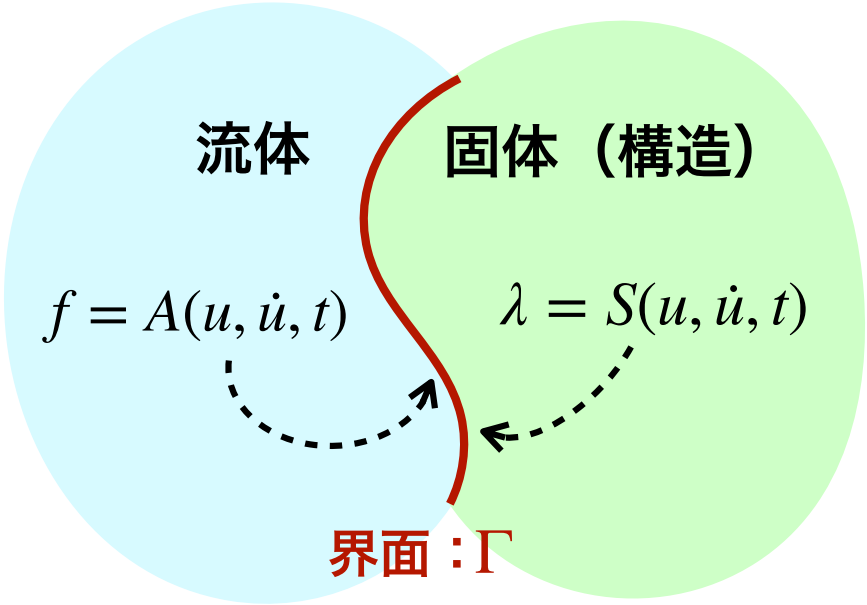
研究背景：流体構造連成解析における界面条件

流体・固体（構造）の支配方程式は，
2つの界面条件によって拘束

- **運動学的適合**：変位uと速度$\dot{u}$
- **力のつり合い**： $f(u, \dot{u}, t) = \lambda(u, \dot{u}, t)$

連成系での変分原理に基づく

$$L = L_f + L_S + \int_\Gamma \lambda(u_f - u_s)$$



解析手法の違いは，「界面条件をどのように，どれだけのコストで満たすか」

Monolithic（一体型）

- 単一連立系，界面条件を厳密に満足
- 既存の高忠実ソルバは活用が困難

Wang et al., 2020, J. Fluids Struct.

Partitioned（分離反復型）

- 既存のソルバを非侵襲的に組合せ可
- 反復低減が研究対象（IQN-ILS etc.）

Delaissé et al., 2023, Arch. Comput. Methods Eng.

データ駆動ROMの併用

- ROMで次時刻の初期推定値改善
- ROMはあくまで予測子，要反復計算

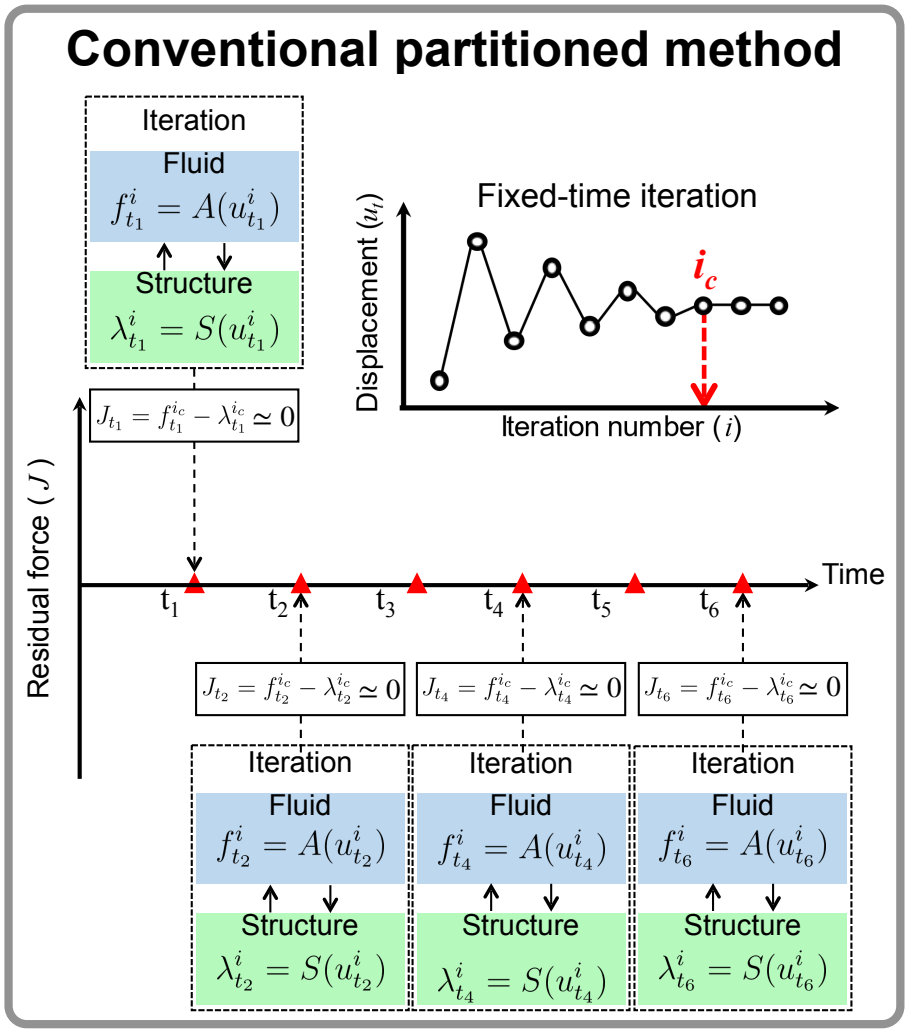
Tiba et al., 2025, Comput. Phys. Commu.

いずれも「界面は拘束条件であり，数学的に満たすべき」という原則

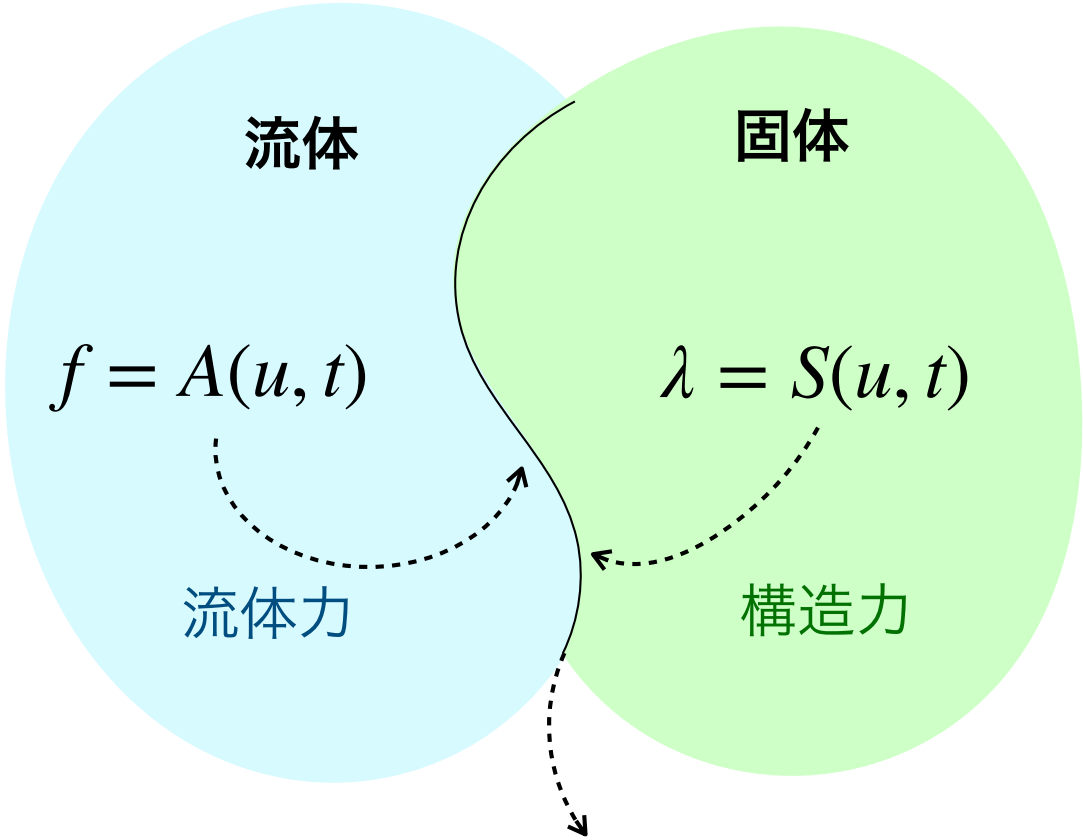
→ **数値的には何らかの反復解法が必要 ＝ ソルバー間の通信**

既存手法：分離反復解法でのfixed time iteration

各時刻において，界面での力のつり合いは瞬時に満たされるべき境界条件



Felippa *et al.*, *CMAME* (2001)



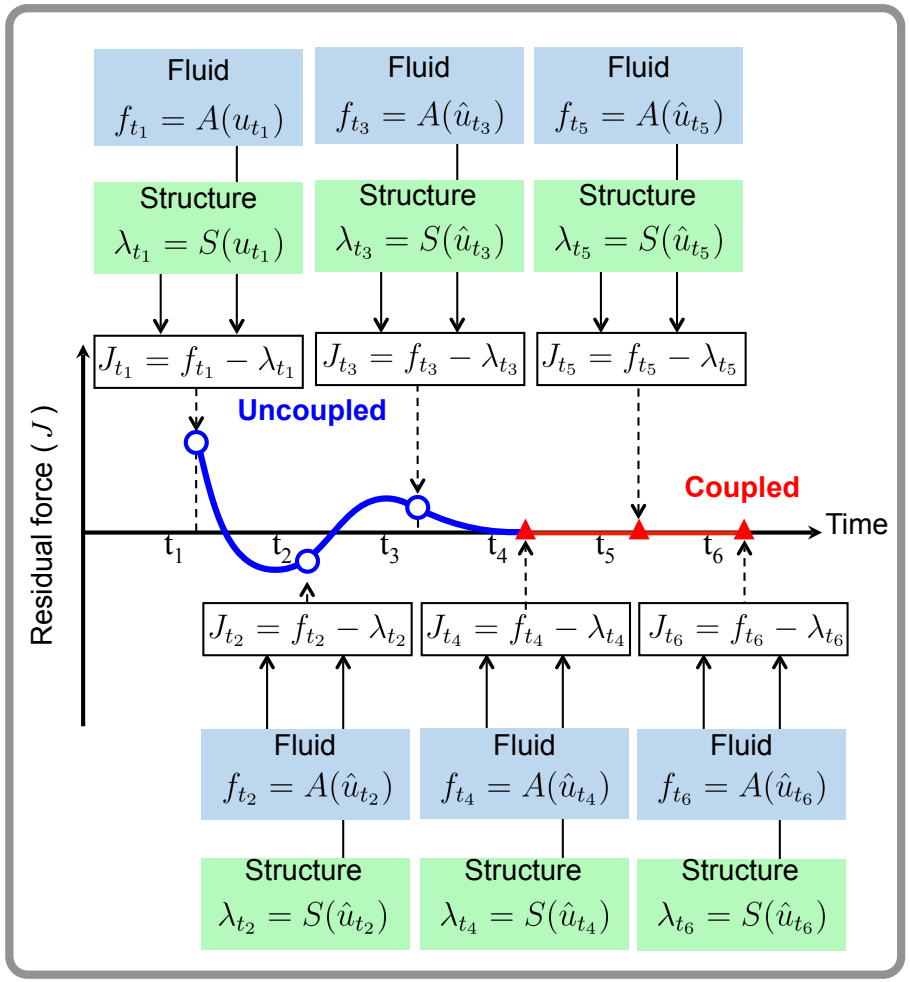
残差力

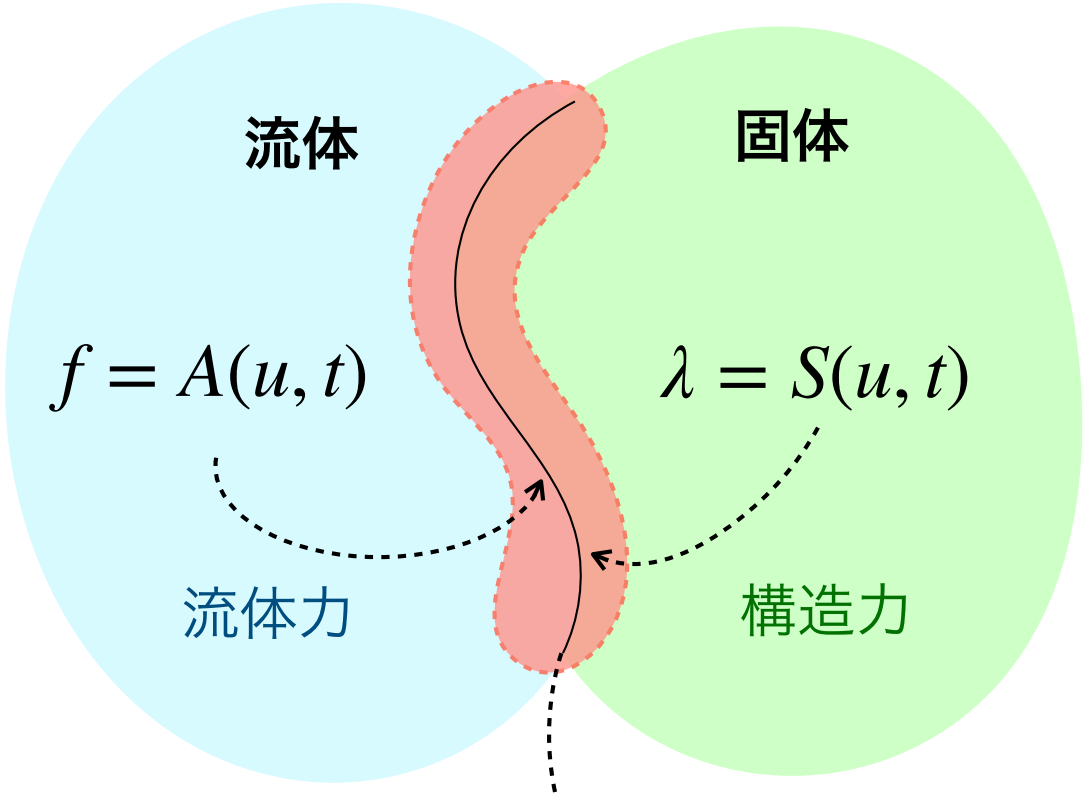
$$J(u,t) = f(u,t) - \lambda(u,t)$$

(u：界面変位)

各時刻で「反復」を行わないことは可能か？

Interface control principle





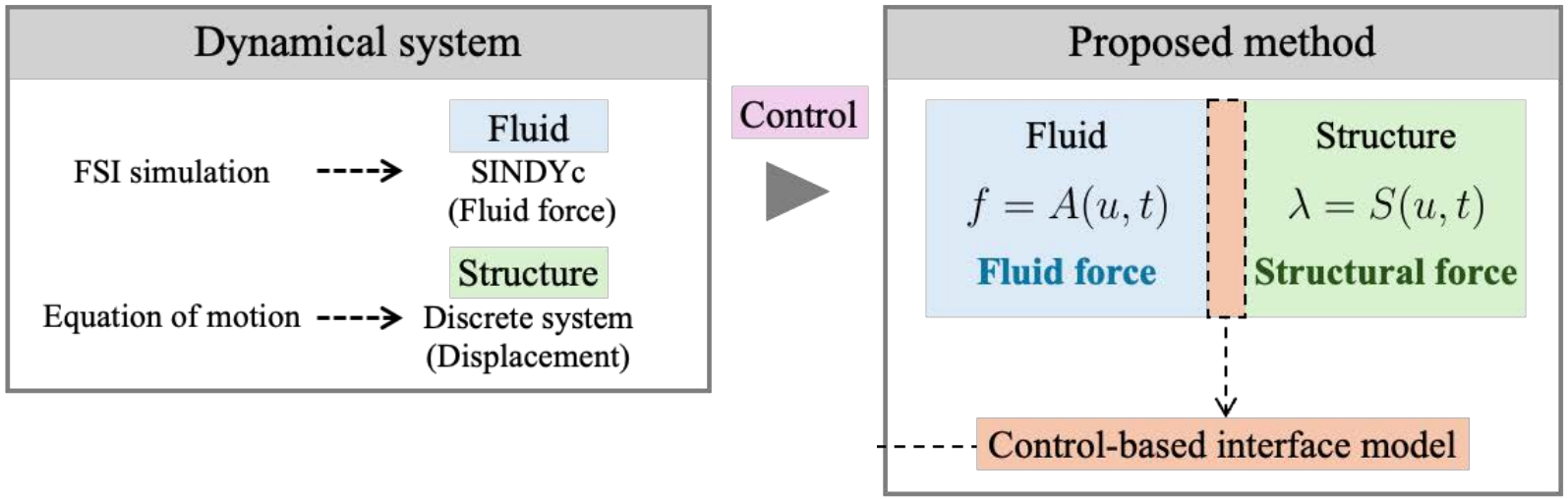
残差力

$$J(u,t) = f(u,t) - \lambda(u,t) \to 0 \quad (t \to \infty)$$

(u : 界面変位)

界面条件の破れを残差力として許し，「制御」する問題に定式化

ICP : Interface Control Principle



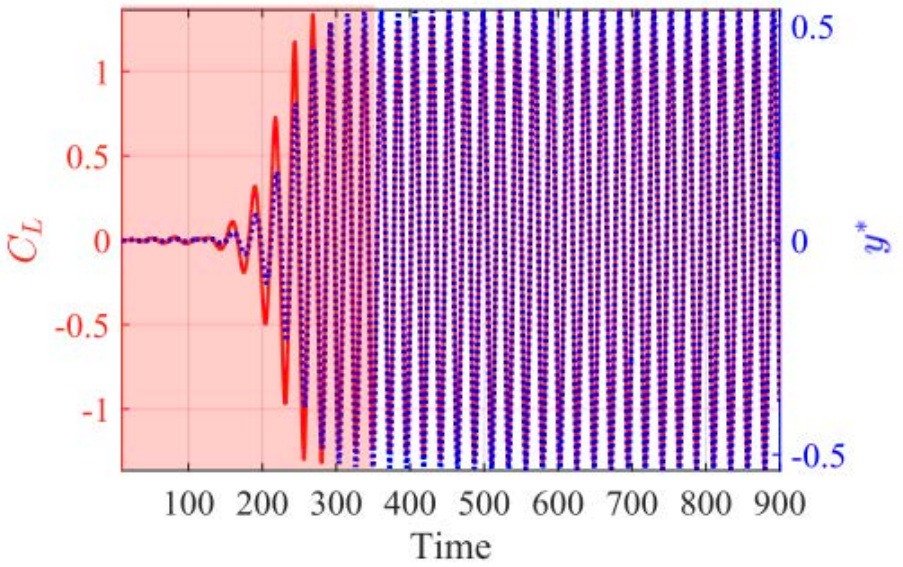
SINDYcによる流体力の低次元モデル化

Nonlinear dynamics of fluid

$$\frac{\mathrm{d}}{\mathrm{d}t}\mathbf{x}(t) = \mathbf{f}(\mathbf{x}(t), \mathbf{u}(t))$$

$$\mathbf{x} = \begin{bmatrix} C_L \\ \dot{C}_L \end{bmatrix} \quad \mathbf{u} = \begin{bmatrix} y* \\ \dot{y}* \end{bmatrix}$$

Training data set



SINDYc model for fluid force

$$\mathbf{X} = \begin{bmatrix} \mathbf{x}^\mathsf{T}(t_1) \\ \mathbf{x}^\mathsf{T}(t_2) \\ \vdots \\ \mathbf{x}^\mathsf{T}(t_m) \end{bmatrix} \quad \mathbf{U} = \begin{bmatrix} \mathbf{u}^\mathsf{T}(t_1) \\ \mathbf{u}^\mathsf{T}(t_2) \\ \vdots \\ \mathbf{u}^\mathsf{T}(t_m) \end{bmatrix}$$

$$\Theta(\mathbf{X}, \mathbf{U}) = \begin{bmatrix} | & | & | & | & | & \\ \mathbf{1} & \mathbf{X} & \mathbf{U} & (\mathbf{X} \otimes \mathbf{X}) & (\mathbf{X} \otimes \mathbf{U}) & \cdots \\ | & | & | & | & | & \end{bmatrix}$$

$$\dot{\mathbf{x}}_k^\mathsf{T} = \Theta(\mathbf{x}_k^\mathsf{T}, \mathbf{u}_k^\mathsf{T})\Xi$$

$$\xi_i^{\mathrm{SINDYc}} = \mathrm{argmin}_{\xi_i^{\mathrm{SINDYc}}} \left\| \dot{\mathbf{X}}_i - \Theta(\mathbf{X}, \mathbf{U})\xi_i^{\mathrm{SINDYc}} \right\|_2 + \alpha \left\| \xi_i^{\mathrm{SINDYc}} \right\|_1$$

Θ : Library of candidate nonlinear functions

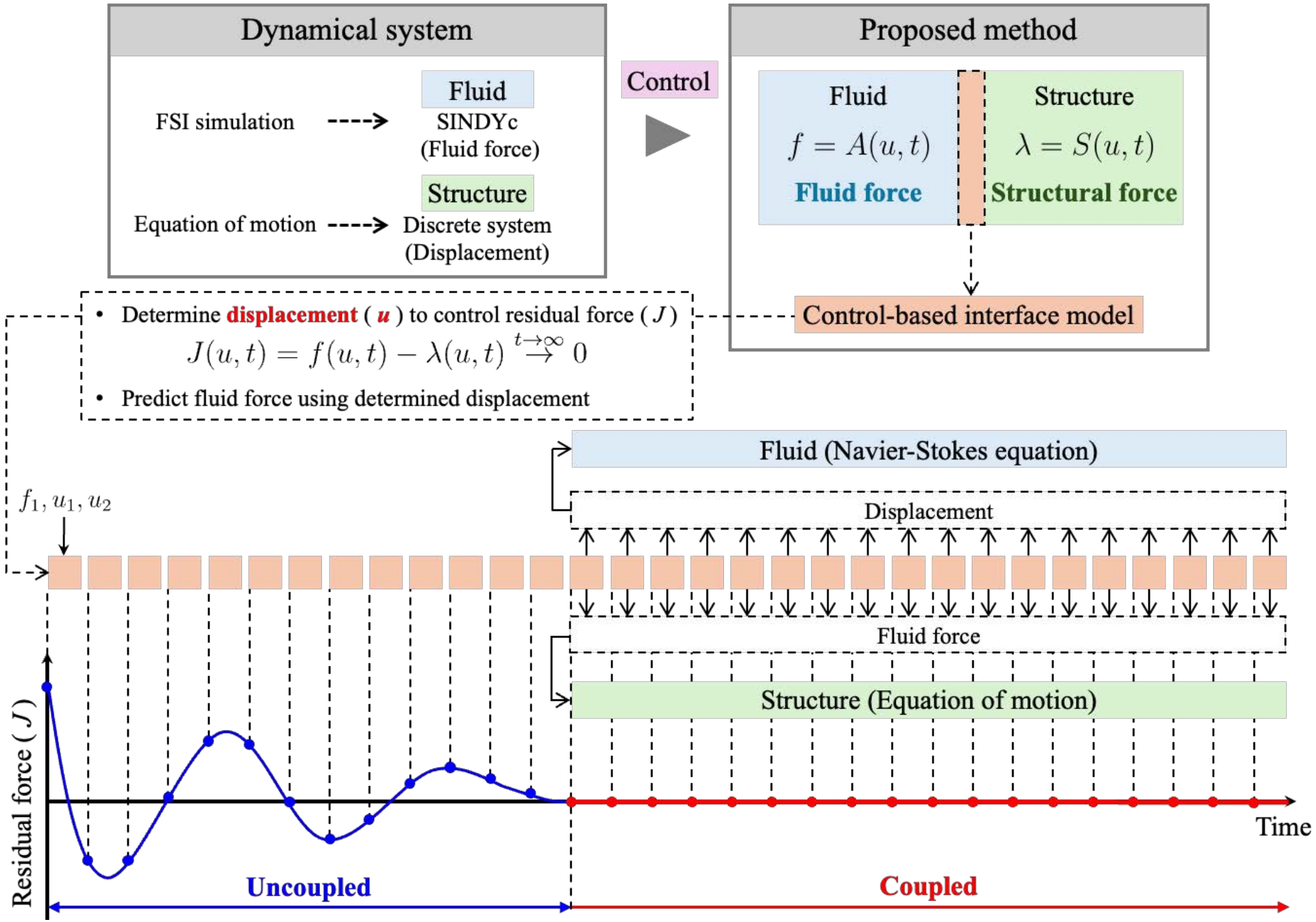
Ξ : Sparse vectors of coefficients

Discrete system

$$\mathbf{x}_{k+1} = \mathbf{x}_k + \Delta t \Xi^\mathsf{T} \Theta^\mathsf{T}(\mathbf{x}_k^\mathsf{T}, \mathbf{u}_k^\mathsf{T})$$

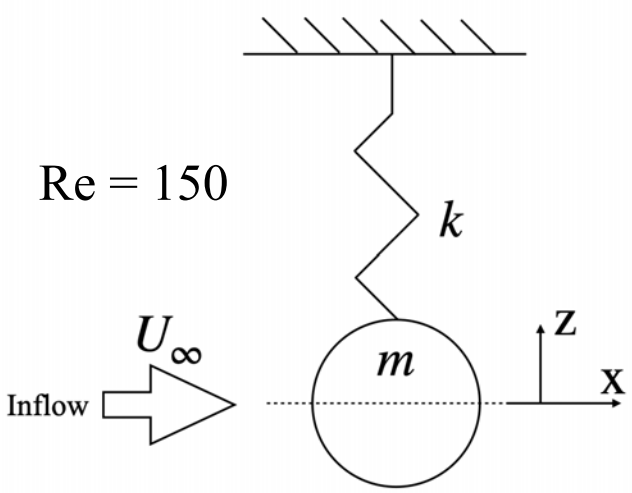
Reconstructed as a nonlinear ROM

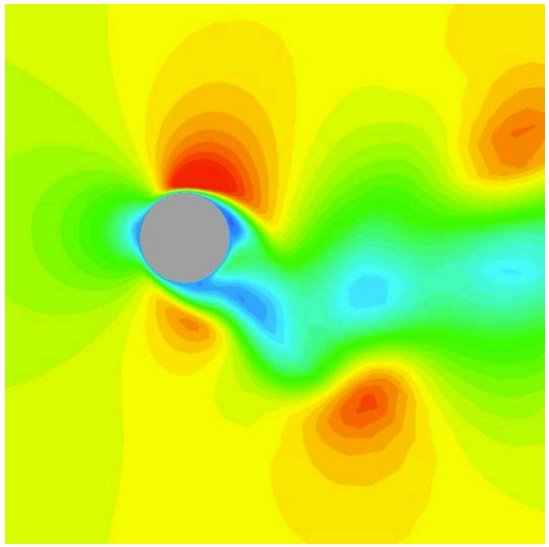
ICP : Interface Control Principle

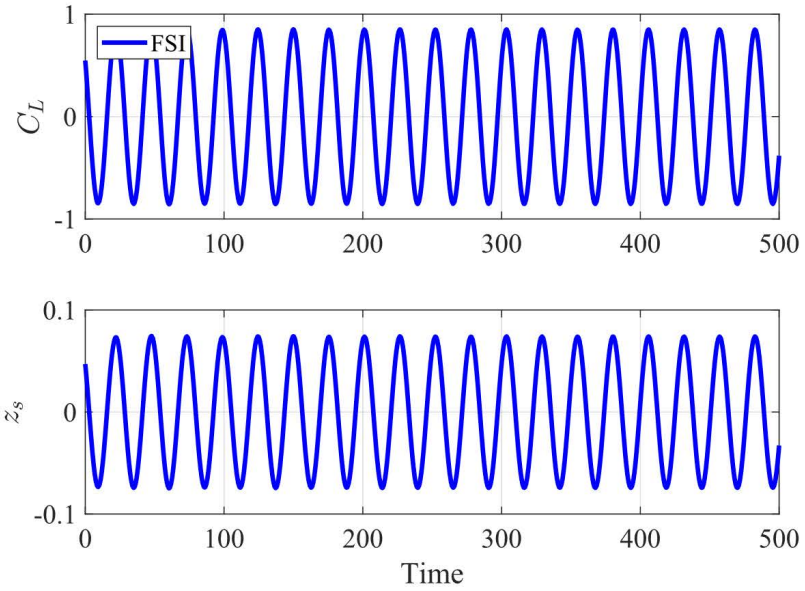


VIV円柱による基礎検証

- **問題設定：**Vortex-induced vibration（VIV）円柱







- **ICP界面モデル：**SINDYcで推定した流体力を真と考えて，状態フィードバック制御

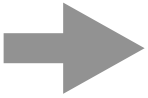
$$x_{k+1} = A_f x_k + B_f u_k$$

$$u_{k+1} = A_s x_k + B_s u_k + G_k$$

x_k：流体変数（構造に働く流体力）

u_k：構造変数（構造の変形量）

G_k：残差力（連成時は０となるべき）



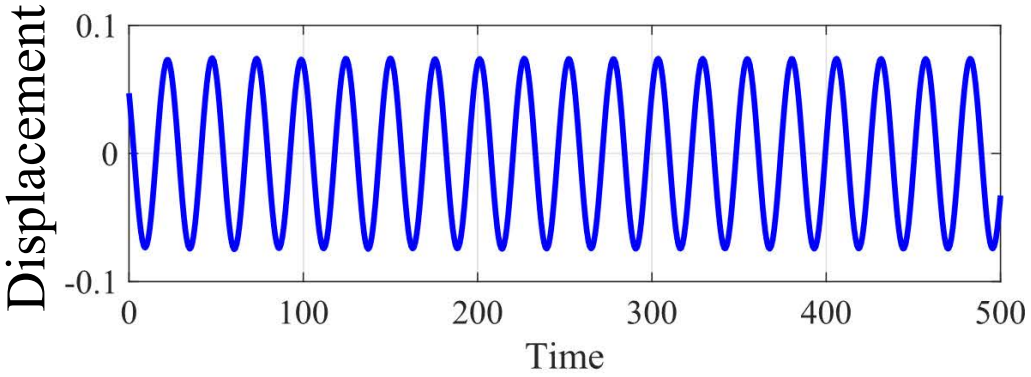
$$x_{k+1} = A_f x_k + B_f u_k$$

$$G_k = u_{k+1} - A_s x_k - B_s u_k$$

$\lim_{k\to\infty} G_k = 0$となる$u_k$を設計する

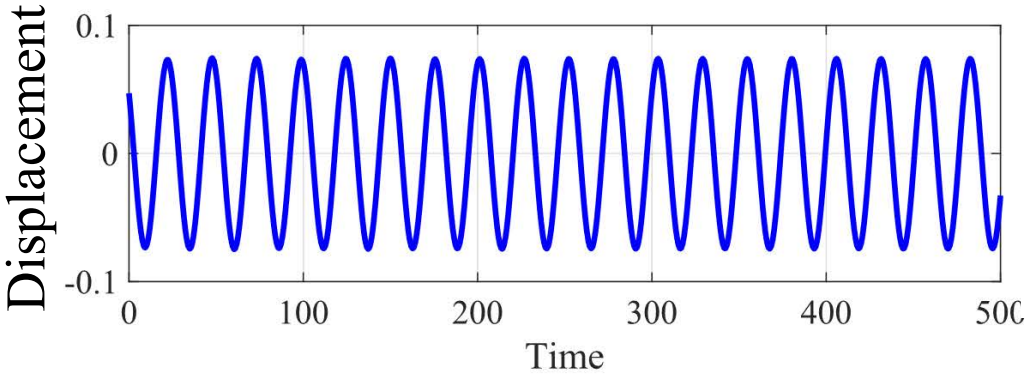
VIV円柱による基礎検証

■ **参照解**：従来の分離反復法による連成 FSI

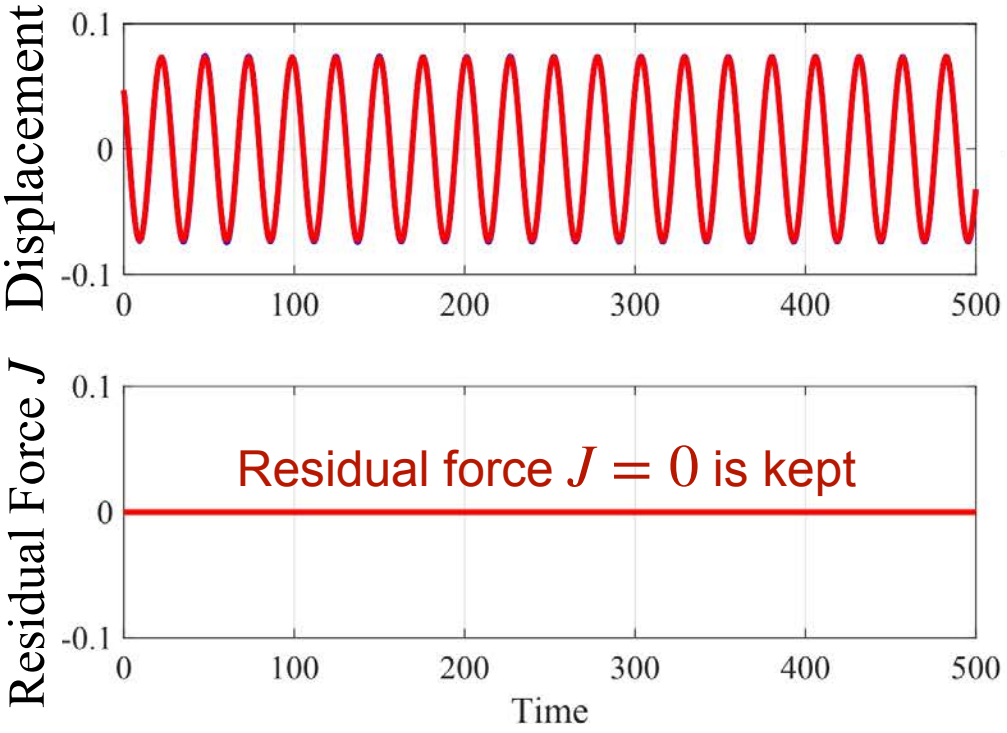


VIV円柱による基礎検証

■ **参照解**：従来の分離反復法による連成 FSI



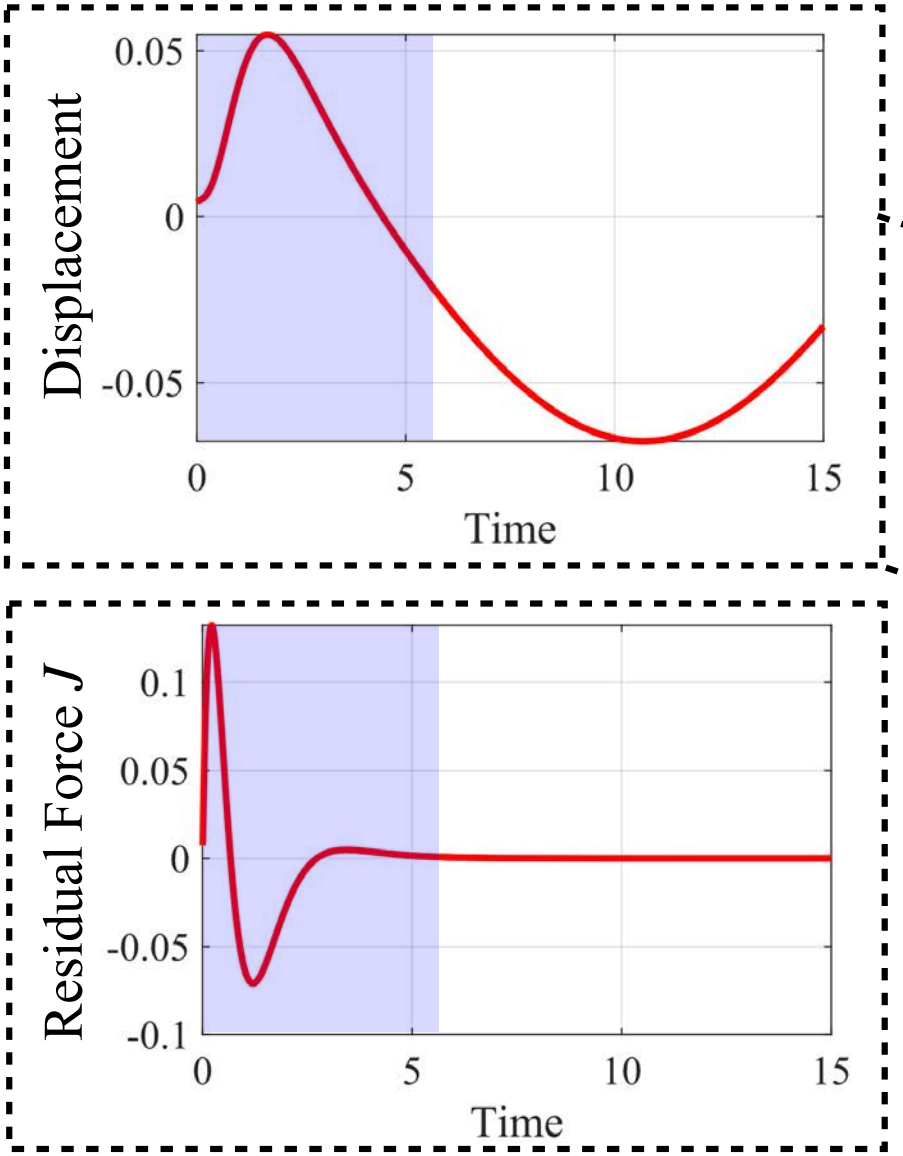
■ **提案手法**：流体力の SINDYc ＋
構造の離散系による界面モデル



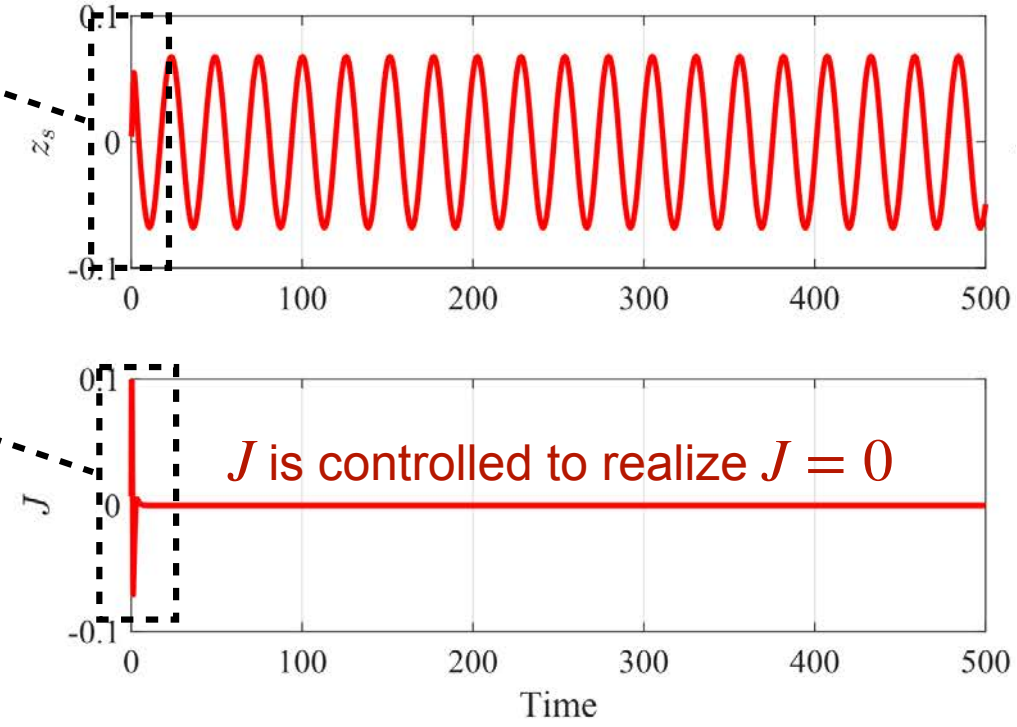
各時間ステップでの流体・構造間の反復は一度も行っていない

VIV円柱による基礎検証

- 任意の非連成状態の初期値からスタートしても，連成状態を実現 $(J \neq 0)$

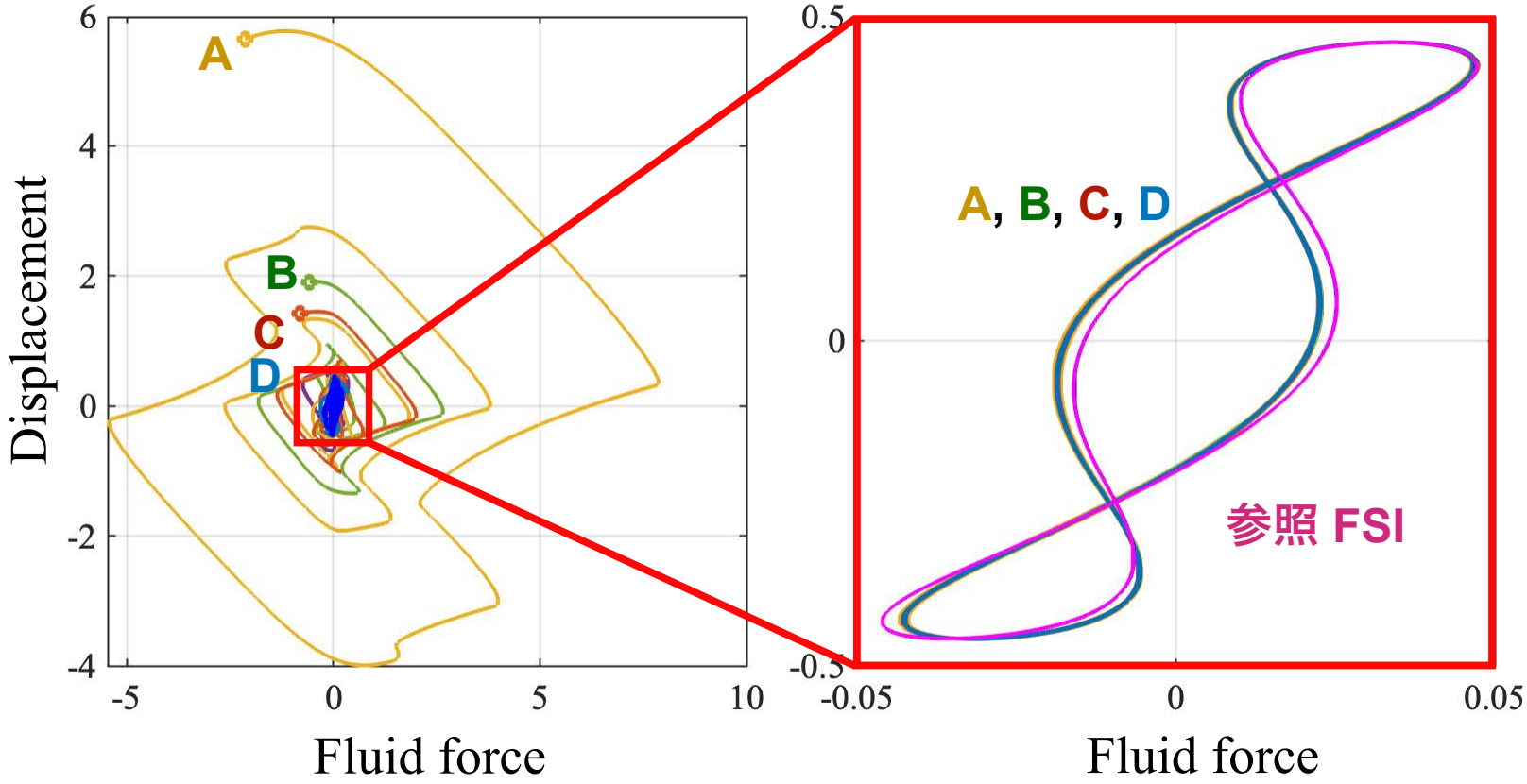


■ 提案手法：流体力の SINDYc ＋
構造の離散系による界面モデル



各時間ステップでの流体・構造間の反復は一度も行っていない

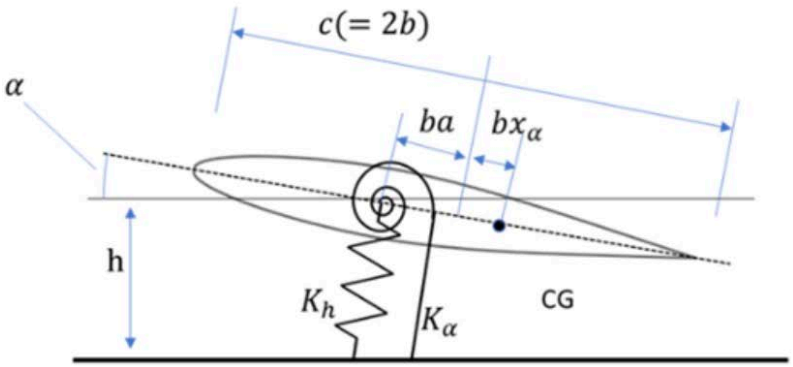
位相空間におけるリミットサイクル



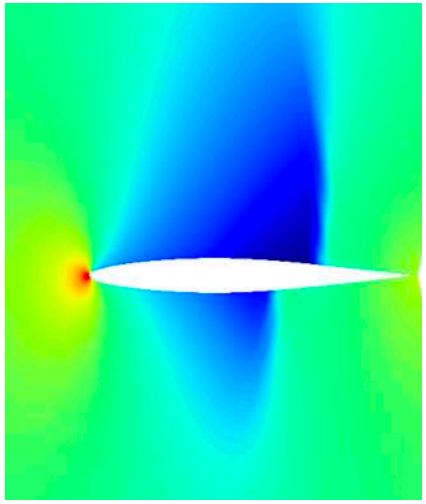
- ４つの初期条件すべてが同一の軌道に収束
- SINDYcによる界面モデルが（比較的）良好に現象を再現

非線形性の強い問題への適用：2次元剛体翼フラッタ

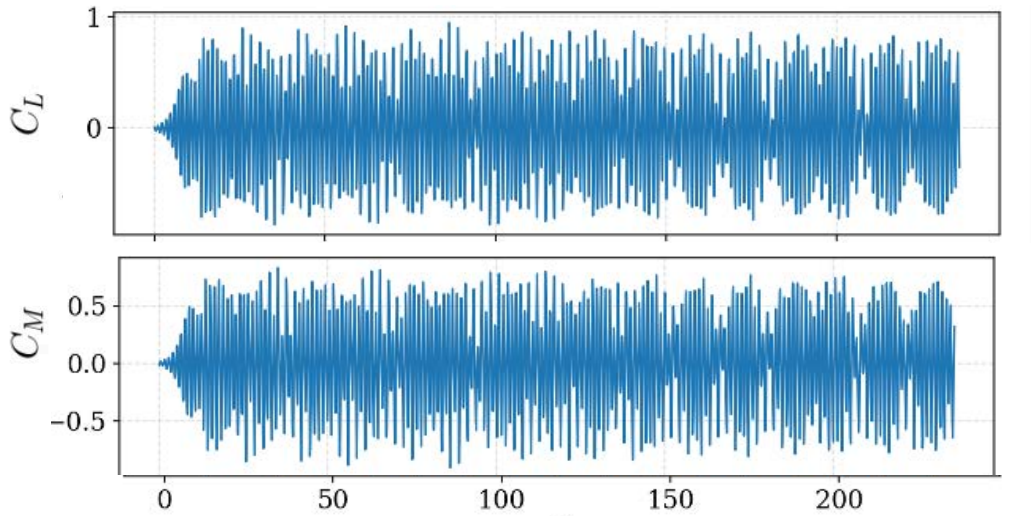
- Mach数=0.9の遷音速域で，複雑な振動状態を表すケース



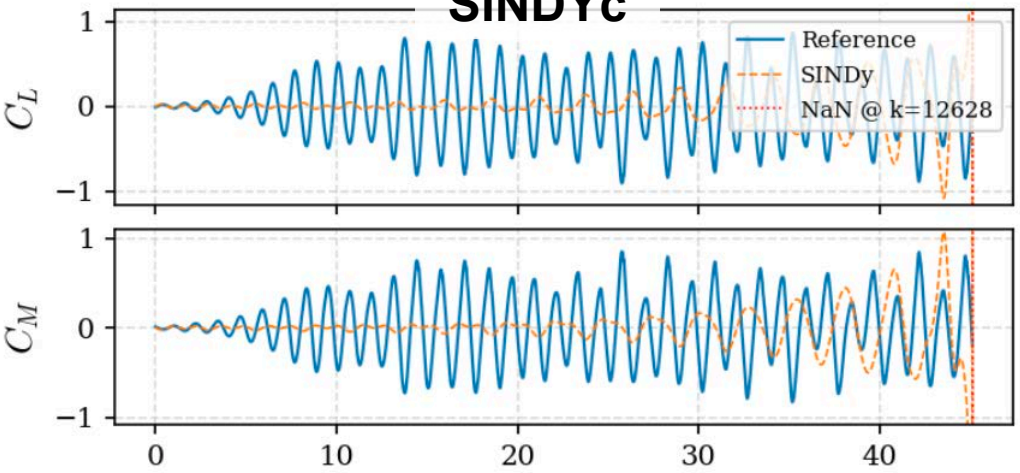
$$
\begin{aligned}
m\ddot{h} + S_\alpha \ddot{\alpha} + K_h h &= -2q_\infty b C_L \\
S_\alpha \ddot{h} + I_\alpha \ddot{\alpha} + K_\alpha \alpha &= 4q_\infty b^2 C_M
\end{aligned}
$$



参照FSI



SINDYc



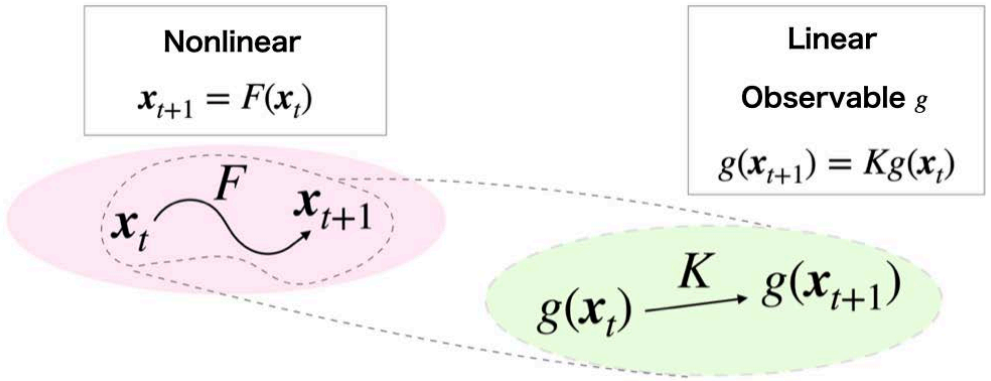
界面モデルの表現能力が不足すると，連成系が不安定化

界面モデルの高度化：Deep Koopman

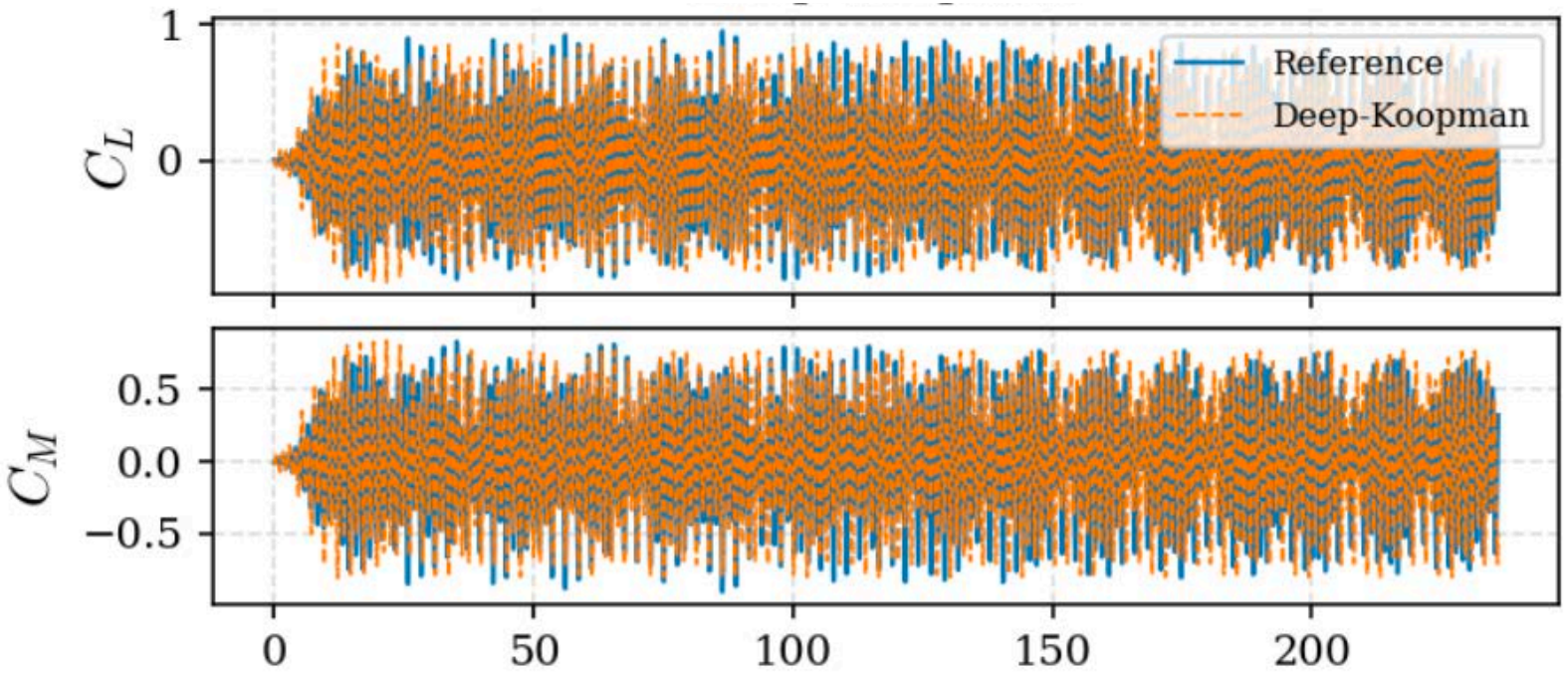
Morton *et al.*, *NeurIPS* 2018

Marumoto et al., *ICFD*2025, 2026

$$x_{t+1} = F(x_t) \longrightarrow \quad g(x_{t+1}) = g(F(x_t)) = \mathcal{K}\, g(x_t)$$



- Autoencoder + Koopman
- エンコーダ・デコーダを学習し，潜在空間で線形化
- SINDYcと異なり，辞書の設計が不要，表現能力をデータから獲得



Introduction of Koopman linearization

Finite-dimensional nonlinear system

$$x_{t+1} = F(x_t, u_t)$$

Koopman theory

$$x = \begin{bmatrix} x_1 \\ \vdots \\ x_n \end{bmatrix} \mapsto g = \begin{bmatrix} \psi_1(x) \\ \vdots \\ \psi_n(x) \\ \vdots \end{bmatrix}$$

finite — infinite

Infinite-dimensional linear system

$$g_{t+1} = \mathrm{K} g_t + L u_t$$

Finite-dimensional approximation

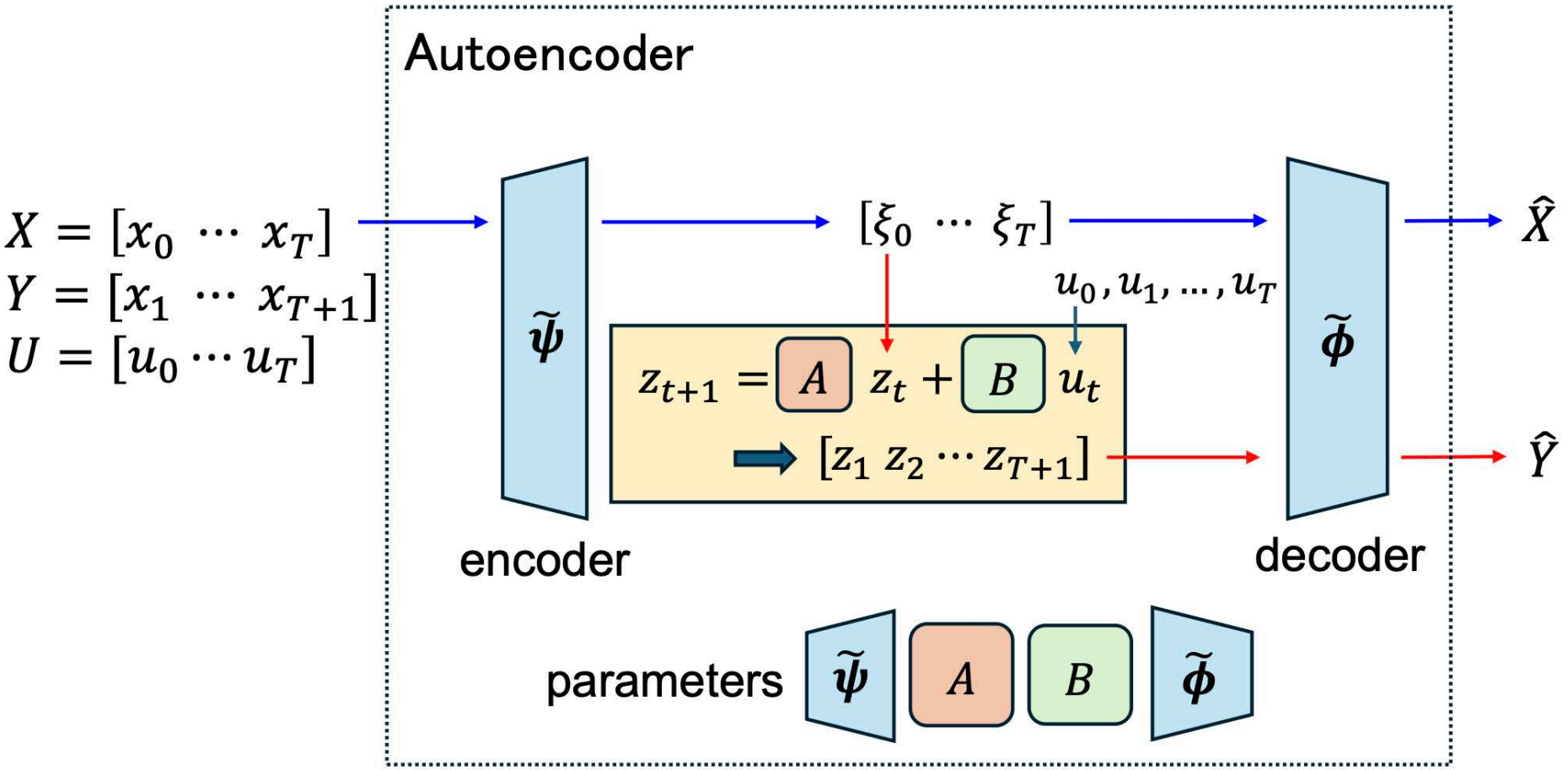
$$g = \begin{bmatrix} \psi_1(x) \\ \vdots \\ \psi_n(x) \\ \vdots \end{bmatrix} \simeq \tilde{\boldsymbol{\psi}} = \begin{bmatrix} \psi_1(x) \\ \vdots \\ \psi_n(x) \\ \vdots \\ \psi_r(x) \end{bmatrix} \mapsto \tilde{\boldsymbol{\phi}} = \begin{bmatrix} \phi_1(\tilde{\boldsymbol{\psi}}(x)) \\ \vdots \\ \phi_n(\tilde{\boldsymbol{\psi}}(x)) \end{bmatrix} = \begin{bmatrix} \hat{x}_1 \\ \vdots \\ \hat{x}_n \end{bmatrix}$$

infinite — finite

Finite-dimensional approximated linear system

$$\tilde{\boldsymbol{\psi}}(x_{t+1}) = A\tilde{\boldsymbol{\psi}}(x_t) + B u_t$$

Introduction of Koopman linearization



Loss function

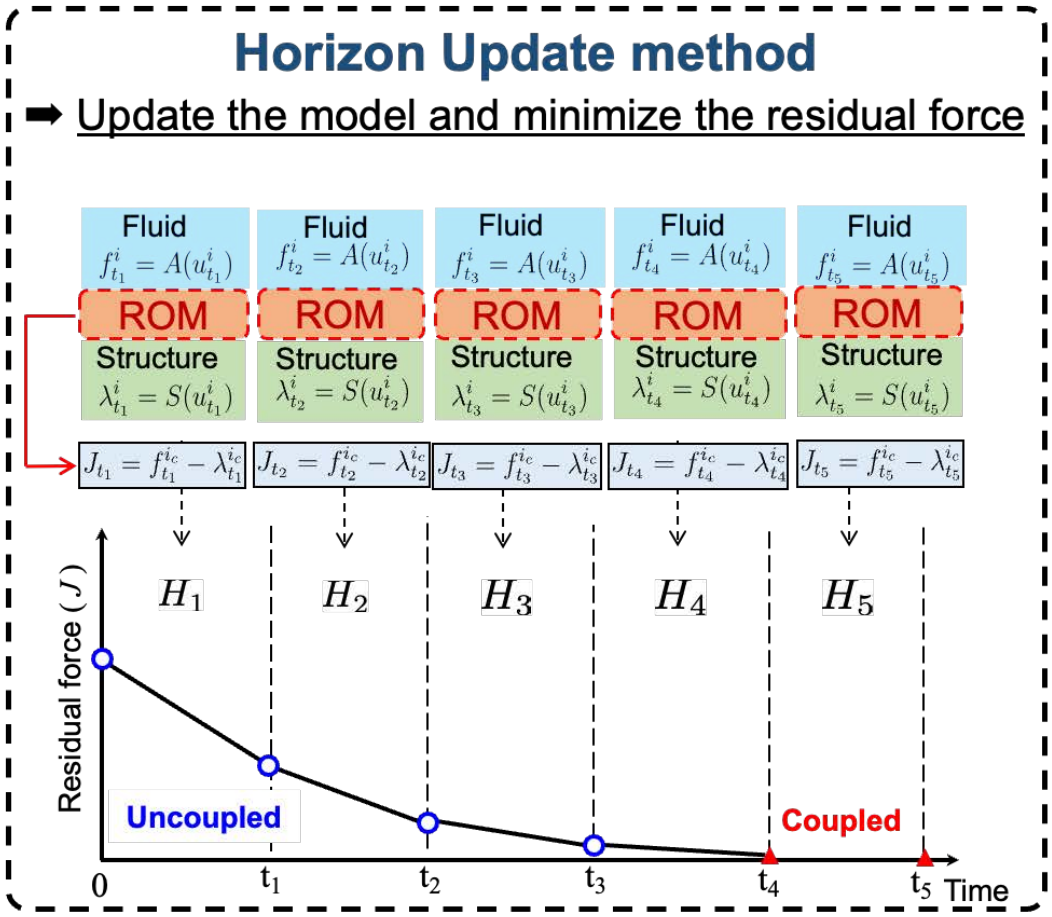
$$L = \left|\hat{X} - X\right| + \left|\hat{Y} - Y\right|$$

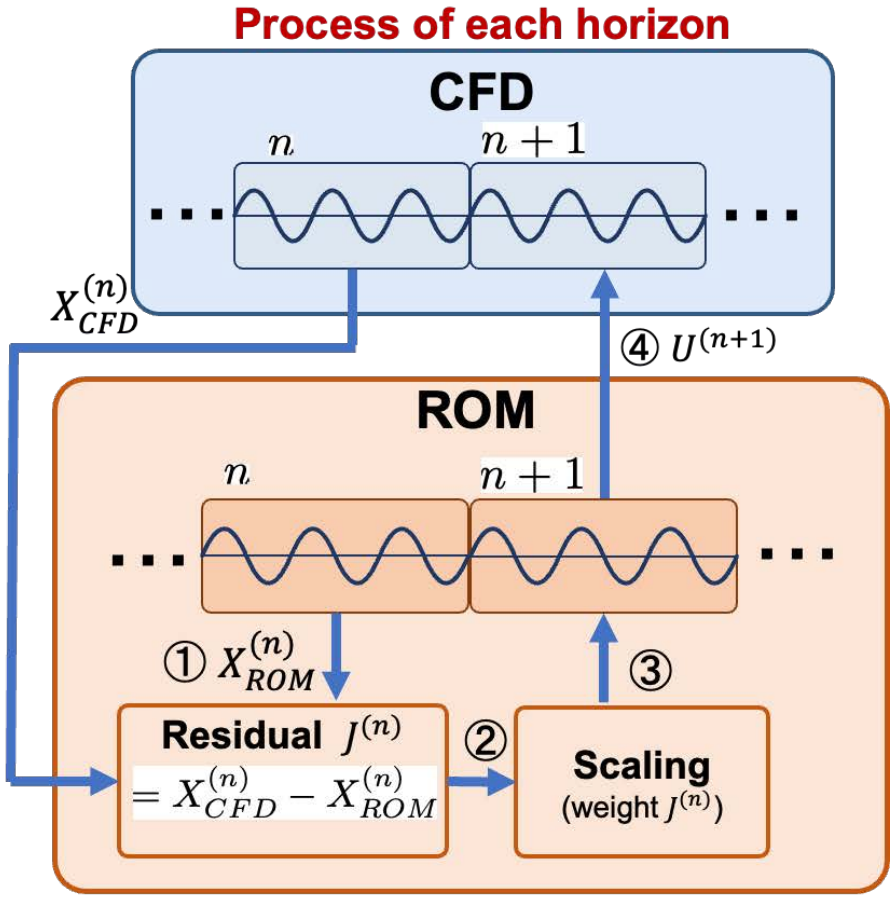
$\left|\hat{X} - X\right|$: reconstruction loss

$\left|\hat{Y} - Y\right|$: prediction loss

Horizon更新：モデルを更新しながら連成を進める

■ 単一モデルで全時間を予測すると，未学習の状態に入った時点で誤差が蓄積



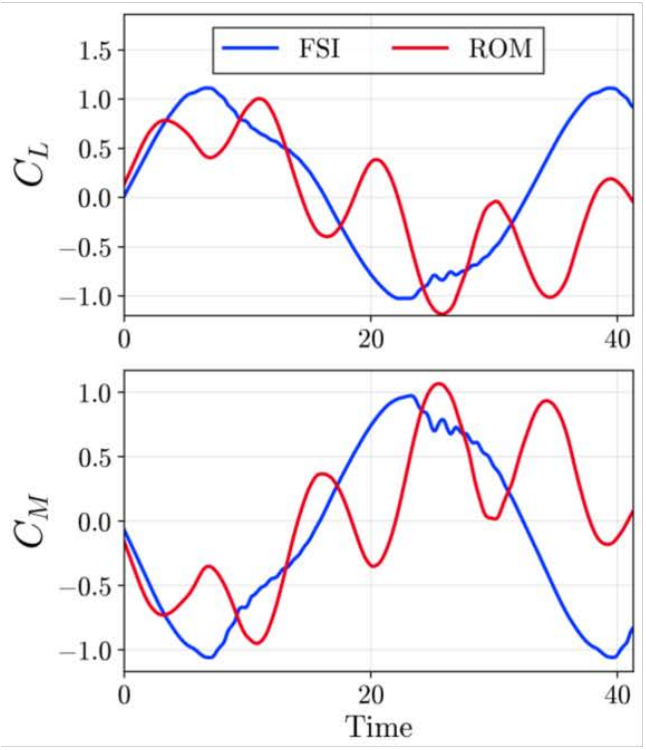


更新されるのはROM．流体・構造間の反復は依然として不要．

Horizon更新に伴う収束

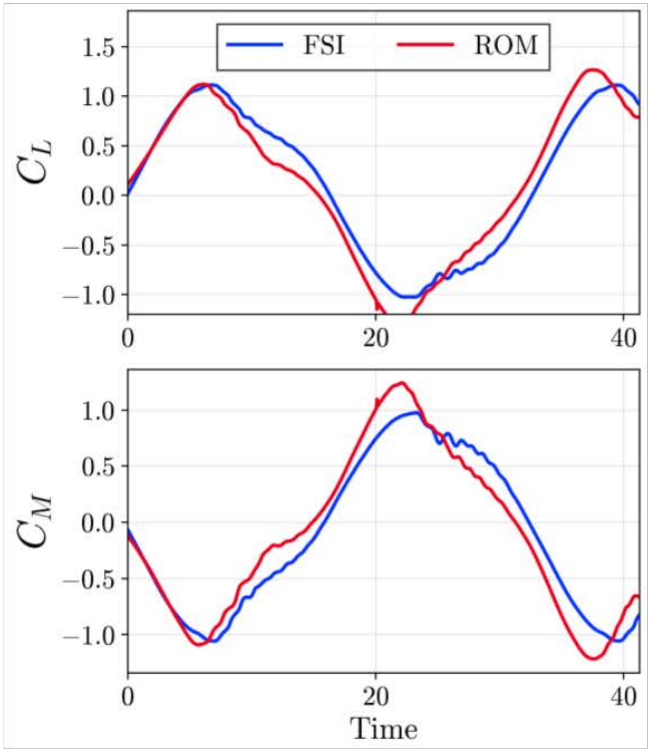
< Horizon 1 >

Estimation error : 70.5% / 65.4%



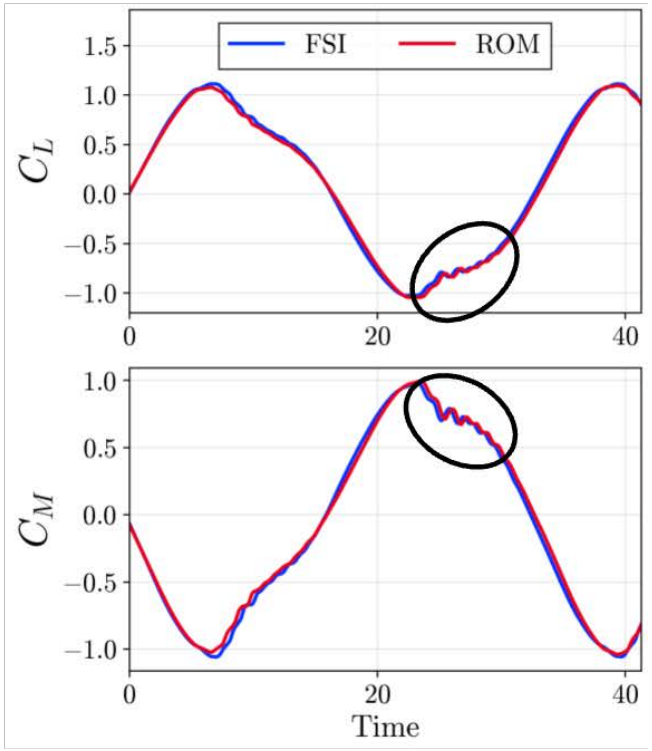
< Horizon 10 >

Estimation error : 19.7% / 19.0%



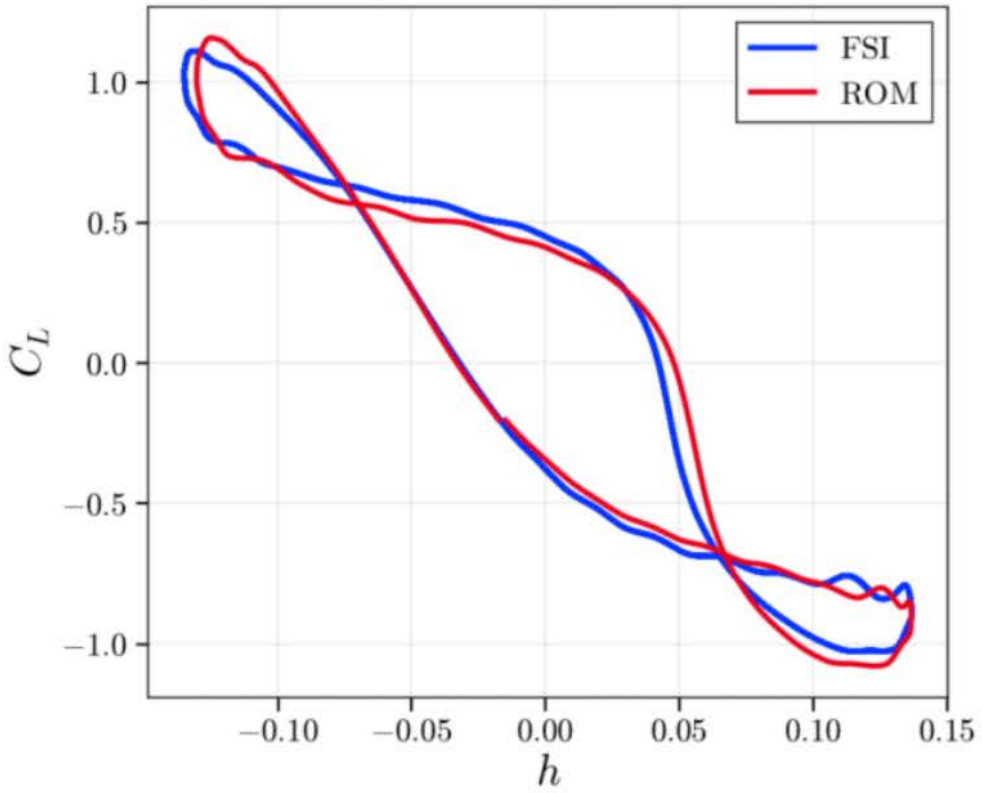
< Horizon 20 >

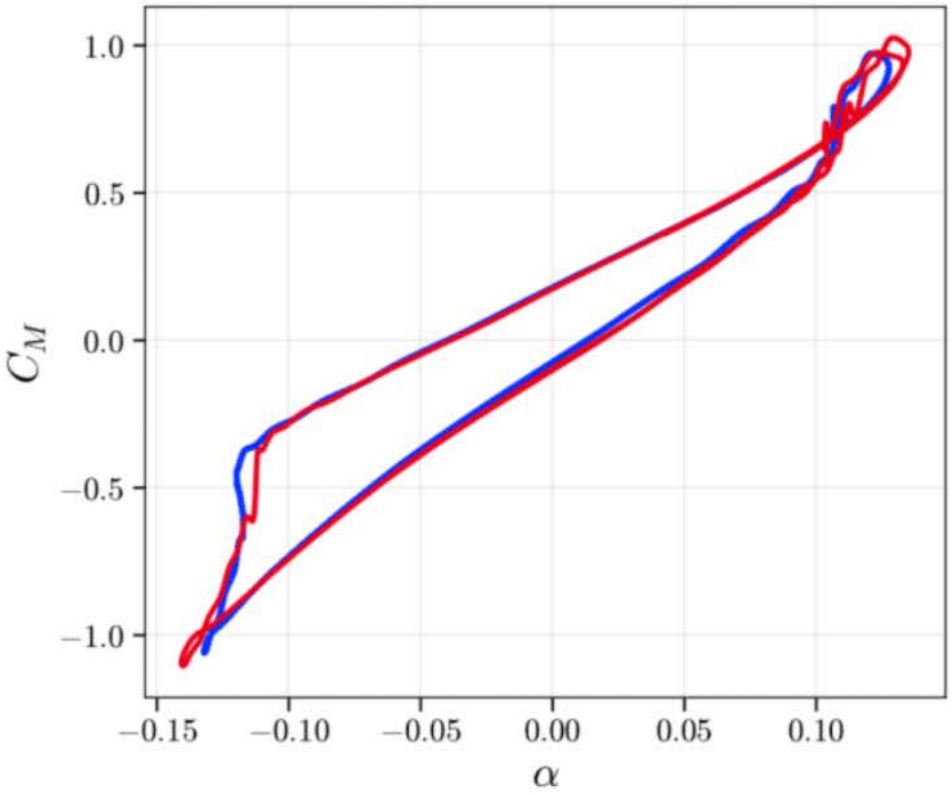
Estimation error : 4.1% / 4.0%



Horizon毎にROMの更新も行うことで，誤差と残差力を同時に減少

結果④：リミットサイクルの再現





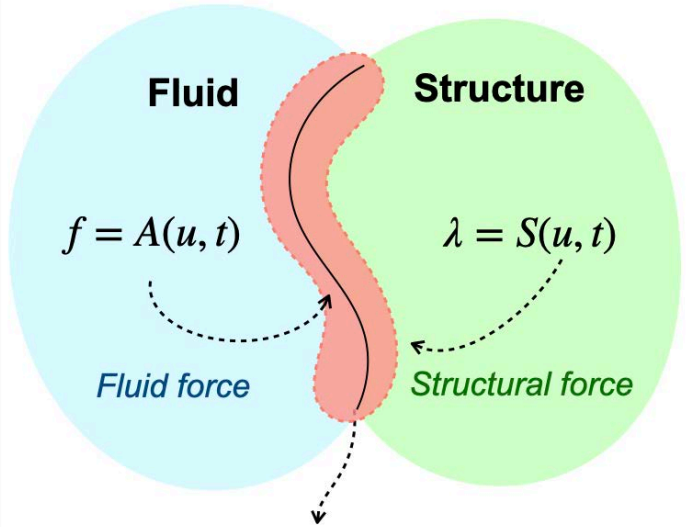
Horizon毎にROMの更新も行うことで，誤差と残差力を同時に減少

まとめ：Interface Control Principle

界面条件の破れ $J = f - \lambda$ を，反復ではなく制御で抑制する

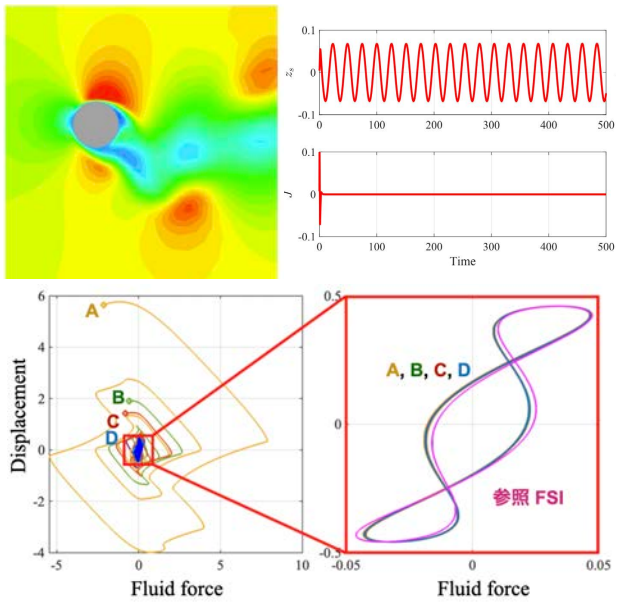
ICP理論

残差力の動力学と制御



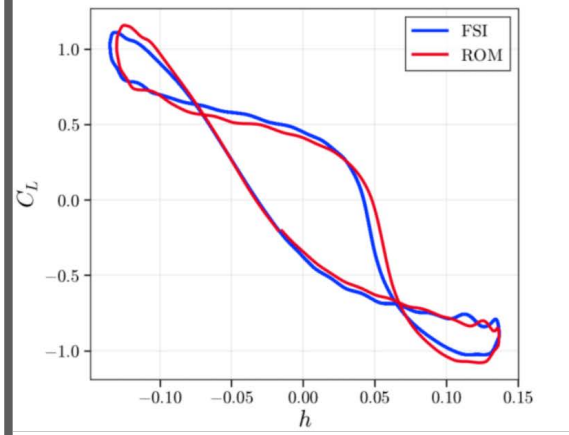
VIV円柱 (基礎検証)

反復なしで連成解を再現



遷音速フラッタ

Deep Koopman + ホライズン更新でLCO を誤差4%程度で予測



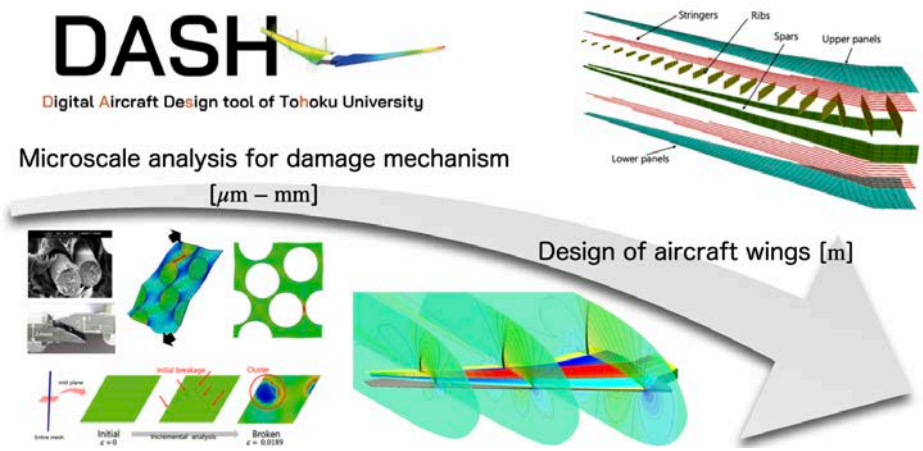
異なる物理の境界に「新しい力学システム」を見出す

Summary

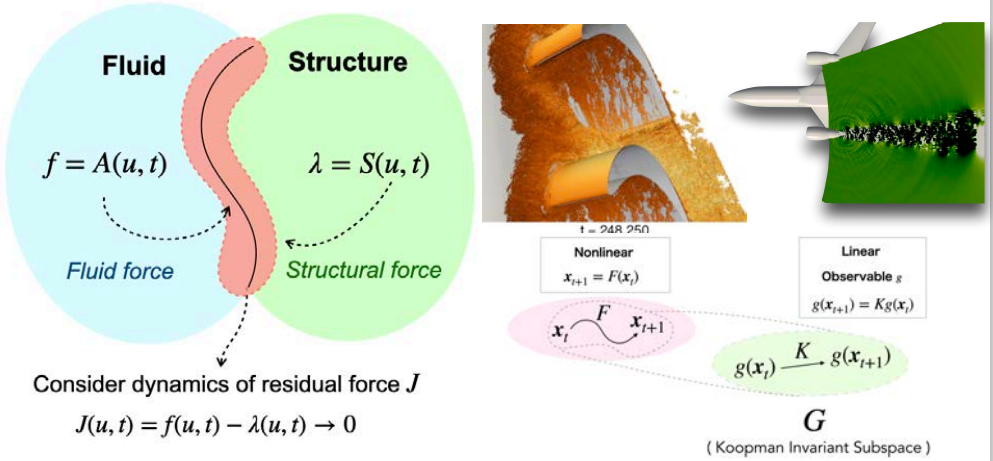
Challenges in technologies for digital aircraft design

- **Multidisciplinary Design Optimization (MDO)**
- **Multi-scale / high-fidelity simulation with modern hardware**
- **Data-driven / assisted multi-physics simulations**

Aircraft Design Tool

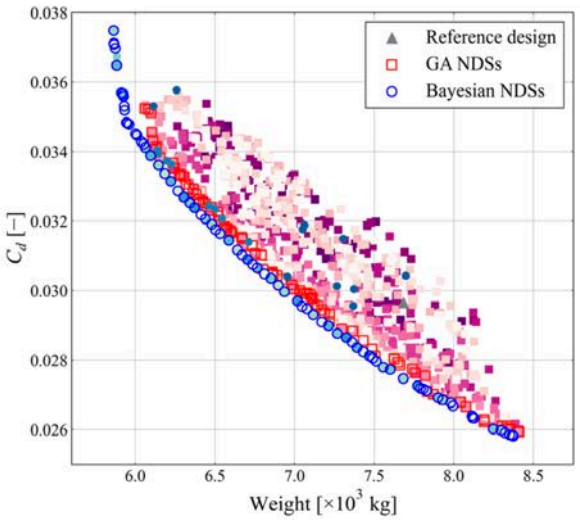


Data-driven FSI



References

[Aircraft design] Composite Structures 383 (2026) 120105 · Open Access



Contents lists available at ScienceDirect

Composite Structures

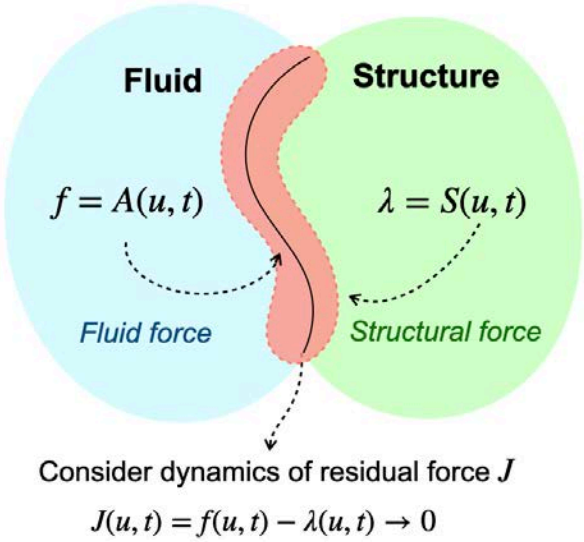
journal homepage: www.elsevier.com/locate/compstruct

Multi-objective Bayesian optimization of composite aircraft wings using various carbon fibers

Yajun Liu [a,1], Yoshiaki Abe [a,*,1], Ryosuke Kano [b,a], Yuki Yatsu [b,a], Katsumi Nakamura [b,a], Koji Shimoyama [d], Tomonaga Okabe [b,c], Shigeru Obayashi [a]

[a] Institute of Fluid Science, Tohoku University, 2-1-1, Katahira, Aobaku, Sendai, 980-8577, Japan
[b] Department of Aerospace Engineering, Tohoku University, 6-6-01, Aramaki-Aza-Aoba, Aobaku, Sendai, 980-8579, Japan
[c] Department of Materials Science and Engineering, University of Washington, BOX 352120, Seattle, WA 98195, USA
[d] Department of Mechanical Engineering, Kyushu University, Fukuoka, 819-0395, Japan

[Date driven FSI] J. Fluids Struct. 146 (2026) 104636 · Open Access



Contents lists available at ScienceDirect

Journal of Fluids and Structures

journal homepage: www.elsevier.com/locate/jfs

Fluid-structure interaction analysis with interface control principle

Chungil Lee [a,1], Yoshiaki Abe [a,1,*], Yu Kawano [b], Tomoki Yamazaki [c,a]

[a] Tohoku University, Institute of Fluid Science, 2-1-1 Katahira, Aoba-ku, Sendai, 9808577, Miyagi, Japan
[b] Hiroshima University, Graduate School of Advanced Science and Engineering, 1-4-1 Kagamiyama, Higashi-Hiroshima, 7398527, Hiroshima, Japan
[c] Tohoku University, Department of Aerospace Engineering, 6-6-01 Aramaki-Aza-Aoba, Aoba-ku, Sendai, 9808579, Miyagi, Japan